Strain Dependent Differences in MAPK Signaling in Yeast

By

Taylor D. Scott

A dissertation submitted in partial fulfillment of

the requirements for the degree of

Doctor of Philosophy

(Cellular and Molecular Biology)

at the

UNIVERSITY OF WISCONSIN-MADISON

2022

Date of final oral examination: 08/15/2022

The dissertation is approved by the following members of the Final Oral Committee

Megan N. McClean, Associate Professor, Biomedical Engineering
Silvia Cavagnero, Professor, Chemistry
Brian Pfleger, Professor, Chemical and Biological Engineering
John Pool, Associate Professor, Genetics

Acknowledgements

A PhD is a long road, and it would not have been possible without the support of many people, both professionally and personally.

First and foremost, I am deeply grateful to my advisor, Dr. Megan McClean, for the guidance and support she provided as I worked on this project. She has fostered an amazing lab culture that keeps me excited to come into lab. She pushed me to think about how to make crazy ideas doable and helped me forge ahead when the science wasn't working. I'm certain I would not have finished this thesis without her help along the way. I am also grateful for the support given by my committee, Dr. Audrey Gasch, Dr. Silvia Cavagnero, Dr. Brian Pfleger, and Dr. John Pool, all of whom provided valuable feedback on the direction and focus of my project. I am also grateful to the UW Flow Cytometry Laboratory, without which I could not have run most of my critical experiments, and the UW DNA Sequencing Center, which performed all of the sequencing for this project.

I would also like to give special thanks to the members of the McClean Lab: Althys Cao, Dr. Anik Chaturbedi, Stephanie Geller, Zack Harmer, Lucy Jiang, Morgan Lekschas, Neydis Moreno Morales, Kevin Stindt, Kieran Sweeney, Renee Szakaly, and Timothy Wakiyama. There's nothing like lunch at The Library or the Terrace to take the edge off of a bad day in lab, and the feedback and comments on my data, drafts, and presentations were invaluable. I also appreciate the support provided by the other CMB students. I would especially like to thank Becky, Dan, Lauren, Sarah, and Tamara. It's hard to navigate grad school and having friends going through the same deadlines and milestones kept me on track and helped me see past the constant imposter syndrome. Not to mention being the best trivia team ever assembled.

Finally, I am grateful for my family: my parents Wes and Andrea, my siblings Molly, Jacob, Alyssa, and my brother-in-law State. They've seen my progress on this project up close and talking to them about the successes and failures helped me keep things in perspective. Even when I doubted my abilities, my

parents provided unquestioning support and confidence that encouraged me to keep going. I am certain this would not have been possible without their constant affirmation and excitement about my progress. Biology is as much about learning as it is about cells, and I'm incredibly grateful that my parents encouraged me to learn throughout my life, and they taught me to seek out information when I got curious about the world.

This work was supported by the National Science Foundation Graduate Research Fellowship Program, the National Institutes of Health, and the Burroughs Wellcome Fund.

Abstract

All cells must respond to extracellular signals in order to exist in a dynamic environment. Between a signal being received at the membrane and the cellular response is a series of tightly regulated molecular reactions which collectively form a signaling network. Mitogen-activated protein kinase (MAPK), among the most common signaling networks, are found in all eukaryotes and are important for cancer biology, developmental biology, and the response to stress. The MAPK networks in the model organism *Saccharomyces cerevisiae*, commonly known as budding yeast, are a model system for studying signal transduction through MAPK networks, and particularly the mechanisms by which cells prevent signal from leaking into connected networks. In this thesis I study how the yeast strain background affects signal flow through MAPK networks and explore potential genetic causes of strain-dependent differences.

I begin with an introduction to the yeast MAPK networks. These networks have been studied for decades, and the structure, activation, and downstream responses of these networks are known in detail. I focus on the upstream activation mechanisms; that is, the events leading to activation of the MAPK. I describe activation of three yeast MAPK networks: the high osmolarity glycerol (HOG) pathway, the mating pathway, and the filamentous growth (FG) pathway. Connections between the pathways (in the form of shared components or reactions) are highlighted, as are regulatory and feedback mechanisms. I then describe two potential mechanisms of insulation—active suppression of the mating/FG pathway by Hog1p and differential activation of scaffolding proteins—which are frequently studied and thought to be responsible for the nearly complete isolation of the networks. Finally, I give examples of important strain backgrounds used in the study of these networks and how the choice of a strain background may influence signaling through the networks.

In chapter two, I compare two strain backgrounds, YPH499 and Σ1278b (Sigma) side-by-side to determine the extent to which they differ in their response to osmostress and pheromone, which signal

through the HOG and mating pathways respectively. The two strain backgrounds have previously been used to study MAPK signaling, but a detailed comparison has not been done. I show that Sigma is more osmosensitive than YPH499 despite growing faster in ordinary, non-stress conditions. I further show that despite this increased osmosensitivity, Sigma is better able to respond to simultaneous osmostress and pheromone, showing a faster activation of the mating pathway after the delay caused by osmostress. I also demonstrate that, while the HOG and mating/FG pathways are insulated in YPH499 as has been previously reported, there is significant and transient leakage from the HOG pathway into the mating/FG pathways in the Sigma background. This leakage, or crosstalk, is dependent on mating/FG pathway components and does not appear to be related to ineffective Hog1p activation. Rather, I find that two phases of crosstalk exist in the Sigma background: an early phase where crosstalk occurs and a late phase where Hog1p suppresses further crosstalk. The late phase Hog1p suppression of crosstalk also occurs in the YPH499 background, but the early crosstalk does not occur. Finally, I show that Rck2p, one target of Hog1p which suppresses crosstalk, plays a more important role in suppressing crosstalk in the Sigma background than in the YPH499 background. This chapter demonstrates that comparing strains can reveal subtle differences in signaling even in well-studied networks.

In chapter three, I map signaling differences to genetic loci or quantitative trait loci (QTL). I crossed YPH499 and Sigma background strains and generated a population of over 600 segregants. I measured the segregants' basal pFUS1-eGFP (mating pathway) activity and the amount of crosstalk in each segregant and found that both traits are heritable. I then used a bulk segregant approach to map the traits to QTL. I identified QTL for basal pFUS1-eGFP expression and crosstalk and tested genes within these QTL by introducing the allele from one parent into the opposite strain background. I did not identify causative genes for crosstalk. I identified *STE50* and *FYV5* as regulating basal mating pathway activity, although the results varied by strain background, suggesting that this trait is epistatic.

I conclude by summarizing my results in the context of known regulators of MAPK signaling in yeast. I also suggest future experiments which would extend this work and provide further insight into my results. MAPK signaling is an important cellular process, and he large number of existing yeast strains provide a resource for exploring how modifications to a signaling network affect pathway output. My results demonstrate that the strain background greatly impacts signaling output, even in closely related laboratory strains, and establishes protocols for assaying signaling traits in closely related strains.

Table of contents

List of Figures

Chapter 1

Chapter 2

Chapter 3

Appendix A

Appendix B

List of Tables

Chapter 2

Chapter 3

Chapter 1: Introduction

Taylor Scott wrote the chapter.

ABSTRACT

Mitogen-activated protein kinase (MAPK) networks are among the most common examples of signaling networks in eukaryotes. They have been implicated in many important biological processes, including cellular growth and division, developmental biology, cancer biology, and stress responses. The yeast MAPK networks are a model system for studying signaling through MAPK networks because of the ease of activating the pathways and the robustness of the responses, in part due to the powerful genetic approaches available in yeast. Decades of research have determined the structure of the networks and the functions of dozens of proteins which participate in the activation of the pathways. In this chapter, I will summarize three important yeast MAPK networks, focusing on activation of the pathways upstream of the cellular response and on feedback and regulation of the pathways. I will also provide an overview of how the networks are connected and what potential mechanisms prevent signal from leaking from one pathway to another, a phenomenon known as crosstalk. Finally, yeast exists in many different strains, laboratory and wild, which display differences in protein abundance and function. I will give examples of strain backgrounds used in the study of yeast MAPK networks and important differences between the strains which affect signaling output.

OVERVIEW

Cells exist in a dynamic environment. They continually are subject to signals in the form of external stress, changes in nutrient availability, and, in many cases, signals from nearby cells. These signals (or stimuli) warrant a cellular response, often in the form of transcriptional changes, metabolic changes, or morphological changes. In order to effectively respond to signals, cells use a tightly regulated series of molecular reactions to process and transmit the signal to the cellular machinery responsible for the response. The set of reactions for a given stimulus/response pair is called a signaling network, and, in general, many signaling networks exist within a given cell.

One common example of signaling networks are the mitogen-activated protein kinase (MAPK) networks, which are conserved among eukaryotes. The core MAPK structure consists of a three-step kinase cascade: a mitogen-activated protein kinase kinase kinase (MAP3K) phosphorylates and activates a mitogen-activated protein kinase kinase (MAP2K), which phosphorylates and activated a mitogen-activated protein kinase (MAPK). The upstream activation mechanisms of the MAP3K are diverse, as are the downstream targets of the MAPK [1]. Multiple MAPK networks may exist within a given cells, each controlling the response to a different stimulus. Three networks of interest are found in the model organism *Saccharomyces cerevisiae*, commonly known as budding yeast [2]. These pathways are the high osmolarity glycerol (HOG) pathway, the mating pathway, and the filamentous growth (FG) pathway. These pathways, despite controlling the responses to vastly different stimuli, share components and activation mechanisms. Consequently, they are frequently used as model systems to study signal transduction through MAPK networks and specifically insulation of connected networks.

I will begin by providing a summary of the activation mechanisms of these three pathways, with particular detail on the mechanisms upstream of and including the core MAPK cascade. Figure 1.1 summarizes the major connections and nodes of the yeast MAPK networks covered in this chapter,

including the kinases of the core MAPK cascades and important proteins necessary to activate the core cascades. I will also describe two complementary mechanisms of signaling insulation which have been shown to prevent signals from leaking from one pathway into another. Finally, I will provide examples of how the strain background used to study these networks influences the findings and, in one case, obscures important signaling events. Signaling is a critically important cellular process, and the yeast MAPK networks are an excellent model system for determining the principles of signal transduction in eukaryotic organisms.

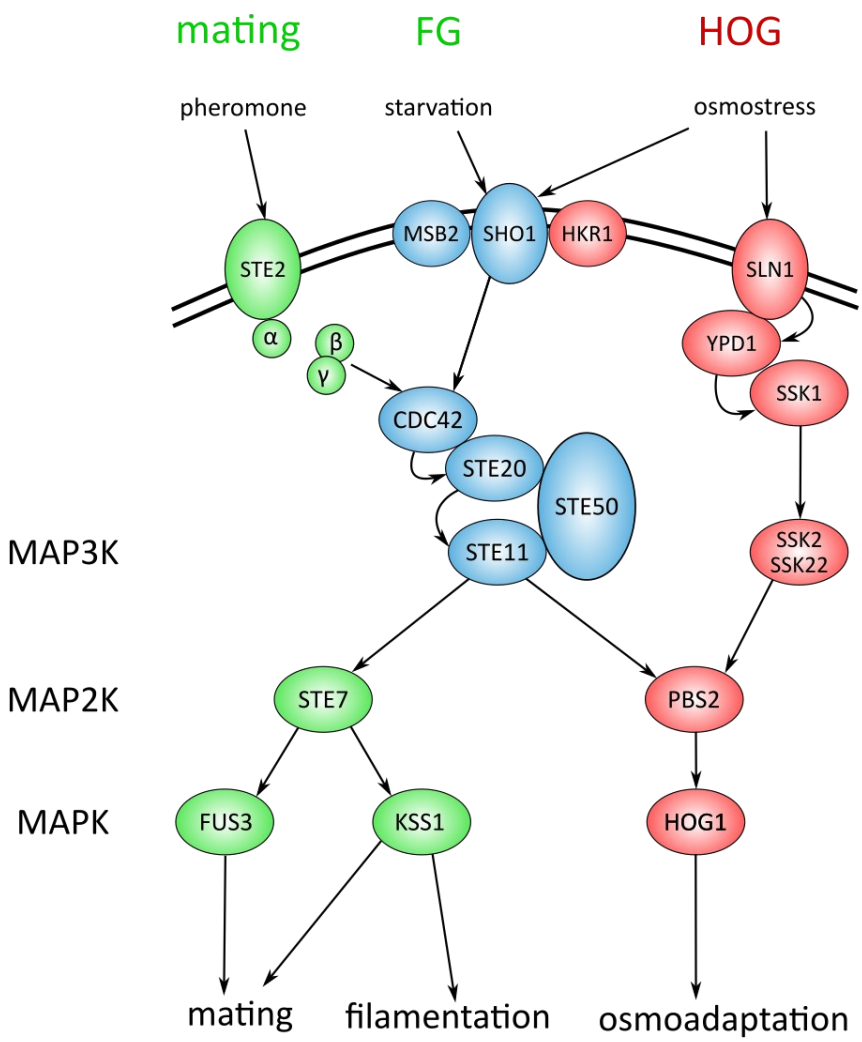

Figure 1.1 Yeast MAPK cascades control the responses to diverse extracellular signals.

Three yeast MAPK networks control the response to pheromone (the mating pathway), nutrient starvation (the filamentous growth [FG]) pathway, and osmostress (the high osmolarity glycerol [HOG]) pathway. The networks consist of two core MAPK kinase cascades, where mating and FG share the same cascade despite different upstream activation mechanisms. Elements of the mating and FG pathways are depicted in green; elements of the HOG pathway are depicted in red; and elements shared by more than one pathway are depicted in blue. Note that the three pathways share the activation of the MAP3K Ste11p by Ste20p, which makes these pathways a model system for the coordination of multiple signaling networks, which respond to disparate stimuli despite sharing components.

YEAST MAPK NETWORKS

The HOG pathway

The high osmolarity glycerol (HOG) pathway is a MAPK pathway controlling the response to osmotic stress, or excess osmolyte in the environment causing water loss. The cell responds by closing glycerol export channels and diverting cellular resources to the production of glycerol, itself an osmolyte, in order to equalize the difference in osmotic pressure and bring water back into the cell [3]. In this section, I will summarize the steps of HOG pathway activation, important events in the cellular response, and regulatory mechanisms.

Activation

HOG pathway activation begins when a yeast cell encounters an osmolyte, any molecule which causes an excess of osmotic pressure outside the cell. There are many potential osmolytes a cell may encounter, but prominent ones are dissolved salts (as in marine environments) and simple sugars (as in the wine making process). In general, the osmolyte does not affect HOG pathway signaling, although there appears to be a cation specific gene response induced when salt is used as an osmolyte [4]. It is important to note that, because the specific stress is osmotic pressure [5], osmolytes which dissociate (e.g., NaCl) impose a greater stress than a non-dissociative osmolyte at the same concentration. For example, 0.4M NaCl or KCl imposes roughly the same osmotic stress as 0.8M sorbitol [6]. Severe water loss is extremely harmful to the cell – at high concentrations of sorbitol, greater than 1M sorbitol, activation of the HOG pathway is delayed because intracellular crowding slows diffusion [7]. These concentrations of sorbitol are not outside of a physiological range. For example, seawater contains approximately 1.15 M dissolved solutes [8], and wine must (crushed grapes) often contains greater than 200 g/L (approximately 1.1M) dissolved sugars [9]. Strong and fast activation of the HOG pathway, then, is necessary for the cell to survive severe and sudden osmotic stress.

Osmolyte-induced water loss activates two parallel branches of HOG pathway activation, dubbed the SLN1 branch and the SHO1 branch, after their respective membrane bound osmosensors. Sln1p is part of a three-component phosphorelay system, similar to the two-component system found in bacteria [10]. Under basal conditions, Sln1p autophosphorylates and the phosphate is transferred first to Ypd1p, then to Ssk1p [10]. Phosphorylated Ssk1p is unable to bind and activate the MAP3Ks Ssk2p and Ssk22p. Under high osmotic stress, autophosphorylation of Sln1p is inhibited, thereby preventing the phosphate transfer to Ssk1p. Unphosphorylated Ssk1p then binds and activates Ssk2p and Ssk22p [11], which initiates, the remainder of the MAPK cascade. Ssk2p and Ssk22p phosphorylate and activate the MAP2K Pbs2p [12], and Pbs2p phosphorylates and activates the MAPK Hog1p [13]. The SLN1 branch is thought to be the fast-activating branch of the HOG pathway. It has been shown that eliminating the SLN1 branch results in two-fold slower activation of Hog1p [14,15], and that the SLN1 branch is more important than the SHO1 branch in responding to rapidly varying osmotic stress [16].

The SHO1 branch exists parallel to the SLN1 branch. At least three osmosensors exist upstream of this branch: Sho1p, Hkr1p, and Msb2p. The precise extent to which these osmosensors function independently is disputed, but it is clear that under osmotic stress they lead to activation of Cdc42p [12,17–20]. Cdc42p, a rho-like GTPase, activates the kinase Ste20p [21], which phosphorylates and activates the MAP3K Ste11p [21,22]. The adaptor protein Ste50p is anchored to the membrane by Opy2p and is involved in the activation of Ste11p by Ste20p [23]. It has been shown that Ste50p has both regulatory functions and scaffolding functions [24–26]. Once Ste11p has been activated, it activates Pbs2p, which then activates Hog1p as in the SLN1 branch [12]. Activation of the SHO1 branch is slower than activation of the SLN1 branch [14,15], raising the question of why it has been maintained. A recent study showed that signaling through the SHO1 branch allows cells to adapt to complex stress patterns, where the level of osmotic shock changes randomly [16]. This leads to a model of HOG pathway activation

in which the SLN1 branch allows the cell to respond quickly to an osmotic shock, while the SHO1 branch gives the cell greater flexibility in responding to dynamic stress.

Kinases involved in MAPK signaling are generally promiscuous, and specificity occurs via binding domains which position phosphorylation sites near the active site [27]. Similarly, scaffold proteins position the kinases in a cascade so that the phosphorylation events can occur efficiently [28]. Both branches of the HOG pathway use the same scaffold, Pbs2p, which is also the MAP2K [29,30]. Pbs2p binds Ste11p, Ssk2p/Ssk22p, and Hog1p, placing the three steps of the cascade in close proximity allowing rapid activation of Hog1p. Other scaffold proteins are involved in upstream activation events. Sho1p is thought to have a scaffolding role, linking together signaling proteins Opy2p and Hkr1p (through Ahk1p) [20,31]. Finally, as mentioned previously, the adaptor protein brings the Ste20p and Ste11p kinases together, allowing Ste20p to activate Ste11p [23,32,33].

After Hog1p is activated, it targets a diverse set of downstream proteins, generally all with the function of increasing intracellular concentration of glycerol. Hog1p is directed to the promoters of stress-responsive genes by the transcription factor Hot1p [34], thereby reducing the global repression of gene expression observed during an osmotic shock [35,36]. Hundreds of genes are induced during an osmotic shock[4,37], and nearly one third of these genes are induced in a Hog1p-dependent manner[4]. One such gene is the glycerol production gene *GPD1*, which is induced through interactions of Hog1p with the transcription factor Hot1p [38], thereby increasing glycerol production[39]. A second gene, *STL1* is induced more than 90-fold under osmotic stress [4,37] and is often used a reporter of HOG pathway signaling. Stl1p is a glycerol symporter essential for cellular uptake of glycerol [40]. In addition, Hog1p targets positive regulators of the glycerol export channel Fps1p, thereby closing the channel and preventing further glycerol export [41]. The net result is that glycerol accumulates in the cell under osmotic shock, thereby promoting recovery from the water loss induced by osmotic stress [3,42].

Feedback and regulation

The HOG pathway is subject to significant feedback and autoregulation. HOG-related production of glycerol naturally limits HOG pathway activity by relieving the osmotic stress [43]. In fact, the HOG pathway has been said to show "perfect adaptation", because once the cell recovers from the water loss, the HOG pathway quickly deactivates and the relevant kinases are dephosphorylated [6]. Studies in microfluidic devices have shown that, given sufficient time to fully deactivate the pathway, the cell is capable of responding fully and robustly to osmotic oscillations with no observed loss of activity [14,44,45]. The rapid dephosphorylation of the HOG pathway components is enabled by various phosphatases, including Ptp2p, Ptp3p, Ptc1p, Ptc2p, and Ptc3p [46–49]. Additionally, Hog1p itself is a source of negative feedback. Active Hog1p phosphorylates Ssk1p and Ssk2p in the SLN1 branch and thereby modulates activity through this branch [50]. The SHO1 branch is also subject to feedback from Hog1p; Sho1p is phosphorylated by Hog1p under osmotic stress, and this phosphorylation dampens signaling through the SHO1 branch [51]. Basal HOG pathway activity is also regulated. Inhibition of Hog1p under basal conditions results in phosphorylated Hog1p, suggesting that Hog1p activity plays a role in maintaining the pathway under basal conditions, and this basal regulation allows for rapid activation of the pathway under osmotic stress [15,50].

The mating pathway

Haploid yeast cells typically reproduce asexually through budding, however two haploid cells of opposite mating types (MATa and MATα) can mate and fuse, forming a zygote which buds diploid cells. The process of mating and fusion is controlled by a MAPK pathway known as the mating pathway. Mating was an early target of yeast research, and there is a long history of study into the molecular basis of its activation and regulation. In this section I will provide an overview of mating pathway activation and regulation mechanisms, both autoregulation and regulation by other cellular machinery.

Activation

Upstream activation of the mating pathway is broadly similar in MATa and MATα cells, but some specific components (e.g., the pheromone receptor) are mating-type specific. For simplicity, I will discuss the mating pathway as it exists in MATa cells. For a MATa cell, mating signaling begins when α-factor, a peptide pheromone secreted by MATα cells, binds the pheromone receptor Ste2p [52]. Ste2p is a G-protein coupled receptor (GPCR) which is basally bound to the heterotrimeric G protein. After pheromone binds, the G protein α subunit (Gpa1p) dissociates from the β and γ subunits (Ste4p and Ste18p). The βγ dimer is stimulatory, and upon release from the inhibitory α subunit, they initiate signaling via association with Cdc24p, Cdc42p, and Ste20p [53,54]. The βγ subunit binds the Cdc24p-Far1p complex and promotes activation of Cdc42p [55,56]. Once activated, Cdc42p binds the inhibitory CRIB domain of Ste20p, which frees the catalytic site and allows Ste20p to phosphorylate and activate the MAP3K Ste11p [57–59]. Signaling follows the familiar MAPK activation regime from this point: active Ste11p phosphorylates the MAP2K Ste7p, activating it, and Ste7p phosphorylates two MAPKs, Fus3p and Kss1p, which are the major effectors of the cellular response to pheromone [60].

The mating pathway is associated with induction of genes required for fusion. The MAPKs, Fus3p and Kss1p, target a transcription factor, Ste12p, in order to effect this response [61]. Ste12p is an activating factor which binds to a short sequence element called the pheromone response element (PRE). PREs are found upstream of many genes induced by the mating pathway, and it has been shown that the presence of a PRE is sufficient to induce expression in response to pheromone [62,63]. Genes induced by the mating pathway include *FUS1* (the most commonly used reporter of mating pathway activity), *MFA1* and *MFA2* (i.e., pheromone peptides), and mating pathway components *FAR1*, *FUS3*, *GPA1*, *STE2*, *SST2*, which serves a feedback mechanism (discussed in more detail below) [64–66]. In the absence of pheromone, Ste12p is bound by the inhibitors Dig1p and Dig2p, which prevents it from activating the genes. Fus3p and Kss1p phosphorylate Dig1p and Dig2p, causing Ste12p to be released and allowing it to

induce the mating-responsive genes. [67–69]. Additionally, unphosphorylated (inactive) Kss1p directly binds and inhibits Ste12p, a further repressive mechanism which prevents inadvertent activation of these genes [70]. The net result of these regulatory mechanisms is that, under basal, unstimulated conditions, the genes are strongly repressed despite Ste12p being bound to the promoters. After pheromone stimulation, the repression is relieved and Ste12p is activated, leading to robust activation of the mating responsive genes.

Fus3p and Kss1p are partially redundant in mating. In particular, cells lacking Fus3p are fully capable of mating, but they mate slower than wildtype cells [71]. It is thought that when both kinases are present, Fus3p plays the major role in mating, but that Kss1p can function in Fus3p's absence. This perhaps due to the sensitivity of the kinases to phosphorylation: Fus3p can induce a transcriptional response at a low threshold of phosphorylation, while a greater percentage of Kss1p molecules must be phosphorylated in order to effect the same response [72]. Additionally, the cell cycle regulator Far1p is targeted by Fus3p (but not Kss1p), accounting for the reduced synchronization in response to α-factor seen in cells lacking Fus3p [61,71].

The prominent scaffold for the mating pathway is Ste5p, which has no catalytic function but serves to link the kinases of the cascade together at the membrane. The scaffolding role of Ste5p is not passive, that is, Ste5p does not function as a scaffold under basal conditions. Rather, under pheromone stimulation, Ste5p is recruited to the membrane by the G protein βγ subunit [73,74]. The kinases Ste11p, Ste7p, Kss1p, and Fus3p bind to Ste5p, allowing the core MAPK cascade to proceed [75–77]. Further, the binding of Ste11p to Ste5p is necessary for full activation of Ste11p. Ste11p contains an N-terminal inhibitory domain, which sterically hinders the catalytic domain [78]. Ste5p has been shown to bind to this inhibitory domain [75,76,79], and hyperactive Ste11p mutants are only fully active in the presence of Ste5p [80].

Feedback and regulation

In general, yeast is incredibly sensitive to pheromone [72], and some of the earliest studies of mating in yeast focused on the ability to pheromone to inhibit the cell cycle of cells of opposite mating types [81]. Unregulated mating pathway activation is lethal [82,83], and the cells is incentivized to limit pathway activity and resume the cell cycle if pheromone stimulation is not sustained. Consequently, the are several mechanisms which negatively regulate the mating pathway after stimulation. First, Fus3p and Kss1p target and activate a mating pathway modulator Sst2p [84,85]. As mentioned above, the α subunit of the G protein is inhibitory, and when stimulated with pheromone, the α subunit dissociates from the βγ dimer, which initiates signaling [86]. Active Sst2p promotes reassociation of the α subunit with the βγ dimer, thereby limiting pathway activation [85]. Furthermore, the pheromone receptor is internalized and recycled upon binding pheromone [87,88]. This limits mating pathway activity in response to transient exposure to pheromone. Fus3p also targets components of the MAPK cascade, seemingly in an inhibitory manner [89], although the extent and exact function of these phosphorylation events is not known. Finally, MATa cells produce a protease, Bar1p, after pheromone stimulation. Bar1p is secreted and degrades α-factor, thereby limiting stimulation [90–93]. Bar1p is induced by Ste12p as described above [62,63,90]. As a result of these feedback mechanisms, the duration of mating pathway activity is limited, allowing cells to resume the cell cycle if a mating partner is not found [85].

Of course, given the evolutionary importance of mating, the mating pathway is also subject to positive feedback to allow for a robust response if a mating partner is present. This is primarily accomplished through transcriptional induction of mating pathway components. Among the genes induced by pheromone are the pheromone receptor *STE2*, the MAPK *FUS3*, and the mating transcription factor *STE12* itself. Also induced are the pheromone genes *MFA1* and *MFA2*. As mentioned above, the pheromone receptor is internalized following pheromone binding, and induction of additional receptor by Ste12p ensures that the number of unoccupied receptors on the membrane remains high, allowing for

continued signaling if pheromone is present. Positive feedback loops have been shown to improve the stability of pathway activation [94,95]. Finally, production of additional a-factor pheromone promotes mating signaling in the cell's prospective mating partners, increasing the chances of successful fusion [65].

The mating pathway is also subject to regulation from outside the network, specifically by the MAT locus, which controls mating type. The MAT locus is on chromosome III and includes two genes, called *MATA1* and *MATA2* in MATa cells and *MATALPHA1* and *MATALPHA2* in MATα cells. These genes encode proteins, a1, a2, α1 and α2, which are master regulators of mating type. Certain genes related to mating are mating type specific, expressed only in MATa cells or MATα cells. Other genes are haploid specific and are strongly repressed in diploids. Differential expression of these genes is due to the interactions of the MAT genes and with a transcription factor Mcm1p. In MATa cells, Mcm1p binds the promoter of the a-specific genes and induces expression, including the pheromone genes *MFA1* and *MFA2*, the α-factor receptor *STE2* [96]. These same genes are repressed in MATα cells by the α2-Mcm1p complex [97]. In MATα cells, Mcm1p by itself does not activate α-specific genes; rather it forms a complex with α2 in order to induce these genes, including the pheromone genes *MFALPHA1, MFALPHA2,* and the a-factor receptor *STE3* [98,99]. In diploids, the α2-Mcm1p complex represses the a-specific genes, while the a1 binds α2 in order to repress the α-specific genes [100,101]. The same a1-α2 complex represses a third set of genes, the haploid specific genes, which are constitutively expressed in haploids. These genes include mating pathway components: *FAR1*, *FUS3*, *STE4*, and *GPA1* [102]. Because these genes are critical components of the mating pathway, the mating pathway remains inactive in diploids and mating is restricted to haploid cells.

The filamentous growth pathway

Yeast cells undergo a ploidy-specific morphological and behavioral shift upon nitrogen starvation. Diploid cells begin a new polarized budding pattern, in which subsequent daughter cells bud opposite of the previous bud site, producing a filament-like chain of cells, all connected at the cell wall [103]. This type of

growth is known as pseudohyphal growth. Haploid cells also begin polarized budding, but rather than forming filaments, haploid cells starved for nitrogen invade the agar [104]. These phenotypes are controlled by the same signaling network, termed the filamentous growth (FG) pathway, which involves both MAPK and cyclic AMP signaling [103–107]. Here, I will focus on the MAPK portion of the filamentous growth pathway, including its activation and regulation.

Activation

Many of the components of FG pathway signaling have been discussed in the context of the mating and HOG pathways. As in the SHO1 branch of the HOG pathway, FG signaling is initiated by the membrane-bound proteins Sho1p and Msb2p [108,109]. It is currently not known how these proteins sense the changes in nitrogen availability [110]. Upon activation, these proteins activate Cdc42p [108], which consequently activates Ste20p [104,105,111], an activation step shared by the HOG, mating, and FG pathways. The RAS homolog Ras2p also signals to Cdc42p and consequently Ste20p [112]. As in the mating pathway, Ste20p then activates the MAP3K Ste11p, which activates the MAP2K Ste7p, which activates the MAPK Kss1p [104,105]. Unlike the mating pathway, the MAPK Fus3p is not involved, and Fus3p cannot produce invasive growth in *kss1Δ* cells [104]. Interestingly, the filamentous phenotype is not affected by *fus3Δ, kss1Δ*, or *fus3Δ kss1Δ* homozygous deletions in diploids [105].

Like the mating pathway and the HOG pathway, activation of the FG pathway is associated with induction of specific genes, such as *SRD1*, *PGU1*, and *DDR48* [113]. It is worth discussing how filamentation genes are distinguished from pheromone responsive genes at the transcriptional level. As with upstream activation, I am focusing on activation of genes specifically induced by the MAPK portion of the filamentous growth pathway, rather than genes induced by cyclic AMP signaling. Like in mating, Ste12p is a transcription factor responsible for activating filamentation responsive genes [104,105]. Unlike mating, however, Ste12p cannot activate the filamentation responsive genes by itself, it does so in a complex with

a second transcription factor, Tec1p [114,115]. The model for filamentation and pheromone discrimination was proposed by Bardwell, et al. in 1998 [68]. Under basal conditions, the Ste12p-Tec1p complex is bound to the promoter but repressed by Dig1p/Dig2p, where unphosphorylated Kss1p may stabilize the interaction of Ste12p-Tec1p with the repressors. After Kss1p is activated, the repression by Dig1p/Dig2p is relieved and Ste12p is phosphorylated and activated, allowing for induction. These genes are not activated under pheromone induction because active Fus3p phosphorylates Tec1p, targeting it for degradation [116–118]. Additional mechanisms insulating the mating and FG pathways (above the transcriptional level) are described below.

Feedback and regulation

Compared to the HOG and mating pathways, relatively little is known about feedback and regulation of the FG pathway. It is known that Msb2p, one of the upstream activators of the FG pathway, and Kss1p, the FG MAPK, are induced by the FG pathway [108]. This, like the induction of Ste12p and Fus3p in the mating pathway, may be a form of positive feedback. It is also worth noting that the filamentation response requires synergistic activation of multiple signaling pathways. For example, the standard strain S288C cannot become filamentous due to a defect in cyclic AMP signaling [119]. It has been suggested that the cyclic AMP pathway itself directly regulates the FG MAPK pathway through the interaction of Ras2p with Cdc42p [112]. This is in contrast to the theory that Ras2p is an intermediate step between Msb2p activation and Cdc42p activation. The evidence for this is that Msb2p directly interacts with Cdc42p, independent of Ras2p [108], which suggests that signal does not need to pass through Ras2p. Despite this, Ras2p can activate Cdc42p, as shown by experiments using constitutively active Ras2p alleles [112]. More work is necessary to understand how the FG pathway is regulated, particularly in terms of positive and negative feedback onto the pathway and its relation to the cyclic AMP signaling pathway.

INSULATION OF THE MAPK NETWORKS

As we have seen, the yeast MAPK networks are intricately connected. The MAPK cascades of the mating pathway and the FG pathway are nearly identical, and the upstream activation of the FG pathway shares many components with upstream activation of the SHO1 branch of the HOG pathway. Further, the three pathways share a specific activation step: Ste20p phosphorylates and activates the MAP3K Ste11p. After signal flows to Ste11p, it can flow to either Pbs2p in the HOG pathway, or Ste7p in the mating and FG pathways. Ste7p itself can phosphorylate two MAPKs: Fus3p and Kss1p. Both kinases are active (with Fus3p more strongly active) under the mating pathway, but only Kss1p is active under the FG pathway. How can the cells distinguish between the different types of stimulation and differentially activate the correct downstream components? After all, given the shared connections, one would expect signal to leak from one pathway into the others, a phenomenon known as crosstalk. For example, after an osmotic shock, active Ste11p could feasibly activate Ste7p instead of Pbs2p. In this section I will describe two prominent mechanisms for pathway insulation, both of which have an extensive body of literature elucidating the necessary factors for maintaining insulation. The first is active inhibition of mating/FG pathway activation by the HOG pathway MAPK Hog1p. The second is insulation via differential binding of scaffolding proteins.

Active inhibition by Hog1p

The role of Hog1p in maintaining separation between HOG pathway and mating/FG pathway signaling was discovered by Sean O'Rourke and Ira Herskowitz in 1998. In their landmark paper, the showed that osmotic stress causes induction of a mating pathway reporter in *hog1Δ* cells or in cells with a catalytically inactive Hog1p [109]. This has been reproduced with several different Hog1p kinase-dead mutations [120,121], as well as with an engineered Hog1p susceptible to inhibition by an ATP analog [121,122]. Further supporting the theory that HOG pathway activity suppresses the mating pathway, it has been shown that co-stimulating cells with pheromone and sorbitol both reduces activation of the mating

pathway and delays the transcriptional response [123,124]. It has also been shown that rapidly oscillating osmotic stress, which hyperactivates the HOG pathway, can cause crosstalk into the FG pathway, though the authors were unable to show leakage into the mating pathway [44]. The precise target that Hog1p phosphorylates in order to suppress the mating pathway is not fully understood, but Ste50p and Rck2p have been suggested [124,125].

Ste50p is an adaptor protein that connects Ste20p with the MAP3K Ste11p. It has been implicated in activation of the HOG pathway, the mating pathway, and the FG pathway, and it appears to have a regulatory role as well as a scaffolding role. Ste50p consist of a sterile alpha motif (SAM) domain and a RAS activating (RA) domain. The SAM domain binds Ste11p [126], and the RA domain binds Cdc42 [33]. It is thought that this binding brings Ste11p to the membrane and into proximity with the Cdc42-Ste20p complex, allowing Ste20p to phosphorylate and signal through the MAPK cascade [23,26,33,127]. Ste50p also modulates Ste11p, which has autophosphorylation activity, by binding an N-terminal inhibitory domain, allowing the catalytic site to become active [78]. Ste50p is not necessary to initiate mating pathway signaling, though it is important for sustaining activity through the pathway [128]. Mutations have been identified which differentially disrupt signaling through the HOG and mating pathways, with some mutations allowing HOG but not mating signaling and vice versa [25,129]. Further, Hog1p targets and phosphorylates Ste50p and phosphosite mutations have been shown to increase crosstalk from the HOG pathway into the mating pathway [125], although this result has been disputed [130]. Uncertainty about the specific mechanism notwithstanding, it is clear that the differential involvement in the HOG, mating, and FG pathways plays an important role in insulating and maintaining specificity.

Rck2p is a MAPK-activated protein kinase and is a downstream target of Hog1p [131]. It is thought that Rck2p modulates translation as part of the response to stress [132,133]. The role Rck2p plays in insulating the HOG and mating/FG pathways is less clear, since insulation is typically observed at the level of transcription (e.g., by a lack of induction of a *FUS1*-lacZ reporter under osmostress). One model,

proposed by Nagiec and Dohlman, is that Rck2p prevents the Ste12p-mediated production of additional Fus3p, thereby interrupting positive feedback necessary for strong mating pathway activity [124]. Rck2p's role in preventing crosstalk into FG targets may be similar—FG pathway components *KSS1* and *MSB2* have been shown to be induced by the FG pathway [108]—but this has not been directly tested. In fact, one study showed that Rck2p is not required to insulate the HOG pathway from the FG pathway [130]. Further work is necessary to determine the exact role Rck2p plays in the HOG response, and specifically how Rck2p interrupts crosstalk in the mating/FG pathways.

Insulation via scaffolding

An alternative mechanism maintaining pathway insulation is differential activation of scaffolding proteins. Activation of the MAPK pathways requires many proteins in close proximity in order to transmit the signal from the membrane-bound receptor to the effector proteins. Scaffold proteins facilitate this by binding multiple signaling kinases and positioning the phosphosites near the active sites. Although many steps of pathway activation may involve scaffolding proteins, I will focus on the scaffold which facilitates the core MAPK cascade; that is, the scaffold which binds the MAP3K, MAP2K, and MAPK. In the HOG pathway, this scaffold is Pbs2p, which is also the MAP2K [29], and in the mating pathway, it is Ste5p [74–76,79,134]. No such protein has been identified for the FG pathway; in particular, Ste5p has been shown not to be involved in FG pathway activation, despite the FG pathway's close similarity to the mating pathway [135]. These scaffolds play an integral role in pathway specificity.

As described above, the mating pathway scaffold Ste5p is necessary for activation of the mating pathway. It is thought that differential recruitment of Ste5p to the membrane allows the cell to distinguish between a pheromone response and an FG response, thereby allowing it to induce only the pheromone responsive genes or the filamentation responsive genes respectively [76,135,136]. According to this theory, when pheromone is present Ste7p and Fus3p are bound to Ste5p and localized to the membrane, allowing signal to flow to Fus3p, the primary activator of the mating pathway. Under nutrient starvation,

Ste5p is not localized to the membrane, and signal therefore flows from free Ste7p to Kss1p, the only MAPK active in the FG pathway [135]. It has further been shown that differential binding of Fus3p and Kss1p to Ste5p allows for rapid and graded Kss1p activation, while Fus3p activation is more switch-like [137]. It has also been shown that Ste5p contains an autoinhibitory domain which inhibits activation of Fus3p, and that this interaction is blocked under pheromone stimulation, providing another mechanism by which Fus3p can be specifically activated only during pheromone stimulation [138,139].

Scaffolding has also been proposed as a mechanism insulating the HOG pathway from the mating/FG pathways, specifically because the mating pathway and the HOG pathway have different scaffolds for the core MAPK cascade [140–142]. A powerful method to study this mechanism is by creating designer kinases and scaffolds, which force association between specific kinases and substrates. Using this system, it has been shown that signal can be directed to a specific pathway, regardless of the input [140,141]. It has also been shown that other MAP2Ks can functionally replace Ste7p in mating signaling as long as the MAP2Ks are tethered to the Ste5p scaffold [142]. These experiments provide strong evidence that scaffolding is one of the critical factors responsible for maintaining pathway insulation. However, they do not explain the active role Hog1p plays in suppressing crosstalk [109], especially because activation of the FG pathway does not require a scaffold [135]. More research is needed in order to determine whether scaffolding can insulate the HOG pathway from the FG pathway, and how suppression by Hog1p interacts with scaffolding insulation.

STRAINS USED TO STUDY MAPK NETWORKS

How does the strain background influence signaling? There exist hundreds of yeast strains, laboratory and wild, that have been generated with unique crosses and under unique environmental pressures, and it is true in general that gene expression varies by strain background [66], as does signaling output (see, for example, [119,143,144]). Yeast MAPK networks have a long history—several genes necessary for mating

were identified in a 1980 screen [145]—and it is impossible to fully characterize the strains used in all important experiments, particularly because many early papers do not provide a full history of the strain backgrounds used [146]. This is particularly true of the mating pathway, studies of which use many strains of unknown lineages. I will provide an overview of a few strain backgrounds used to study MAPK-related signaling in yeast, including strain features potentially relevant to signaling.

The HOG pathway has generally been studied in the standard strain background S288C. This is desirable because the history of S288C is well documented [146] and S288C derivatives were used for the yeast genome sequencing project [147]. The first study identifying the HOG pathway (showing signal transduction between Pbs2p and Hog1p) used S288C derivatives [13]. Subsequently, studies identifying the SLN1 branch [10], the SHO1 branch [12], and the connections between Ste11p and Pbs2p and Ssk2p/Ssk22p and Pbs2p [29,30] also used S288C derivatives. It is worth acknowledging potential consequences of studying osmostress in S288C. The aquaporins Aqy1p and Aqy2p are known to be nonfunctional in the S288C background [144,148,149] and this has been directly linked to a loss of fitness under oscillating hypo- and hyperosmotic stress [148,149]. The effect of this on HOG pathway activation has not been explored, nor has a detailed comparison of HOG pathway dynamics in different strains.

Studies of the FG pathway do not use S288C for a practical reason—S288C is filamentation deficient and does not display either a pseudohyphal (in diploids) or invasive (in haploids) phenotype [103]. In contrast, the Σ1278b background readily displays a filamentous phenotype [103–105], and it is the strain of choice for FG pathway studies. Σ1278b was constructed in the 1960s and is thought to share ancestors with S288C [146,150]. Despite this, genome sequencing shows significant divergence from the reference genome and only 46% of the open reading frames are identical to the S288C reference [151]. The specific filamentation defect found in S288C has been mapped to a non-functional transcription factor Flo8p [119] which is activated by cyclic AMP signaling [152]. Although this defect is unrelated to MAPK activation, it raises the question of whether the loss of selective pressure to maintain filamentation under

stress conditions in S288C or one of its ancestors affects activation of the FG MAPK pathway. It is also possible that pressure to maintain the mating pathway in S288C is sufficient to maintain the FG pathway, given that the FG pathway and mating use many of the same components.

One important strain in yeast MAPK signaling is the EG123 background. Very few details about this strain are known. It was first reported in the literature in 1984, and although the paper describes its genotype, it does not give information about its ancestry or construction [153]. This was unfortunately common at the time [146]. After its use in the original 1984 paper, it was used in many studies of the mating pathway, for example in references [154–158] among others. Perhaps most importantly, it was used in O'Rourke and Herkskowitz's landmark study establishing that the HOG pathway suppresses crosstalk into the mating pathway [109]. Consequently, it has been used in several studies investigating the role of Hog1p in suppressing crosstalk [17,120,121]. Presumably, this strain is, like S288C, filamentation deficient, because O'Rourke and Herskowitz used a Σ1278b-background strain to investigate the role of Hog1p in preventing crosstalk into the FG pathway [109]. However, to my knowledge the strain has not been sequenced and details of its ancestry have not been compiled or made available. Fortunately, Hog1's role in suppressing crosstalk does not appear to be an artifact of the EG123 background. O'Rourke and Herskowitz's results have been replicated in many strain backgrounds, including S288C and Σ1278b [124,130].

CONCLUSIONS

The yeast MAPK networks are a model system for signal transduction in eukaryotes. The three pathways discussed have distinct activation mechanisms and signal types, from a peptide binding a GPCR in the mating pathway, to the biophysical change of water loss in the HOG pathway. The HOG pathway is a particularly useful model for parallel activation branches and adaptation, the mating pathway is a model for G protein activated signaling and switch-like activation, and the FG pathway and mating pathways are

an excellent example of how distinct stimuli can signal through the same subset of signaling molecules yet still maintain separate response. Finally, the pathways are regulated with many levels of feedback, and are models for how signaling networks interface with general transcriptional control, the cell cycle, and other (non-MAPK) signaling pathways.

Many studies have elucidated the structures of these pathways and their mechanisms of activation. A common thread linking the pathways is the activation of Ste11p by the Cdc42p-Ste20p complex. In the mating pathway, pheromone binding the receptor initiates signaling to Ste20p via G proteins; in the HOG and FG pathways, the signaling is done by membrane-bound sensors. These mechanisms converge on Ste11p, and Ste11p could be activated by multiple signaling pathways at once. How can the cell faithfully transmit signals when the three pathways share this connection? The mechanisms have yet to be fully determined, but active suppression of the mating/FG pathways by the HOG pathway and the differential role of scaffolding proteins certainly play major roles. From these pathways, we learn fundamentals of how cells coordinate signals, especially in the context of needing to multiplex signals through a limited set of signaling molecules.

One important confounding factor in the study of signaling networks is the strain background, which affects gene expression and (through mutations) protein function. While study of the HOG pathway generally uses the S288C background, S288C cannot display the filamentous phenotype due to a defect in cyclic AMP signaling. Therefore, study of the FG pathway is done in a different laboratory strain, Σ1278b, which is filamentation competent. How did the loss of filamentation in S288C affect the interplay between the HOG and FG pathways? This question is especially salient because the HOG and FG pathways share several upstream activators (Sho1p, Msb2p, Cdc42p, Ste20p, and Ste11p). Finally, the seminal paper showing that Hog1p suppresses crosstalk used an obscure strain background, EG123, whose ancestry was not described when it was introduced [153]. This strain has not (to my knowledge) been sequenced, so it is unclear where it fits in the landscape of strain genotypes and phenotypes.

Signaling is a fundamental cellular activity, and it is important to understand how cells organize their signaling networks in order to respond correctly to a given stimulus. Studying the yeast MAPK networks provides the opportunity to understand how genotype maps to phenotype and how differences in expression contribute to differences in signal flow. The decades of research into yeast MAPK networks gives us excellent knowledge of the network structures to use as a scaffold upon which to study the system as a whole. These studies could be conducted in a targeted manner – mutating specific genes or titrating a particular component – but existing yeast strains signal differently and provide an opportunity to study this problem in a more natural system, where the system evolved to accommodate the need to respond to multiple stimuli. In the following chapters I will explore differences in signaling between two laboratory yeast strains—YPH499 (which is congenic to S288C, though it has significantly more genetic variation than strains directly derived from S288C) [159,160], and Σ1278b, described above—and investigate potential genetic causes for these differences. In doing so, I show how changes to the cellular context, such as differences in expression or point mutations, can change the behavior of MAPK signaling networks, despite ostensibly the same components and reactions.

REFERENCES

1 Widmann C, Gibson S, Jarpe MB & Johnson GL (1999) Mitogen-Activated Protein Kinase: Conservation of a Three-Kinase Module From Yeast to Human. *Physiological Reviews* **79**, 143–180.

2 Chen RE & Thorner J (2007) Function and regulation in MAPK signaling pathways: Lessons learned from the yeast Saccharomyces cerevisiae. *Biochimica et Biophysica Acta (BBA) - Molecular Cell Research* **1773**, 1311–1340.

3 Hohmann S (2002) Osmotic Stress Signaling and Osmoadaptation in Yeasts. *Microbiol Mol Biol Rev* **66**, 300–372.

4 Posas F, Chambers JR, Heyman JA, Hoeffler JP, Nadal E de & Ariño J (2000) The Transcriptional Response of Yeast to Saline Stress. *J Biol Chem* **275**, 17249–17255.

5 Tamás MJ, Rep M, Thevelein JM & Hohmann S (2000) Stimulation of the yeast high osmolarity glycerol (HOG) pathway: evidence for a signal generated by a change in turgor rather than by water stress. *FEBS Letters* **472**, 159–165.

6 Muzzey D, Gómez-Uribe CA, Mettetal JT & van Oudenaarden A (2009) A Systems-Level Analysis of Perfect Adaptation in Yeast Osmoregulation. *Cell* **138**, 160–171.

7 Miermont A, Waharte F, Hu S, McClean MN, Bottani S, Léon S & Hersen P (2013) Severe osmotic compression triggers a slowdown of intracellular signaling, which can be explained by molecular crowding. *PNAS* **110**, 5725–5730.

8 Millero FJ, Feistel R, Wright DG & McDougall TJ (2008) The composition of Standard Seawater and the definition of the Reference-Composition Salinity Scale. *Deep Sea Research Part I: Oceanographic Research Papers* **55**, 50–72.

9 Heinisch JJ & Rodicio R (2017) Stress Responses in Wine Yeast. In *Biology of Microorganisms on Grapes, in Must and in Wine* (König H, Unden G, & Fröhlich J, eds), pp. 377–395. Springer International Publishing, Cham.

10 Maeda T, Wurgler-Murphy SM & Saito H (1994) A two-component system that regulates an osmosensing MAP kinase cascade in yeast. *Nature* **369**, 242–245.

11 Posas F & Saito H (1998) Activation of the yeast SSK2 MAP kinase kinase kinase by the SSK1 two-component response regulator. *EMBO J* **17**, 1385–1394.

12 Maeda T, Takekawa M & Saito H (1995) Activation of yeast PBS2 MAPKK by MAPKKKs or by binding of an SH3-containing osmosensor. *Science* **269**, 554–558.

13 Brewster JL, Valoir T de, Dwyer ND, Winter E & Gustin MC (1993) An osmosensing signal transduction pathway in yeast. *Science* **259**, 1760–1763.

14 Hersen P, McClean MN, Mahadevan L & Ramanathan S (2008) Signal processing by the HOG MAP kinase pathway. *Proceedings of the National Academy of Sciences* **105**, 7165–7170.

15 Macia J, Regot S, Peeters T, Conde N, Solé R & Posas F (2009) Dynamic Signaling in the Hog1 MAPK Pathway Relies on High Basal Signal Transduction. *Sci Signal* **2**, ra13–ra13.

16 Granados AA, Crane MM, Montano-Gutierrez LF, Tanaka RJ, Voliotis M & Swain PS (2017) Distributing tasks via multiple input pathways increases cellular survival in stress. *eLife Sciences* **6**, e21415.

17 O'Rourke SM & Herskowitz I (2002) A third osmosensing branch in Saccharomyces cerevisiae requires the Msb2 protein and functions in parallel with the Sho1 branch. *Mol Cell Biol* **22**, 4739–4749.

18 Tanaka K, Tatebayashi K, Nishimura A, Yamamoto K, Yang H-Y & Saito H (2014) Yeast osmosensors Hkr1 and Msb2 activate the Hog1 MAPK cascade by different mechanisms. *Science Signaling* **7**.

19 Zuzuarregui A, Li T, Friedmann C, Ammerer G & Alepuz P (2015) Msb2 is a Ste11 membrane concentrator required for full activation of the HOG pathway. *Biochimica et Biophysica Acta - Gene Regulatory Mechanisms* **1849**, 722–730.

20 Tatebayashi K, Yamamoto K, Nagoya M, Takayama T, Nishimura A, Sakurai M, Momma T & Saito H (2015) Osmosensing and scaffolding functions of the oligomeric four-transmembrane domain osmosensor Sho1. *Nature Communications* **6**, 6975.

21 Raitt DC, Posas F & Saito H (2000) Yeast Cdc42 GTPase and Ste20 PAK-like kinase regulate Sho1-dependent activation of the Hog1 MAPK pathway. *EMBO J* **19**, 4623–4631.

22 Wu C, Whiteway M, Thomas DY & Leberer E (1995) Molecular Characterization of Ste20p, a Potential Mitogen-activated Protein or Extracellular Signal-regulated Kinase Kinase (MEK) Kinase Kinase from Saccharomyces cerevisiae(∗). *Journal of Biological Chemistry* **270**, 15984–15992.

23 Wu C, Jansen G, Zhang J, Thomas DY & Whiteway M (2006) Adaptor protein Ste50p links the Ste11p MEKK to the HOG pathway through plasma membrane association. *Genes Dev* **20**, 734–746.

24 Ramezani Rad M, Jansen G, Bühring F & Hollenberg CP (1998) Ste50p is involved in regulating filamentous growth in the yeast Saccharomyces cerevisiae and associates with Ste11p. *Mol Gen Genet* **259**, 29–38.

25 Jansen G, Bühring F, Hollenberg CP & Ramezani Rad M (2001) Mutations in the SAM domain of STE5O differentially influence the MAPK-mediated pathways for mating, filamentous growth and osmotolerance in Saccharomyces cerevisiae. *Mol Gen Genet* **265**, 102–117.

26 Posas F, Witten EA & Saito H (1998) Requirement of STE50 for osmostress-induced activation of the STE11 mitogen-activated protein kinase kinase kinase in the high-osmolarity glycerol response pathway. *Mol Cell Biol* **18**, 5788–5796.

27 Bardwell L (2006) Mechanisms of MAPK signalling specificity. *Biochem Soc Trans* **34**, 837–841.

28 Witzel F, Maddison L & Blüthgen N (2012) How scaffolds shape MAPK signaling: what we know and opportunities for systems approaches. *Frontiers in Physiology* **3**.

29 Posas F & Saito H (1997) Osmotic activation of the HOG MAPK pathway via Ste11p MAPKKK: Scaffold role of Pbs2p MAPKK. *SCIENCE* **276**, 1702–1708.

30 Tatebayashi K, Takekawa M & Saito H (2003) A docking site determining specificity of Pbs2 MAPKK for Ssk2/Ssk22 MAPKKKs in the yeast HOG pathway. *EMBO J* **22**, 3624–3634.

31 Nishimura A, Yamamoto K, Oyama M, Kozuka-Hata H, Saito H & Tatebayashi K (2016) Scaffold Protein Ahk1, Which Associates with Hkr1, Sho1, Ste11, and Pbs2, Inhibits Cross Talk Signaling from the Hkr1 Osmosensor to the Kss1 Mitogen-Activated Protein Kinase. *Mol Cell Biol* **36**, 1109–1123.

32 Tatebayashi K, Yamamoto K, Tanaka K, Tomida T, Maruoka T, Kasukawa E & Saito H (2006) Adaptor functions of Cdc42, Ste50, and Sho1 in the yeast osmoregulatory HOG MAPK pathway. *EMBO J* **25**, 3033–3044.

33 Truckses DM, Bloomekatz JE & Thorner J (2006) The RA domain of Ste50 adaptor protein is required for delivery of ste11 to the plasma membrane in the filamentous growth signaling pathway of the yeast Saccharomyces cerevisiae. *Mol Cell Biol* **26**, 912–928.

34 Alepuz PM, de Nadal E, Zapater M, Ammerer G & Posas F (2003) Osmostress-induced transcription by Hot1 depends on a Hog1-mediated recruitment of the RNA Pol II. *EMBO J* **22**, 2433–2442.

35 Cook KE & O'Shea EK (2012) Hog1 controls global reallocation of RNA Pol II upon osmotic shock in Saccharomyces cerevisiae. *G3 (Bethesda)* **2**, 1129–1136.

36 Nadal-Ribelles M, Conde N, Flores O, González-Vallinas J, Eyras E, Orozco M, de Nadal E & Posas F (2012) Hog1 bypasses stress-mediated down-regulation of transcription by RNA polymerase II redistribution and chromatin remodeling. *Genome Biology* **13**, R106.

37 Rep M, Krantz M, Thevelein JM & Hohmann S (2000) The Transcriptional Response of Saccharomyces cerevisiae to Osmotic Shock. *J Biol Chem* **275**, 8290–8300.

38 Albertyn J, Hohmann S, Thevelein JM & Prior BA (1994) GPD1, which encodes glycerol-3-phosphate dehydrogenase, is essential for growth under osmotic stress in Saccharomyces cerevisiae, and its expression is regulated by the high-osmolarity glycerol response pathway. *Mol Cell Biol* **14**, 4135–4144.

39 Nevoigt E & Stahl U (1996) Reduced pyruvate decarboxylase and increased glycerol-3-phosphate dehydrogenase [NAD+] levels enhance glycerol production in Saccharomyces cerevisiae. *Yeast* **12**, 1331–1337.

40 Ferreira C, van Voorst F, Martins A, Neves L, Oliveira R, Kielland-Brandt MC, Lucas C & Brandt A (2005) A Member of the Sugar Transporter Family, Stl1p Is the Glycerol/H+ Symporter in Saccharomyces cerevisiae. *MBoC* **16**, 2068–2076.

41 Lee J, Reiter W, Dohnal I, Gregori C, Beese-Sims S, Kuchler K, Ammerer G & Levin DE (2013) MAPK Hog1 closes the S. cerevisiae glycerol channel Fps1 by phosphorylating and displacing its positive regulators. *Genes Dev* **27**, 2590–2601.

42 Klipp E, Nordlander B, Krüger R, Gennemark P & Hohmann S (2005) Integrative model of the response of yeast to osmotic shock. *Nat Biotechnol* **23**, 975–982.

43 Reed RH, Chudek JA, Foster R & Gadd GM (1987) Osmotic significance of glycerol accumulation in exponentially growing yeasts. *Appl Environ Microbiol* **53**, 2119–2123.

44 Mitchell A, Wei P & Lim WA (2015) Oscillatory stress stimulation uncovers an Achilles' heel of the yeast MAPK signaling network. *Science* **350**, 1379–1383.

45 Mettetal JT, Muzzey D, Gómez-Uribe C & Oudenaarden A van (2008) The Frequency Dependence of Osmo-Adaptation in *Saccharomyces cerevisiae*. *Science* **319**, 482–484.

46 Wurgler-Murphy SM, Maeda T, Witten EA & Saito H (1997) Regulation of the Saccharomyces cerevisiae HOG1 mitogen-activated protein kinase by the PTP2 and PTP3 protein tyrosine phosphatases. *Mol Cell Biol* **17**, 1289–1297.

47 Mattison CP & Ota IM (2000) Two protein tyrosine phosphatases, Ptp2 and Ptp3, modulate the subcellular localization of the Hog1 MAP kinase in yeast. *Genes Dev* **14**, 1229–1235.

48 Jacoby T, Flanagan H, Faykin A, Seto AG, Mattison C & Ota I (1997) Two Protein-tyrosine Phosphatases Inactivate the Osmotic Stress Response Pathway in Yeast by Targeting the Mitogen-activated Protein Kinase, Hog1 *. *Journal of Biological Chemistry* **272**, 17749–17755.

49 Warmka J, Hanneman J, Lee J, Amin D & Ota I (2001) Ptc1, a Type 2C Ser/Thr Phosphatase, Inactivates the HOG Pathway by Dephosphorylating the Mitogen-Activated Protein Kinase Hog1. *Mol Cell Biol* **21**, 51–60.

50 Sharifian H, Lampert F, Stojanovski K, Regot S, Vaga S, Buser R, Lee SS, Koeppl H, Posas F, Pelet S & Peter M (2015) Parallel feedback loops control the basal activity of the HOG MAPK signaling cascade. *Integrative Biology* **7**, 412–422.

51 Hao N, Behar M, Parnell SC, Torres MP, Borchers CH, Elston TimothyC & Dohlman HG (2007) A Systems-Biology Analysis of Feedback Inhibition in the Sho1 Osmotic-Stress-Response Pathway. *Curr Biol* **17**, 659–667.

52 Jenness DD, Burkholder AC & Hartwell LH (1983) Binding of α-factor pheromone to yeast a cells: Chemical and genetic evidence for an α-factor receptor. *Cell* **35**, 521–529.

53 Blumer KJ & Thorner J (1990) Beta and gamma subunits of a yeast guanine nucleotide-binding protein are not essential for membrane association of the alpha subunit but are required for receptor coupling. *Proceedings of the National Academy of Sciences* **87**, 4363–4367.

54 Leberer E, Dignard D, Harcus D, Thomas DY & Whiteway M (1992) The protein kinase homologue Ste20p is required to link the yeast pheromone response G-protein beta gamma subunits to downstream signalling components. *EMBO J* **11**, 4815–4824.

55 Nern A & Arkowitz RA (1999) A Cdc24p-Far1p-Gβγ Protein Complex Required for Yeast Orientation during Mating. *Journal of Cell Biology* **144**, 1187–1202.

56 Butty A-C, Pryciak PM, Huang LS, Herskowitz I & Peter M (1998) The Role of Far1p in Linking the Heterotrimeric G Protein to Polarity Establishment Proteins During Yeast Mating. *Science* **282**, 1511–1516.

57 Leberer E, Wu C, Leeuw T, Fourest-Lieuvin A, Segall JE & Thomas DY (1997) Functional characterization of the Cdc42p binding domain of yeast Ste20p protein kinase. *EMBO J* **16**, 83–97.
58 Lamson RE, Winters MJ & Pryciak PM (2002) Cdc42 Regulation of Kinase Activity and Signaling by the Yeast p21-Activated Kinase Ste20. *Molecular and Cellular Biology* **22**, 2939–2951.
59 Ash J, Wu C, Larocque R, Jamal M, Stevens W, Osborne M, Thomas DY & Whiteway M (2003) Genetic Analysis of the Interface Between Cdc42p and the CRIB Domain of Ste20p in Saccharomyces cerevisiae. *Genetics* **163**, 9–20.
60 Bardwell L (2005) A walk-through of the yeast mating pheromone response pathway. *Peptides* **26**, 339–350.
61 Elion EA, Satterberg B & Kranz JE (1993) FUS3 phosphorylates multiple components of the mating signal transduction cascade: evidence for STE12 and FAR1. *MBoC* **4**, 495–510.
62 Hagen DC, McCaffrey G & Sprague GF (1991) Pheromone response elements are necessary and sufficient for basal and pheromone-induced transcription of the FUS1 gene of Saccharomyces cerevisiae. *Molecular and Cellular Biology* **11**, 2952–2961.
63 Kronstad JW, Holly JA & MacKay VL (1987) A yeast operator overlaps an upstream activation site. *Cell* **50**, 369–377.
64 Hartig A, Holly J, Saari G & MacKay VL (1986) Multiple regulation of STE2, a mating-type-specific gene of Saccharomyces cerevisiae. *Mol Cell Biol* **6**, 2106–2114.
65 Ren B, Robert F, Wyrick JJ, Aparicio O, Jennings EG, Simon I, Zeitlinger J, Schreiber J, Hannett N, Kanin E, Volkert TL, Wilson CJ, Bell SP & Young RA (2000) Genome-Wide Location and Function of DNA Binding Proteins. *Science* **290**, 2306–2309.
66 Roberts CJ, Nelson B, Marton MJ, Stoughton R, Meyer MR, Bennett HA, He YD, Dai H, Walker WL, Hughes TR, Tyers M, Boone C & Friend † Stephen H. (2000) Signaling and Circuitry of Multiple MAPK Pathways Revealed by a Matrix of Global Gene Expression Profiles. *Science* **287**, 873–880.
67 Olson KA, Nelson C, Tai G, Hung W, Yong C, Astell C & Sadowski I (2000) Two Regulators of Ste12p Inhibit Pheromone-Responsive Transcription by Separate Mechanisms. *Molecular and Cellular Biology* **20**, 4199–4209.
68 Bardwell L, Cook JG, Zhu-Shimoni JX, Voora D & Thorner J (1998) Differential regulation of transcription: Repression by unactivated mitogen-activated protein kinase Kss1 requires the Dig1 and Dig2 proteins. *Proceedings of the National Academy of Sciences* **95**, 15400–15405.
69 Tedford K, Kim S, Sa D, Stevens K & Tyers M (1997) Regulation of the mating pheromone and invasive growth responses in yeast by two MAP kinase substrates. *Current Biology* **7**, 228–238.
70 Bardwell L, Cook JG, Voora D, Baggott DM, Martinez AR & Thorner J (1998) Repression of yeast Ste12 transcription factor by direct binding of unphosphorylated Kss1 MAPK and its regulation by the Ste7 MEK. *Genes Dev* **12**, 2887–2898.
71 Elion EA, Brill JA & Fink GR (1991) Functional Redundancy in the Yeast Cell Cycle: FUS3 and KSS1 Have Both Overlapping and Unique Functions. *Cold Spring Harbor Symposia on Quantitative Biology* **56**, 41–49.
72 Winters MJ & Pryciak PM (2018) Analysis of the thresholds for transcriptional activation by the yeast MAP kinases Fus3 and Kss1. *Molecular Biology of the Cell* **29**, 669–682.
73 Dowell SJ, Bishop AL, Dyos SL, Brown AJ & Whiteway MS (1998) Mapping of a Yeast G Protein βγ Signaling Interaction. *Genetics* **150**, 1407–1417.
74 Pryciak PM & Huntress FA (1998) Membrane recruitment of the kinase cascade scaffold protein Ste5 by the Gβγ complex underlies activation of the yeast pheromone response pathway. *Genes and Development* **12**, 2684–2697.
75 Choi KY, Satterberg B, Lyons DM & Elion EA (1994) Ste5 tethers multiple protein kinases in the MAP kinase cascade required for mating in S. cerevisiae. *Cell* **78**, 499–512.

76 Marcus S, Polverino A, Barr M & Wigler M (1994) Complexes between STE5 and components of the pheromone-responsive mitogen-activated protein kinase module. *Proc Natl Acad Sci U S A* **91**, 7762–7766.

77 Bardwell AJ, Flatauer LJ, Matsukuma K, Thorner J & Bardwell L (2001) A conserved docking site in MEKs mediates high-affinity binding to MAP kinases and cooperates with a scaffold protein to enhance signal transmission. *J Biol Chem* **276**, 10374–10386.

78 Wu C, Leberer E, Thomas DY & Whiteway M (1999) Functional Characterization of the Interaction of Ste50p with Ste11p MAPKKK in Saccharomyces cerevisiae. *MBoC* **10**, 2425–2440.

79 Printen JA & Sprague Jr. GF (1994) Protein-protein interactions in the yeast pheromone response pathway: Ste5p interacts with all members of the MAP kinase cascade. *GENETICS* **138**, 609–619.

80 Stevenson BJ, Rhodes N, Errede B & Sprague Jr. GF (1992) Constitutive mutants of the protein kinase STE11 activate the yeast pheromone response pathway in the absence of the G protein. *Genes Dev* **6**, 1293–1304.

81 Duntze W, MacKay V & Manney TR (1970) Saccharomyces cerevisiae: A Diffusible Sex Factor. *Science*.

82 Chan RK & Otte CA (1982) Physiological characterization of Saccharomyces cerevisiae mutants supersensitive to G1 arrest by a factor and alpha factor pheromones. *Molecular and Cellular Biology* **2**, 21–29.

83 Chan RK & Otte CA (1982) Isolation and genetic analysis of Saccharomyces cerevisiae mutants supersensitive to G1 arrest by a factor and alpha factor pheromones. *Mol Cell Biol* **2**, 11–20.

84 Garrison TR, Zhang Y, Pausch M, Apanovitch D, Aebersold R & Dohlman HG (1999) Feedback Phosphorylation of an RGS Protein by MAP Kinase in Yeast. *Journal of Biological Chemistry* **274**, 36387–36391.

85 Dohlman HG, Song J, Ma D, Courchesne WE & Thorner J (1996) Sst2, a negative regulator of pheromone signaling in the yeast Saccharomyces cerevisiae: expression, localization, and genetic interaction and physical association with Gpa1 (the G-protein alpha subunit). *Molecular and Cellular Biology* **16**, 5194–5209.

86 Apanovitch DM, Slep KC, Sigler PB & Dohlman HG (1998) Sst2 is a GTPase-activating protein for Gpa1: purification and characterization of a cognate RGS-Galpha protein pair in yeast. *Biochemistry* **37**, 4815–4822.

87 Jenness DD & Spatrick P (1986) Down regulation of the alpha-factor pheromone receptor in S. cerevisiae. *Cell* **46**, 345–353.

88 Chen L & Davis NG (2000) Recycling of the Yeast a-Factor Receptor. *J Cell Biol* **151**, 731–738.

89 Yu RC, Pesce CG, Colman-Lerner A, Lok L, Pincus D, Serra E, Holl M, Benjamin K, Gordon A & Brent R (2008) Negative feedback that improves information transmission in yeast signalling. *Nature* **456**, 755–761.

90 Manney TR (1983) Expression of the BAR1 gene in Saccharomyces cerevisiae: induction by the alpha mating pheromone of an activity associated with a secreted protein. *Journal of Bacteriology* **155**, 291–301.

91 Ciejek E & Thorner J (1979) Recovery of S. cerevisiae a cells from G1 arrest by α factor pheromone requires endopeptidase action. *Cell* **18**, 623–635.

92 Ballensiefen W & Schmitt HD (1997) Periplasmic Barl Protease of Saccharomyces Cerevisiae is Active Before Reaching its Extracellular Destination. *European Journal of Biochemistry* **247**, 142–147.

93 MacKay VL, Welch SK, Insley MY, Manney TR, Holly J, Saari GC & Parker ML (1988) The Saccharomyces cerevisiae BAR1 gene encodes an exported protein with homology to pepsin. *Proceedings of the National Academy of Sciences* **85**, 55–59.

94 Ingolia NT & Murray AW (2007) Positive-Feedback Loops as a Flexible Biological Module. *Current Biology* **17**, 668–677.

95 Takahashi S & Pryciak PM (2008) Membrane Localization of Scaffold Proteins Promotes Graded Signaling in the Yeast MAP Kinase Cascade. *Curr Biol* **18**, 1184–1191.
96 Elble R & Tye BK (1991) Both activation and repression of a-mating-type-specific genes in yeast require transcription factor Mcm1. *Proceedings of the National Academy of Sciences* **88**, 10966–10970.
97 Smith DL & Johnson AD (1992) A molecular mechanism for combinatorial control in yeast: MCM1 protein sets the spacing and orientation of the homeodomains of an alpha 2 dimer. *Cell* **68**, 133–142.
98 Bruhn L & Sprague GF (1994) MCM1 point mutants deficient in expression of alpha-specific genes: residues important for interaction with alpha 1. *Mol Cell Biol* **14**, 2534–2544.
99 Hagen DC, Bruhn L, Westby CA & Sprague GF (1993) Transcription of alpha-specific genes in Saccharomyces cerevisiae: DNA sequence requirements for activity of the coregulator alpha 1. *Mol Cell Biol* **13**, 6866–6875.
100 Jensen R, Sprague GF & Herskowitz I (1983) Regulation of yeast mating-type interconversion: feedback control of HO gene expression by the mating-type locus. *Proc Natl Acad Sci U S A* **80**, 3035–3039.
101 Goutte C & Johnson AD (1988) a1 protein alters the DNA binding specificity of alpha 2 repressor. *Cell* **52**, 875–882.
102 Nagaraj VH, O'Flanagan RA, Bruning AR, Mathias JR, Vershon AK & Sengupta AM (2004) Combined analysis of expression data and transcription factor binding sites in the yeast genome. *BMC Genomics* **5**, 59.
103 Gimeno CJ, Ljungdahl PO, Styles CA & Fink GR (1992) Unipolar cell divisions in the yeast S. cerevisiae lead to filamentous growth: Regulation by starvation and RAS. *Cell* **68**, 1077–1090.
104 Roberts RL & Fink GR (1994) Elements of a single map kinase cascade in Saccharomyces cerevisiae mediate two developmental programs in the same cell type: Mating and invasive growth. *GENES DEV* **8**, 2974–2985.
105 Liu H, Styles CA & Fink GR (1993) Elements of the Yeast Pheromone Response Pathway Required for Filamentous Growth of Diploids. *Science* **262**, 1741–1744.
106 Stanhill A, Schick N & Engelberg D (1999) The Yeast Ras/Cyclic AMP Pathway Induces Invasive Growth by Suppressing the Cellular Stress Response. *Mol Cell Biol* **19**, 7529–7538.
107 Pan X & Heitman J (1999) Cyclic AMP-Dependent Protein Kinase Regulates Pseudohyphal Differentiation in Saccharomyces cerevisiae. *Mol Cell Biol* **19**, 4874–4887.
108 Cullen PJ, Sabbagh W, Graham E, Irick MM, van Olden EK, Neal C, Delrow J, Bardwell L & Sprague GF (2004) A signaling mucin at the head of the Cdc42- and MAPK-dependent filamentous growth pathway in yeast. *Genes Dev* **18**, 1695–1708.
109 O'Rourke SM & Herskowitz I (1998) The Hog1 MAPK prevents cross talk between the HOG and pheromone response MAPK pathways in Saccharomyces cerevisiae. *Genes Dev* **12**, 2874–2886.
110 Cullen PJ & Sprague Jr. GF (2012) The regulation of filamentous growth in yeast. *Genetics* **190**, 23–49.
111 Peter M, Neiman AM, Park HO, van Lohuizen M & Herskowitz I (1996) Functional analysis of the interaction between the small GTP binding protein Cdc42 and the Ste20 protein kinase in yeast. *EMBO J* **15**, 7046–7059.
112 Mösch HU, Roberts RL & Fink GR (1996) Ras2 signals via the Cdc42/Ste20/mitogen-activated protein kinase module to induce filamentous growth in Saccharomyces cerevisiae. *Proc Natl Acad Sci U S A* **93**, 5352–5356.
113 Madhani HD, Galitski T, Lander ES & Fink GR (1999) Effectors of a developmental mitogen-activated protein kinase cascade revealed by expression signatures of signaling mutants. *Proc Natl Acad Sci U S A* **96**, 12530–12535.
114 Madhani HD & Fink GR (1997) Combinatorial control required for the specificity of yeast MAPK signaling. *Science* **275**, 1314–1317.

115 Laloux I, Jacobs E & Dubois E (1994) Involvement of SRE element of Ty1 transposon in TEC1-dependent transcriptional activation. *Nucleic Acids Res* **22**, 999–1005.
116 Bao MZ, Schwartz MA, Cantin GT, Yates JR & Madhani HD (2004) Pheromone-dependent destruction of the Tec1 transcription factor is required for MAP kinase signaling specificity in yeast. *Cell* **119**, 991–1000.
117 Brückner S, Köhler T, Braus GH, Heise B, Bolte M & Mösch H-U (2004) Differential regulation of Tec1 by Fus3 and Kss1 confers signaling specificity in yeast development. *Curr Genet* **46**, 331–342.
118 Chou S, Huang L & Liu H (2004) Fus3-regulated Tec1 degradation through SCFCdc4 determines MAPK signaling specificity during mating in yeast. *Cell* **119**, 981–990.
119 Liu H, Styles CA & Fink GR (1996) Saccharomyces Cerevisiae S288c Has a Mutation in Flo8, a Gene Required for Filamentous Growth. *Genetics* **144**, 967–978.
120 Westfall PJ & Thorner J (2006) Analysis of Mitogen-Activated Protein Kinase Signaling Specificity in Response to Hyperosmotic Stress: Use of an Analog-Sensitive HOG1 Allele. *Eukaryotic Cell* **5**, 1215–1228.
121 Westfall PJ, Patterson JC, Chen RE & Thorner J (2008) Stress resistance and signal fidelity independent of nuclear MAPK function. *Proceedings of the National Academy of Sciences* **105**, 12212–12217.
122 Patterson JC, Klimenko ES & Thorner J (2010) Single-Cell Analysis Reveals That Insulation Maintains Signaling Specificity Between Two Yeast MAPK Pathways with Common Components. *Sci Signal* **3**, ra75–ra75.
123 McClean MN, Mody A, Broach JR & Ramanathan S (2007) Cross-talk and decision making in MAP kinase pathways. *Nat Genet* **39**, 409–414.
124 Nagiec MJ & Dohlman HG (2012) Checkpoints in a Yeast Differentiation Pathway Coordinate Signaling during Hyperosmotic Stress. *PLOS Genetics* **8**, e1002437.
125 Hao N, Zeng Y, Elston TC & Dohlman HG (2008) Control of MAPK specificity by feedback phosphorylation of shared adaptor protein Ste50. *J Biol Chem* **283**, 33798–33802.
126 Kwan JJ, Warner N, Maini J, Chan Tung KW, Zakaria H, Pawson T & Donaldson LW (2006) Saccharomyces cerevisiae Ste50 binds the MAPKKK Ste11 through a head-to-tail SAM domain interaction. *J Mol Biol* **356**, 142–154.
127 Grimshaw SJ, Mott HR, Stott KM, Nielsen PR, Evetts KA, Hopkins LJ, Nietlispach D & Owen D (2004) Structure of the Sterile α Motif (SAM) Domain of the Saccharomyces cerevisiae Mitogen-activated Protein Kinase Pathway-modulating Protein STE50 and Analysis of Its Interaction with the STE11 SAM *. *Journal of Biological Chemistry* **279**, 2192–2201.
128 Xu G, Jansen G, Thomas DY, Hollenberg CP & Rad MR (1996) Ste50p sustains mating pheromone-induced signal transduction in the yeast Saccharomyces cerevisiae. *MOL MICROBIOL* **20**, 773–783.
129 Sharmeen N, Sulea T, Whiteway M & Wu C (2019) The adaptor protein Ste50 directly modulates yeast MAPK signaling specificity through differential connections of its RA domain. *Mol Biol Cell* **30**, 794–807.
130 Shock TR, Thompson J, Yates JR & Madhani HD (2009) Hog1 Mitogen-Activated Protein Kinase (MAPK) Interrupts Signal Transduction between the Kss1 MAPK and the Tec1 Transcription Factor To Maintain Pathway Specificity. *Eukaryotic Cell* **8**, 606–616.
131 Bilsland-Marchesan E, Ariño J, Saito H, Sunnerhagen P & Posas F (2000) Rck2 Kinase Is a Substrate for the Osmotic Stress-Activated Mitogen-Activated Protein Kinase Hog1. *Molecular and Cellular Biology* **20**, 3887–3895.
132 Teige M, Scheikl E, Reiser V, Ruis H & Ammerer G (2001) Rck2, a member of the calmodulin-protein kinase family, links protein synthesis to high osmolarity MAP kinase signaling in budding yeast. *Proceedings of the National Academy of Sciences* **98**, 5625–5630.
133 Warringer J, Hult M, Regot S, Posas F & Sunnerhagen P (2010) The HOG Pathway Dictates the Short-Term Translational Response after Hyperosmotic Shock. *Mol Biol Cell* **21**, 3080–3092.

134 Mahanty SK, Wang Y, Farley FW & Elion EA (1999) Nuclear Shuttling of Yeast Scaffold Ste5 Is Required for Its Recruitment to the Plasma Membrane and Activation of the Mating MAPK Cascade. *Cell* **98**, 501–512.

135 Flatauer LJ, Zadeh SF & Bardwell L (2005) Mitogen-activated protein kinases with distinct requirements for Ste5 scaffolding influence signaling specificity in Saccharomyces cerevisiae. *Mol Cell Biol* **25**, 1793–1803.

136 Reményi A, Good MC, Bhattacharyya RP & Lim WA (2005) The role of docking interactions in mediating signaling input, output, and discrimination in the yeast MAPK network. *Molecular Cell* **20**, 951–962.

137 Hao N, Nayak S, Behar M, Shanks RH, Nagiec MJ, Errede B, Hasty J, Elston TC & Dohlman HG (2008) Regulation of Cell Signaling Dynamics by the Protein Kinase-Scaffold Ste5. *Molecular Cell* **30**, 649–656.

138 Zalatan JG, Coyle SM, Rajan S, Sidhu SS & Lim WA (2012) Conformational control of the Ste5 scaffold protein insulates against MAP kinase misactivation. *Science* **337**, 1218–1222.

139 Good M, Tang G, Singleton J, Reményi A & Lim WA (2009) The Ste5 Scaffold Directs Mating Signaling by Catalytically Unlocking the Fus3 MAP Kinase for Activation. *Cell* **136**, 1085–1097.

140 Harris K, Lamson RE, Nelson B, Hughes TR, Marton MJ, Roberts CJ, Boone C & Pryciak PM (2001) Role of scaffolds in MAP kinase pathway specificity revealed by custom design of pathway-dedicated signaling proteins. *Curr Biol* **11**, 1815–1824.

141 Park S-H, Zarrinpar A & Lim WA (2003) Rewiring MAP kinase pathways using alternative scaffold assembly mechanisms. *Science* **299**, 1061–1064.

142 Won AP, Garbarino JE & Lim WA (2011) Recruitment interactions can override catalytic interactions in determining the functional identity of a protein kinase. *Proceedings of the National Academy of Sciences* **108**, 9809–9814.

143 Treusch S, Albert FW, Bloom JS, Kotenko IE & Kruglyak L (2015) Genetic Mapping of MAPK-Mediated Complex Traits Across S. cerevisiae. *PLoS Genet* **11**.

144 Laizé V, Gobin R, Rousselet G, Badier C, Hohmann S, Ripoche P & Tacnet F (1999) Molecular and Functional Study ofAQY1fromSaccharomyces cerevisiae:Role of the C-Terminal Domain. *Biochemical and Biophysical Research Communications* **257**, 139–144.

145 Hartwell LH (1980) Mutants of Saccharomyces cerevisiae unresponsive to cell division control by polypeptide mating hormone. *Journal of Cell Biology* **85**, 811–822.

146 Mortimer RK & Johnston JR (1986) Genealogy of Principal Strains of the Yeast Genetic Stock Center. *Genetics* **113**, 35–43.

147 Oliver SG, van der Aart QJM, Agostoni-Carbone ML, Aigle M, Alberghina L, Alexandraki D, Antoine G, Anwar R, Ballesta JPG, Benit P, Berben G, Bergantino E, Biteau N, Bolle PA, Bolotin-Fukuhara M, Brown A, Brown AJP, Buhler JM, Carcano C, Carignani G, Cederberg H, Chanet R, Contreras R, Crouzet M, Daignan-Fornier B, Defoor E, Delgado M, Demolder J, Doira C, Dubois E, Dujon B, Dusterhoft A, Erdmann D, Esteban M, Fabre F, Fairhead C, Faye G, Feldmann H, Fiers W, Francingues-Gaillard MC, Franco L, Frontali L, Fukuhara H, Fuller LJ, Galland P, Gent ME, Gigot D, Gilliquet V, Glansdorff N, Goffeau A, Grenson M, Grisanti P, Grivell LA, de Haan M, Haasemann M, Hatat D, Hoenicka J, Hegemann J, Herbert CJ, Hilger F, Hohmann S, Hollenberg CP, Huse K, Iborra F, Indje KJ, Isono K, Jacq C, Jacquet M, James CM, Jauniaux JC, Jia Y, Jimenez A, Kelly A, Kleinhans U, Kreisl P, Lanfranchi G, Lewis C, vanderLinden CG, Lucchini G, Lutzenkirchen K, Maat MJ, Mallet L, Mannhaupet G, Martegani E, Mathieu A, Maurer CTC, McConnell D, McKee RA, Messenguy F, Mewes HW, Molemans F, Montague MA, Muzi Falconi M, Navas L, Newlon CS, Noone D, Pallier C, Panzeri L, Pearson BM, Perea J, Philippsen P, Pierard A, Planta RJ, Plevani P, Poetsch B, Pohl F, Purnelle B, Ramezani Rad M, Rasmussen SW, Raynal A, Remacha M, Richterich P, Roberts AB, Rodriguez F, Sanz E, Schaaff-Gerstenschlager I, Scherens B, Schweitzer B, Shu Y, Skala J, Slonimski

PP, Sor F, Soustelle C, Spiegelberg R, Stateva LI, Steensma HY, Steiner S, Thierry A, Thireos G, Tzermia M, Urrestarazu LA, Valle G, Vetter I, van Vliet-Reedijk JC, Voet M, Volckaert G, Vreken P, Wang H, Warmington JR, von Wettstein D, Wicksteed BL, Wilson C, Wurst H, Xu G, Yoshikawa A, Zimmermann FK & Sgouros JG (1992) The complete DNA sequence of yeast chromosome III. *Nature* **357**, 38–46.

148 Bonhivers M, Carbrey JM, Gould SJ & Agre P (1998) Aquaporins in Saccharomyces: GENETIC AND FUNCTIONAL DISTINCTIONS BETWEEN LABORATORY AND WILD-TYPE STRAINS*. *Journal of Biological Chemistry* **273**, 27565–27572.

149 Carbrey JM, Bonhivers M, Boeke JD & Agre P (2001) Aquaporins in Saccharomyces: Characterization of a second functional water channel protein. *Proceedings of the National Academy of Sciences* **98**, 1000–1005.

150 Grenson M, Mousset M, Wiame JM & Bechet J (1966) Multiplicity of the amino acid permeases in Saccharomyces cerevisiae. I. Evidence for a specific arginine-transporting system. *Biochim Biophys Acta* **127**, 325–338.

151 Dowell RD, Ryan O, Jansen A, Cheung D, Agarwala S, Danford T, Bernstein DA, Rolfe PA, Heisler LE, Chin B, Nislow C, Giaever G, Phillips PC, Fink GR, Gifford DK & Boone C (2010) Genotype to Phenotype: A Complex Problem. *Science* **328**, 469–469.

152 Rupp S, Summers E, Lo HJ, Madhani H & Fink G (1999) MAP kinase and cAMP filamentation signaling pathways converge on the unusually large promoter of the yeast FLO11 gene. *EMBO J* **18**, 1257–1269.

153 Siliciano PG & Tatchell K (1984) Transcription and regulatory signals at the mating type locus in yeast. *Cell* **37**, 969–978.

154 Dolan JW & Fields S (1990) Overproduction of the yeast STE12 protein leads to constitutive transcriptional induction. *Genes Dev* **4**, 492–502.

155 Clark KL & Sprague GF (1989) Yeast pheromone response pathway: characterization of a suppressor that restores mating to receptorless mutants. *Molecular and Cellular Biology* **9**, 2682–2694.

156 Fields S, Chaleff DT & Sprague Jr. GF (1988) Yeast STE7, STE11, and STE12 genes are required for expression of cell-type-specific genes. *MOL CELL BIOL* **8**, 551–556.

157 Sen M & Marsh L (1994) Noncontiguous domains of the alpha-factor receptor of yeasts confer ligand specificity. *Journal of Biological Chemistry* **269**, 968–973.

158 Michaelis S & Herskowitz I (1988) The a-factor pheromone of Saccharomyces cerevisiae is essential for mating. *Molecular and Cellular Biology* **8**, 1309–1318.

159 Sikorski RS & Hieter P (1989) A system of shuttle vectors and yeast host strains designed for efficient manipulation of DNA in Saccharomyces cerevisiae. *Genetics* **122**, 19–27.

160 Song G, Dickins BJA, Demeter J, Engel S, Dunn B & Cherry JM (2015) AGAPE (Automated Genome Analysis PipelinE) for Pan-Genome Analysis of Saccharomyces cerevisiae. *PLOS ONE* **10**, e0120671.

Chapter 2: Strain dependent differences in coordination of yeast signaling networks

This chapter was adapted from the paper published at:

Scott, T.D., Xu, P., and McClean M.N. (2022). Strain dependent differences in coordination of yeast signaling networks. *BioRxiv*. https://doi.org/10.1101/2022.06.09.495559.

Ping Xu performed the fluorescent *in situ* hybridization experiments. Taylor Scott performed the remaining experiments and analyzed the data for all experiments. Taylor Scott and Ping Xu constructed strains and plasmids. Taylor Scott and Megan McClean wrote the paper.

ABSTRACT

The yeast mitogen-activated protein kinase pathways serve as a model system for understanding how network interactions affect the way in which cells coordinate the response to multiple signals. We have quantitatively compared two yeast strain backgrounds, YPH499 and Σ1278b (both of which have previously been used to study these pathways) and found several important differences in how they coordinate the interaction between the high osmolarity glycerol (HOG) and mating pathways. In the Σ1278b background, in response to simultaneous stimulus, mating pathway activation is dampened and delayed in a dose dependent manner. In the YPH499 background, only dampening is dose dependent. Further, leakage from the HOG pathway into the mating pathway (crosstalk) occurs during osmostress in the Σ1278b background only. The mitogen-activated protein kinase Hog1p suppresses crosstalk late in an induction time course in both strains but does not affect the early crosstalk seen in the Σ1278b background. Finally, the kinase Rck2p plays a greater role suppressing late crosstalk in the Σ1278b background than in the YPH499 background. Our results demonstrate that comparisons between laboratory yeast strains provide an important resource for understanding how signaling network interactions are tuned by genetic variation. These results show that even well-studied model systems are not homogenous in their output, and that existing natural variation between strains is a powerful resource for studying how networks can be subtly altered while maintaining functional signaling.

INTRODUCTION

Cells exist in dynamic changing environments and must coordinate their respond to multiple stimuli in order to survive and thrive. The cellular response to a stimulus may be organized into a series of tightly regulated reactions which together form a signaling network. The mitogen-activated protein kinase (MAPK) network architecture is a common example of a signaling network and is conserved among eukaryotes [1]. The core structure consists of a three-step kinase cascade, in which a MAP kinase kinase kinase (MAP3K) becomes activated by diverse upstream mechanisms. Once activated, it phosphorylates and activates a MAP kinase kinase (MAP2K), which phosphorylates and activates the MAPK. Once activated, the MAPK phosphorylates diverse targets throughout the cell in order to effect the cellular response. Multiple MAPK networks may exist in a cell, each controlling the response to one or more stimuli, and these networks may share kinases. MAPK networks play an important role in many fields of study, including disease etiology and drug development [2], developmental biology [3], and *in silico* control of cellular processes[4].

The budding yeast (*Saccharomyces cerevisiae)* MAPK networks are an attractive model system for studying signal flow through MAPK networks because their stimuli are well known, and they have a relatively simple structure. Two pathways of interest are the high osmolarity glycerol (HOG) pathway, which controls the response to high osmotic stress, and the mating/FG pathway, which is activated by pheromone and nutrient starvation (Figure 2.1). The HOG pathway consists of two parallel activation branches, known as the SLN1 branch (containing the MAP3Ks Ssk2p and Ssk22p) [5,6] and the SHO1 branch (containing the MAP3K Ste11p) [6,7], which converge on the MAP2K Pbs2p. Pbs2p activates the sole MAPK, Hog1p [8]. Activation of the Hog1p can be measured via the transcriptional reporter *STL1*, which is strongly activated by HOG pathway activity in a Hog1p-dependent manner [9,10]. The mating/FG pathways share a single activation branch [11] in which the MAP3K Ste11p is activated by the Cdc42-Ste20 complex [12–16] before phosphorylating and activating the MAP2K Ste7p [17,18], which activates the

MAPKs Fus3p and Kss1p [19–22]. While Fus3p and Kss1p are traditionally thought of as the MAPKs for the mating and FG pathways respectively, they are partially redundant in mating [23] and are both activated in response to pheromone [24–27]. *FUS1* is a common transcriptional reporter of mating/FG MAPK activity, and it is induced by both phosphorylated Fus3p and Kss1p [28].

A striking feature of these networks is that they share an activation mechanism, namely the activation of Ste11p by Cdc42-Ste20 (Figure 2.1). Despite this connection, the pathways are (in general) insulated and it is thought that a combination of scaffolding and inhibition via Hog1p suppresses activation of the mating/FG pathways in response to osmostress [29–31]. This discovery initiated extensive research into how the connection between the two pathways is regulated, and various approaches have been used to study this phenomenon, the majority of which have involved large changes to the network structure. For example, it has been shown that deleting Hog1p results in significant leakage of osmostress signal into the mating/FG pathways (a phenomenon known as crosstalk) [29], as does chemical inhibition of Hog1p or rendering Hog1p kinase dead [32,33]. Similarly, crosstalk is seen when the MAP2K binding domains of Hog1p and Kss1p or Fus3p are swapped, effectively physically rewiring the networks [34]. How much, though, does signal insulation and crosstalk vary between wild-type strains, where there is natural genetic variation, but the networks remain intact?

Here we quantitatively examine signaling in two strain backgrounds, YPH499 and Σ1278b (Sigma), and compare their response to osmostress and pheromone. YPH499 is congenic with S288C and has previously been used to study crosstalk between these pathways [35,36]. Sigma is commonly used to study filamentation and has long been used to study the mating and FG pathways [11,37,38]. These two strains are genetically very similar, diverging by ~0.3% which is similar to the divergence between unrelated humans[39–41]. Whole genome sequencing studies have shown that while both strains are domesticated laboratory strains, Sigma is more significantly diverged from S288C [39,41]. Importantly,

the components of the HOG and mating/FG MAPK pathways are present in both strains and therefore the two strains have the same apparent network structure.

We show that, despite the two strains having the same network structure, they show qualitative and quantitative differences in the response to osmostress and pheromone. This is true when the strains are stimulated with osmostress alone, and when the cells are exposed to simultaneous osmostress and pheromone. We also show that the well-known suppression of the mating/FG pathways by the HOG pathway activity can be separated into two phases, a previously unknown early, strain-dependent phase and the known late, Hog1p-dependent phase. In the early phase, crosstalk occurs in Sigma but not in YPH499 cells. We also show that a known HOG-dependent suppressor of crosstalk, kinase Rck2p, has a more significant role in Sigma than in YPH499. By comparing two strains, we demonstrate that different strains vary significantly in their signaling output, despite apparently identical network structures.

RESULTS

Sigma and YPH499 have different osmosensitivity

We wished to quantitatively compare the effects of simultaneous osmostress and pheromone in the YPH499 and Sigma backgrounds. However, the effects of simultaneous induction are known to correlate with the severity of osmostress, and we therefore needed to establish the relative osmosensitivity of the two strains. When grown in liquid culture and on agar plates, Sigma is more osmosensitive than YPH499, though not grossly and both strains recover well from an osmotic shock.

When YPH499 and Sigma cells were spotted onto YPD agar with and without sorbitol, both strains showed decreased growth with increasing sorbitol (Figure 2.2A). Comparing the two strains after 24 hours growth, however, showed that Sigma grows comparatively worse than YPH499 at higher concentrations of sorbitol, with the defect clearly visible beginning at 0.75M sorbitol. This defect lessened after 45 hours growth, consistent with adaptation to the hyperosmolar environment. Quantification of spot growth

confirms these general trends when the Sigma growth is normalized to YPH499 growth (Figure 2.2B). At 24 hours and at 45 hours, the relative growth of Sigma decreased linearly with increasing sorbitol indicating that more osmostress imposed a more severe growth defect in Sigma than in YPH499. At 24 hours, the slope of the best fit line is -0.41 M^{-1}, indicating the growth defect on 1M sorbitol YPD agar was approximately 41% greater in Sigma than in YPH499. In contrast, the slope of the line at 45 hours is -0.19 M^{-1}, meaning that the growth defect per molar sorbitol at 45 hours was only 19% greater than in YPH499.

Similar results were found in liquid culture (Figure 2.2C). We have consistently seen that, in several media types, Sigma yeast grows to a higher density than YPH499 yeast in liquid culture without osmostress (data not shown). To test the effects of osmostress in liquid growth, we measured optical density at 600 nm (OD600) after 16 hours growth and 41 hours growth in liquid YPD with and without sorbitol. After 16 hours growth in YPD without sorbitol, Sigma cultures were about twice as dense as YPH499 cultures (0.9 additional doublings). The addition of sorbitol to the media however significantly decreased Sigma's growth advantage at 16 hours: at 0.75M sorbitol, the excess growth was reduced to 0.5 additional doublings, and at 1.5M sorbitol the Sigma cultures were *less* grown than the YPH499 cultures, having doubled 0.3 times fewer than the YPH499 cultures. After 45 hours, the effects of sorbitol are largely abrogated: the number of additional doublings in the cultures with sorbitol was slightly lower than the cultures without sorbitol although the difference was not statistically significant.

Finally, Sigma shows greater induction of a HOG pathway transcriptional reporter than YPH499 at most doses of sorbitol (Figure 2.2D). We measured induction of tdTomato driven by the *STL1* promoter (pSTL1-tdTomato) after 45 minutes in varying concentrations of sorbitol using flow cytometry. In both strain backgrounds maximum pSTL1-tdTomato induction was achieved at 0.7M – 0.8M sorbitol before decreasing at higher concentrations of sorbitol. In the Sigma background, however, maximum pSTL1-tdTomato induction was nearly 30-fold, while the maximum induction in YPH499 was only 15-fold. Additionally, pSTL1-tdTomato induction at high concentrations of sorbitol decreased more sharply in

Sigma than in YPH499, and in particular pSTL1-tdTomato was less induced in Sigma at 1M and 1.25M sorbitol.

Mating pathway activation under osmostress is faster in Sigma than in YPH499

Having seen that Sigma is more osmosensitive than YPH499, we reasoned that the effect of osmostress on mating pathway induction should be more severe in Sigma than in YPH499 at a given concentration of sorbitol. Increasing osmostress has been shown to both dampen and delay mating pathway activation when cells are simultaneously exposed to an osmolyte (such as sorbitol or NaCl) [42], and we therefore hypothesized that Sigma should show greater dampening and a longer delay in mating pathway activation than YPH499. To test this, we induced Sigma and YPH499 cells with 10 μM α-factor and varying concentrations of sorbitol (0M – 1.5M) and measured expression of eGFP driven by the *FUS1* promoter (pFUS1-eGFP). The time courses of mating response in the pheromone/sorbitol induced cells, plotted as a percentage of the pFUS1-eGFP level in a time-matched sample induced with pheromone alone, had a characteristic shape (Figure 2.3A). There is a large initial dampening in the mating response which gradually recovers to a less extreme final dampening level. We quantify the initial dampening by taking the minimum value of the mating response and the final dampening by taking the average of the final two measurements at 150 minutes and 180 minutes post-induction, by which point the cells had fully recovered from the osmotic shock. To quantify the delay, we find the full-width half minimum (FWHM) by calculating the width of the initial dampening peak at the dampening level halfway between the initial dampening and the final dampening. A greater FWHM indicates a longer time to recover to the final dampening level.

In YPH499 (Figure 2.3B) and in Sigma (Figure 2.3C), increasing sorbitol caused increasing dampening in mating pathway activation, both initially and finally. Notably, we observed no strain-dependent difference in dampening (Figure 2.3D). This was true when considering initial dampening (dashed line) and final dampening (solid line) at every level of osmostress. In both strains, the minimum

mating response (initial dampening) at 0.25M sorbitol was approximately 90% of a sample induced with pheromone alone. These samples recovered to a final mating response greater than 95% of the pheromone only sample (YPH499, 98.4%; Sigma, 95.1%). Under more severe osmostress (1.25M sorbitol), the initial dampening was much greater, approximately 30% in both strains (YPH499, 26.7%; Sigma, 30.6%). Similarly, the final dampening was also more severe, and the cells recovered to only 50% of a pheromone only sample (YPH499, 46.4%; Sigma, 50.1%). At the most severe osmostress tested (1.5M sorbitol), the cells did not recover to a final dampening level but remained depressed for the duration of the time course. The final dampening level at this osmostress is 27.8% in YPH499 and 20.0% in Sigma.

Unlike the dampening effect, the delay in mating activation caused by osmostress was clearly strain-dependent (Figure 2.3E). In YPH499, the delay of the mating response curves was roughly constant at 45-50 minutes at each test sorbitol concentration. In contrast, the delay in Sigma increased with increasing sorbitol, from 11 minutes at 0.25M sorbitol to 40 minutes at 1.25M sorbitol. We were unable to calculate the FWHM for our 1.5M sorbitol time courses because the curves did not recover to a final dampening level but instead decreased throughout the time course.

Sigma yeast show induction of the mating pathway under osmostress

The finding that Sigma yeast have a starkly shorter delay in mating pathway activation under simultaneous osmostress and pheromone induction was surprising because it is known that activation of the Hog1p inhibits induction of mating pathway transcripts [29,32,33,36,43]. Counter to this, in examining a sorbitol-only control, we noticed that Sigma increased pFUS1-eGFP expression under sorbitol induction, even in the absence of pheromone (Figure 2.3F). When Sigma and YPH499 cells were exposed to 0.75M sorbitol, the Sigma cells showed a maximum of 1.3-fold increase in pFUS1-eGFP at approximately 30-45 minutes post-induction. In contrast, the maximum induction in YPH499 was negligible (1.05-fold), and its induction was uniformly lower than the induction seen in Sigma. This finding was unexpected, and we performed further experiments to verify that Sigma is showing mating pathway induction under osmostress. We

collected time courses in a variety of mating and HOG pathway mutants following a 0.75M sorbitol induction (the results of which are detailed below) in 24-well plates which are less susceptible to edge effects and well-to-well variability than the 96-well plates used in the simultaneous sorbitol and pheromone experiments. These experiments were performed in an identical manner, and the wild-type controls represent 20 biological replicates performed on different days. The collected controls from these mutant experiments (Figure 2.4A) show that Sigma induced pFUS1-eGFP under osmostress significantly more than YPH499. Sigma achieved maximum induction at approximately 45 minutes post-induction; at this time point, the pFUS1-eGFP induction in Sigma cells (normalized to the 0-minute time point) was 1.24-fold compared to 1.08-fold in YPH99, and pFUS1-eGFP induction in Sigma was significantly higher than in YPH499 at every time point from 20 minutes to 60 minutes post-induction. We also measured pFUS1-eGFP induction at different concentrations of sorbitol at 45 minutes post-induction (Figure 2.4B). pFUS1-eGFP induction in Sigma was strongly dose-dependent, achieving its maximum induction at a moderate level of osmostress, approximately 0.6M-0.8M sorbitol. In contrast, YPH499 cells did not show significant pFUS1-eGFP induction at any concentration of sorbitol. As seen in the pSTL1-tdTomato dose-response curve in Figure 2.2D, the pFUS1-eGFP induction in Sigma decreased at higher concentrations of sorbitol and we saw negligible induction at concentrations greater than 1M sorbitol.

To confirm that this apparent induction was happening at the level of transcription, we directly observed *FUS1* transcripts using single-cell fluorescent *in situ* hybridization (scFISH). In both strain backgrounds, there were few *FUS1* transcripts present in an uninduced sample (Figure 2.4C, left images). In Sigma, however, many cells had FUS1 transcripts following a 15-minute induction with 0.75M sorbitol (Figure 2.4C, bottom right). We did not see the same in YPH499 cells (Figure 2.4C, top right). As seen with flow cytometry, induction of *FUS1* transcripts under sorbitol in Sigma was dose dependent and at 0.5M and 0.75M sorbitol, roughly 40% of cells had *FUS1* transcripts, an increase from 20% at 0M sorbitol (Figure

2.4D). In YPH499 however, no dose-dependent induction was observed and the number of cells with *FUS1* transcripts remained at 10-20% at every concentration of sorbitol.

Sorbitol induction of pFUS1-eGFP in Sigma is *STE11* and *FUS3/KSS1* dependent

We wondered whether the pFUS1-eGFP induction in Sigma represented true crosstalk, this is, whether the induction was due to signal leaking from the HOG pathway into the mating/FG pathways. To test this, we collected sorbitol induction time courses in mating/FG pathway deletions. The Sigma-background deletions are discussed here. Ste11p is a shared component of the HOG and mating pathways and can phosphorylate either Pbs2p (in the HOG pathway) or Ste7p (in the mating/FG pathways). Deleting *STE11*, therefore, should disrupt the connection between the pathways and prevent pFUS1-eGFP induction due to osmostress in the Sigma background. As expected, pFUS1-eGFP induction was drastically reduced in Sigma *ste11Δ* cells (Figure 2.5A). In fact, in a 60-minute time course under 0.75M sorbitol, pFUS1-eGFP induction in Sigma *ste11Δ* cells was indistinguishable from that in YPH499 wild-type cells. Activation of Ste11p may plausibly result in phosphorylation of either Fus3p or Kss1p, and activation of either kinase would cause an increase in pFUS1-eGFP production. We therefore collected time courses in *fus3Δ* and *kss1Δ* deletions as well as a *fus3Δ kss1Δ* double deletion. As seen in the *ste11Δ* deletion, pFUS1-eGFP induction in Sigma *fus3Δ kss1Δ* cells was reduced to levels seen in YPH499 wild-type cells (Figure 2.5B). This indicates that Fus3p and/or Kss1p activity is responsible for the increased pFUS1-eGFP induction seen in the Sigma background under osmostress. In contrast, we found that pFUS1-eGFP induction in the Sigma background was unchanged when *FUS3* and *KSS1* were deleted separately (Figure 2.5C, D). This is true for the duration of the 60-minute time course. This suggests that signal leaks from Ste11p into both kinases and activation of either kinase is sufficient to induce our reporter.

Mechanisms of HOG-dependent crosstalk inhibition are strain dependent

HOG pathway activity is known to suppress crosstalk in part through activation of the MAPK activated protein kinase Rck2p, perhaps through translational suppression of mating pathway components [42]. We

wondered whether a defect in Rck2p activation could explain the crosstalk seen in the Sigma background. We collected 60-minute time courses under 0.75M sorbitol in YPH499 and Sigma wild-type, *rck2Δ*, and *hog1Δ* cells (Figure 2.6). In both strains, the *rck2Δ* and the *hog1Δ* deletions each produced excess crosstalk compared to the wild-type cells. Interestingly, this excess crosstalk occurred late in the induction time course, and, in particular, it occurred after the crosstalk seen in the Sigma wild-type cells. In the YPH499 background, both deletions showed a significant increase in pFUS1-eGFP induction compared to the wild-type beginning at 30 minutes post-induction (Figure 2.6A). In the Sigma background, the *rck2Δ* showed excess induction beginning at 30 minutes post-induction and the *hog1Δ* showed additional crosstalk beginning at 45 minutes post-induction (Figure 2.6B). We also found that the role of *rck2Δ* in the YPH499 background was limited compared to the Sigma background. Specifically, the maximum amount of crosstalk in the YPH499 *rckΔ* was considerably lower than in the YPH499 *hog1Δ* cells (*rck2Δ* = 1.32 ± 0.05; *hog1Δ* = 2.00 ± 0.04). In contrast, Sigma *rck2Δ* cells achieved roughly the same level of crosstalk as the *hog1Δ* cells over 60 minutes (*rck2Δ* = 1.66 ± 0.07; *hog1Δ* = 1.69 ± 0.08), though the signal was clearly attenuating in the *rck2Δ* mutant.

Early crosstalk in Sigma is independent of HOG pathway activity

Having seen that deleting *HOG1* produces crosstalk late in an induction time course, we wondered whether other disruptions of Hog1p activity also produce crosstalk late in a time course. We measured crosstalk in two additional mutants in which Hog1p activity is disrupted. First, we examined *ssk1Δ* deletions. Ssk1p is an essential component of the fast-activating SLN1 branch of the HOG pathway and deleting *SSK1* significantly slows activation of Hog1p [44–46]. In the Sigma background, the *ssk1Δ* cells and wild-type cells showed identical pFUS1-eGFP induction for the first 30 minutes post-induction, but the *ssk1Δ* cells showed increased induction at 45 minutes and 60 minutes post-osmotic shock (Figure 2.7A). In the YPH499 background, results were similar. The *ssk1Δ* cells showed higher induction than wild-type cells at 45- and 60-minutes post-induction (Figure 2.7C). There was also a slight but significant

increase in induction at 30 minutes post-shock in the YPH499 background that we did not observe in the Sigma background.

We also disrupted Hog1p activity directly by introducing the kinase-dead *HOG1*^{D144A} allele which displays no kinase activity [32]. In the Sigma background the *HOG1*^{D144A} mutant cells and wild-type cells exhibited identical levels of pFUS1-eGFP induction for the first 30 minutes following the osmotic shock, but the mutants showed higher crosstalk at 45 and 60 minutes (Figure 2.7B). Similarly, in the YPH499 background the *HOG1*^{D144A} mutants showed much higher induction at 45 minutes and 60 minutes post-induction with a slight increase at 30 minutes post-induction (Figure 2.7D). In both strain backgrounds, and similarly to the *hog1Δ* time courses, pFUS1-eGFP induction in the *HOG1*^{D144A} mutants increases continuously throughout the time course while the induction is limited in the *ssk1Δ* cells. Because the HOG pathway disruptions do not affect the crosstalk seen in Sigma during the first 30 minutes of an induction, we conclude that the mechanism which permits early crosstalk in the Sigma background is not dependent on HOG pathway activity.

DISCUSSION

Osmostress has strain dependent effects on mating pathway activation

The two strains used in this study, Sigma and YPH499, show differences in osmosensitivity. Sigma grows worse than YPH499 on YPD agar and in liquid YPD when sorbitol is present, and Sigma shows stronger activation of a HOG pathway transcriptional reporter than YPH499 at most concentrations of sorbitol. This result is not unexpected because Sigma contains functional aquaporins Aqy1p and Aqy2p while thegenes encoding these proteins in YPH499 contain a premature stop codon rendering them less functional than the Sigma variant [47–49]. Consequently, Sigma cells are more prone to water loss following an osmotic shock. The loss of Aqy1p and Aqy2p function has been directly tied to increased osmotolerance in growth on YPD agar and in hyperosmotic/hypoosmotic cycling [47,48]. It has been shown that the water loss at

high concentrations of sorbitol significantly slows diffusion of signaling molecules and slows HOG pathway activation [50]. This is the likely cause of the decreased reporter induction at high concentrations of sorbitol (Figure 2.2D). Sigma is predicted to lose water more readily than YPH499 due to its functional aquaporins, which would explain both the increased transcriptional activation at lower concentrations of sorbitol (because the stress is more severe) and the decreased activation at high concentrations of sorbitol (because slowed diffusion is more severe).

As has been previously reported, simultaneous osmostress and pheromone results in a significant dampening and delay to mating pathway activation [42]. This is expected because activation of the HOG pathway is fast relative to mating pathway activation and Hog1p activity strongly inhibits the mating pathway. Because Hog1p activity (both amplitude and duration) correlates with osmostress [45], the simplest explanation of the dampening and delay effect is that it is a direct result of Hog1p activity under osmostress. Surprisingly, we find that the dampening effect is identical in our two strain backgrounds, despite Sigma being more osmosensitive. This is true at every tested concentration of sorbitol, ranging from a small osmostress to a severe osmostress, and is true both initially and at saturation. Despite the similarity in dampening, our results indicate that the delay is strongly strain dependent. Sigma has a shorter delay at every concentration of sorbitol, and the delay in Sigma is dose dependent while it is constant in YPH499. Nagiec and Dohlman found a dose dependent delay in the S288C background (with which YPH499 is congenic), so it is curious that we observe a constant delay in our experiments [42]. A potential explanation for this is that our strains harbor a *bar1Δ* deletion while the strains used by Nagiec do not. Bar1p is a protease which degrades pheromone [51,52] and its expression is induced by mating pathway activation as a form of negative feedback [53,54]. Consequently, the pheromone activation time courses saturate after a few hours in *BAR1* strains but do not in *bar1Δ* strains. Thus, our measure of delay is based on the time it takes doubly stimulated cells to produce pFUS1-eGFP at the same rate as cells induced with pheromone alone, instead of being a direct measure of time-to-saturation as measured by

Nagiec and Dohlman. Nonetheless, the difference in delay seen in the two strains is striking and indicates that inhibition of the mating pathway in Sigma is not directly related to the severity of osmostress as has been previously suggested.

HOG pathway signal transiently leaks into the mating pathway in Sigma yeast

We find transient induction of the mating/FG pathways under osmostress alone in Sigma yeast, and this induction is consistent with signal leakage from the HOG pathway into the mating/FG pathways through the Ste11p node. This was unexpected because the known targets of Hog1p activity which suppress the mating pathway, namely Ste50p and Rck2p, are present in Sigma and the structure of the HOG and mating pathways is the same in both strains. This result indicates that the insulation between the HOG and the mating/FG pathways is strain dependent. Crosstalk is typically studied in the context of a large disruption to the signaling networks (for example, deletion of Hog1p or deletion of Hog1p targets), largely because crosstalk is not observed in wild-type cells. Here we show that crosstalk can occur in a native network absent large disruptions, but it is strain-dependent and transient. Importantly, this crosstalk occurs under physiologically relevant stress profiles. For example, during wine-making yeast must survive an initial sugar content of 15-28% (w/v) [55], which assuming glucose is the primary sugar, produces an osmoshock equivalent to 0.8M - 1.6M sorbitol. A previous study observed crosstalk into a mating/FG reporter under complex, quickly oscillating stress [56]. Here, our stress is a simple, static shock which more likely to be found in a natural environment. Further study of this phenomenon will provide insight into the factors which contribute to or suppress crosstalk in a fully functioning network.

Rck2p-dependent inhibition of crosstalk is strain dependent

Rck2p is an important factor in HOG-dependent suppression of crosstalk. The exact mechanism by which Rck2p suppresses crosstalk is unknown, but it has been suggested that activation of Rck2p translationally suppresses activation of mating pathway products and disrupts the positive feedback necessary to fully activate the mating pathway [42]. We found that in Sigma, deleting *RCK2* produces similar levels of

crosstalk as deleting *HOG1*. In fact, crosstalk in the *rck2Δ* mutant was higher than in the *hog1Δ* at some time points. This suggests that Rck2p is the factor responsible for suppressing late crosstalk in the Sigma background. In contrast, we observed in YPH499 that crosstalk is attenuated relative to *hog1Δ* cells, and while *rck2Δ* cells produce excess crosstalk relative to WT cells, this crosstalk is significantly lower than the crosstalk seen in *hog1Δ* cells. A previous study (in the S288C background) showed that Rck2p is not solely responsible for HOG-dependent suppression of crosstalk [42], so it is surprising that crosstalk in Sigma *rck2Δ* cells reaches similar levels to that seen in Sigma *hog1Δ* cells. Further experiments are needed to understand the differences in the strain backgrounds which cause this difference in Rck2p-mediated insulation.

The HOG pathway regulates late, but not early, crosstalk

Our initial hypothesis for the crosstalk seen in the Sigma background was that a defect in HOG pathway signaling allowed some transient crosstalk prior to robust activation of Hog1p. Our results, however, suggest that, while HOG pathway activity inhibits late crosstalk, it does not explain the early crosstalk seen in the Sigma background. In the *ssk1Δ* mutants, the fast-activating SLN1 branch of the HOG pathway is disrupted, and it has been shown that activation of the HOG pathway is roughly two-fold slower in *ssk1Δ* cells [44–46]. The *hog1Δ* and *HOG1*^{D144A} mutants both eliminate Hog1p activity, the former by eliminating Hog1p itself and the latter by rendering Hog1p kinase dead [32]. We used both mutations because the MAPK pathway kinases are promiscuous and will phosphorylate any target that can bind [34,57,58], therefore removing Hog1p as a binding partner for Pbs2p may impact signaling through the network for reasons other than Hog1p activity. If the crosstalk in Sigma were due to ineffective Hog1p activity, we expect to see excess crosstalk in the mutants at the time points at which we see crosstalk in Sigma. In all three cases, we *do* see additional crosstalk, but it occurs *after* the crosstalk seen in wild-type cells. That is, the time courses of *ssk1Δ*, *hog1Δ*, and *HOG1*^{D144A} mutants are identical to wild-type time courses for 30 minutes post-induction but show increased induction at the 45- and 60-minute time points. In YPH499,

these mutants show slightly increased crosstalk at 30 minutes and substantially increased crosstalk at 45- and 60-minutes post-induction.

This result allows us to divide crosstalk into two phases: early and late. Early following an osmotic shock (roughly the first 30 minutes), crosstalk is permitted in the Sigma background but not the YPH499 background. Late in the time course, beginning at roughly 30 minutes, additional crosstalk is suppressed by Hog1p activity in both strain backgrounds. Because Hog1p activity is merely delayed and not eliminated in *ssk1Δ* cells, our findings suggest that there is a critical window following osmostress in which Hog1p must be active in order to suppress late crosstalk. Without a functioning SLN1 branch, activation of Hog1p occurs outside this window and late crosstalk is permitted, though it is attenuated as the cell responds to the stress and turns off the HOG pathway. This model agrees with a previous study which found that Hog1p needed to be active for 20 to 30 minutes in order to suppress crosstalk, but that inhibition of Hog1p after 30 minutes did not cause crosstalk, indicating that continuous Hog1p activity is not needed to suppress crosstalk throughout an osmotic shock [36].

The factors which permit early crosstalk in Sigma but suppress early crosstalk in YPH499 are unknown and further studies are necessary to determine how these factors are regulated. Our results indicate that suppression via these factors is not Hog1p dependent because crosstalk in the HOG-disrupted mutants remained low at 20- and 30-minutes post-induction in the YPH499 background and was unchanged in the Sigma background. One potential HOG-independent mechanisms of crosstalk inhibition is scaffolding [30]. However, there is only a single point mutation in Ste5p (the mating pathway scaffold [59] in the Sigma background (D877G) which occurs outside any kinase binding sites; Pbs2p (the HOG pathway scaffold [7,60]) is identical in the two strains. Further, our results show that Kss1p is sufficient to allow crosstalk in the Sigma background, and activation of Kss1p does not require a scaffold [61]. Thus, differences in the scaffold proteins themselves are unlikely to be the cause of the early

crosstalk seen in the Sigma background, though further studies are needed to conclusively eliminate this mechanism.

CONCLUSION

Studies of signaling in yeast frequently use mutations or deletions to discover how different nodes in a signaling network affect signal flow through the network. While these experiments yield invaluable information about network structure and function, they also introduce large changes into the network. For example, deleting *HOG1* not only eliminates Hog1p activity but also eliminates Pbs2p's binding partner and target and significantly impairs the cell's ability to adapt to osmostress. We were interested in what differences in signaling can exist in cells which retain the native network structure. We have quantitatively compared two strains which ostensibly have identical HOG and mating pathway structure; that is, neither strain harbors a deletion of any MAPK component. Despite this, we found differences in MAPK signaling between these strains. The Sigma background is, compared to the S288C-congenic YPH499 background, more osmosensitive when measured through growth on solid YPD agar, growth in liquid YPD, and expression of an osmostress-responsive reporter. The increased osmosensitivity, though, does not cause increased dampening of the mating pathway when cells are costimulated with osmostress and pheromone, and, surprisingly, the Sigma background has a shorter delay in mating pathway activation at most concentrations of sorbitol. We also observe crosstalk from the HOG pathway into the mating pathway when wild-type Sigma cells are stimulated with osmostress alone, a result which to our knowledge has not been reported in any *S. cerevisiae* strain. Our results indicate that this signal leakage occurs through Ste11p and Fus3p/Kss1p, which is consistent with the known links between the HOG and mating pathways. Importantly, this crosstalk occurs early in an osmostress induction time course, prior to the known HOG-dependent inhibition of crosstalk. Finally, we have also shown that known mechanisms of crosstalk inhibition may vary differ between strain backgrounds. The crosstalk seen in Sigma background *rck2Δ* cells is comparable to that seen in Sigma *hog1Δ* cells, while in the YPH499 background

rck2Δ exhibit significantly lower crosstalk than *hog1Δ* cells. Our results demonstrate that a careful comparison of laboratory yeast strains can provide insight into how signaling is regulated in the context of a natural, undisrupted signaling network. Undoubtedly there is some difference in the Sigma and YPH499 networks which permits crosstalk, but this difference could be the result of a subtle mechanism, such as differences in expression or point mutations caused by natural genetic variation, and not the result of a large disruption to the network. Future work to discover how other strains regulate the HOG and mating pathways, particularly in comparison to S288C-derived strains, will provide insight into the diverse mechanisms by which signaling may be regulated. More broadly, existing genetic diversity among strains in model organisms is a powerful tool for expanding our knowledge of biological processes [62]. Our results show that, even in well-studied model systems, signaling properties are not homogenous and may significantly vary between strains. Studying this natural variation will reveal how pathways can be tuned and maintained as different strains adapt to their environmental niches.

MATERIALS AND METHODS

Yeast strains and methods

Yeast culture and growth were performed using standard methods [63] and transformations were done using a lithium acetate transformation protocol [64]. For scFISH and flow cytometry experiments, cultures were grown in low fluorescence media (1.7 g/L Yeast Nitrogen Base without ammonium sulfate, without folic acid, without riboflavin [MP Biomedicals # 114030512]; 5 g/L ammonium sulfate; 20 g/L dextrose) supplemented with amino acids. Other experiments were performed in standard YPD media or synthetic complete media with the appropriate amino acid dropped out.

Genes were deleted using homologous integration of a drug selection cassette amplified from pMM0129, pMM0130, or pMM0131 and verified by colony PCR. CRISPR/Cas9-mediated allele replacements were performed by first deleting the gene of interest with a drug selection cassette followed

by transformation of a CRISPR plasmid expressing a guide RNA targeting the drug resistance gene and repair template amplified from a plasmid or genomic DNA as appropriate [65] (CRISPR plasmids were a gift from Audrey Gasch). Transformant colonies were passaged 3X in YPD media to lose the CRISPR plasmids and the integration of the allele was confirmed by sequencing. Where necessary, drug selection markers on plasmids were exchanged using circular polymerase extension cloning [66,67]. A complete list of strains and plasmids can be found in Tables S1 and S2.

The YPH499-background strain with integrated pSTL1-tdTomato and pFUS1-eGFP fluorescent reporters (yMM0736) was a gift from Jeremy Thorner, as were the plasmids containing these reporters (pMM0154 and pMM1055). The pFUS1-eGFP reporter was amplified from pMM0154 and cloned into the pYIPlac211 backbone between the BamHI and EcoRI sites. Sigma-background strain with these reporters were constructed as described [36] by digesting the reporter plasmids with an enzyme which cuts once in the promoter (NruI for *STL1* and BsaAI for *FUS1*) prior to integration. This method integrates the reporter alongside the original (undisrupted) gene.

To facilitate experiments in 96-well plates, the Sigma background was rendered non-clumpy by introducing the $AMN1^{D368V}$, which allows daughter cells to cleanly separate from mother cells [68–70] (Figure 2.8). $AMN1^{D368V}$ was introduced into yMM1174 using CRISPR/Cas9 as described above.

Osmosensitivity

To quantify osmosensitivity on YPD agar, three colonies each of YPH499 and Sigma were grown to mid-log and spotted YPD plates with various concentrations of sorbitol. Plates were imaged using a ChemiDoc (Bio-Rad) at 24 hr and 45 hr and spot intensity was quantified using the gel analyzer tool in ImageJ. Intensity on YPD+sorbitol plates was normalized to intensity on the YPD (no osmostress) plate to determine growth, and the resulting mean growth of the Sigma spots was divided by the mean growth of the YPH499 spots to determine the growth defect of Sigma relative to YPH499. The standard error of the

mean was found for the growth quantification and was propagated in the relative growth defect calculating using the standard formula.

To quantify osmosensitivity in a well-mixed culture, 3 colonies each of YPH499 and Sigma were grown to mid-log then diluted to approximately 1.5×10^6 cells/mL in YPD with or without sorbitol. Cultures were incubated with rotation at 30°C and samples were taken at 16 hr and at 41 hr. Density was quantified as the optical density at 600 nm using a spectrophotometer and samples were diluted to within the linear range of our spectrophotometer prior to measurement. Doublings were calculated by taking $\log_2 \frac{\mathrm{OD600_t}}{\mathrm{OD600_0}}$, and the number of doublings in YPH499 was subtracted from the number of doublings in Sigma to calculate the excess doublings in Sigma. The standard error of the mean for the doublings was found and propagated in the excess doublings calculation using the standard formula.

Induction time courses

Overnight cultures of the appropriate yeast strains were diluted to $1.5\text{-}3 \times 10^6$ cells/mL in LFM and allowed to grow 6-8 hr at 30°C to the mid-log phase. To induce, a sample of the mid-log culture was pipetted into a 96-well (Figure 2.3) or 24-well plate (Figure 2.2D, 2.4A,B, 2.5-2.8) containing media with sorbitol and/or pheromone. After inducing for the desired time, cycloheximide was added to a final concentration of 100 µg/mL to halt translation. Plates were sealed with BreatheEasy film and incubated shaking at 30℃ for 16-18 hr to allow fluorescent proteins to mature. For time courses, samples were induced beginning with the latest timepoint and continuing in reverse so that cycloheximide was added to all samples at the same time and all samples were allowed to fold for the same amount of time. Cycloheximide was added to the well containing the 0-minute time point prior to induction. For experiments in 24-well plates (using clumpy yMM1174-derived Sigma strains), 3X volume PBS+0.1% Tween-20 (pre-chilled to 4℃) was added to each well and plates were placed on ice. Each well was sonicated (amplitude 5, 1 sec on, 1 sec off, 1 min total) before 225 µL was transferred to a 96-well plate pre-loaded with 25 µL 0.1% methylene blue as a live-

dead stain. For experiments in 96-well plates (using non-clumpy yMM1584-derived Sigma strains), 4X volume PBS+0.1% Tween+0.0125% methylene blue was added to each well and plates were immediately placed on ice. Samples were kept on ice and in the dark prior to flow cytometry.

Flow cytometry

Samples were run on an Attune NxT Focusing Cytometer. Measurements were taken in the forward scatter (FSC), side scatter (SSC), BL1 (488nm laser, 530/30 filter, 503LP dichroic mirror), YL1 (561nm laser, 585/16 filter, 577LP dichroic mirror) and RL2 (633 nm laser, 720/30 filter, 690LP dichroic mirror) channels. Samples were first gated for eGFP+ (BL1H) and tdTomato+ (YL1H) events which removed a significant portion of the debris and dead cells. Samples were then gated for cells using FSC-A vs SSC-A, then two successive gates for single cells were drawn using FSC-A vs FSC-H and SSC-A vs SSC-H respectively. Finally, a gate for live cells was drawn using RL2-H vs FSC-H to gate for low RL2 (live) cells. See supplementary figure 2.9 for a representative example of the gating procedure in YPH499 (Figure 2.9A) and Sigma (Figure 2.9B). At least 50,000 total events were collected for each sample. The median BL1-H and YL1-H were taken as the eGFP value and the tdTomato value respectively for each sample. For double stimulus experiments, eGFP values of the sorbitol + pheromone induced samples were normalized to a time-matched sample stimulated with pheromone alone. For crosstalk inductions, the eGFP values were normalized to a time-matched control sample induced with 0M sorbitol media to account for differences in basal pFUS1-eGFP production. All analysis was performed using FlowJo version 10.8.

Fluorescent *in situ* hybridization

Strains were grown as described above and collected for fixation and processing as described in [71]. FISH probes were designed using the Biosearch Technologies Stellaris Designer with Quasar 670 (*FUS1* probes) or Quasar 570 (*STL1* probes). Probes sequences are available in tables S3 and S4. Images were acquired as z-stacks every 0.2 mm with an epifluorescent Nikon Eclipse-TI inverted microscope using a 100x Nikon Plan Apo oil immersion objective and Clara CCD camera (Andor DR328G, South Windsor, Connecticut,

United States of America). Quasar 670 emission was visualized at 700 nm upon excitation at 620 nm (Chroma 49006_Nikon ET-Cy5 filter cube, Chroma Technologies, Bellows Falls, Vermont, USA). Quasar 570 emission was visualized at 605 nm upon excitation at 545 nm (Chroma 49004_Nikon ET-Cy3 filter cube). Transcripts were counted by semiautomated transcript detection and counting in MATLAB using scripts adapted from [72].

REFERENCES

1 Widmann C, Gibson S, Jarpe MB & Johnson GL (1999) Mitogen-Activated Protein Kinase: Conservation of a Three-Kinase Module From Yeast to Human. *Physiological Reviews* **79**, 143–180.

2 Braicu C, Buse M, Busuioc C, Drula R, Gulei D, Raduly L, Rusu A, Irimie A, Atanasov AG, Slaby O, Ionescu C & Berindan-Neagoe I (2019) A Comprehensive Review on MAPK: A Promising Therapeutic Target in Cancer. *Cancers (Basel)* **11**, 1618.

3 Lavoie H, Gagnon J & Therrien M (2020) ERK signalling: a master regulator of cell behaviour, life and fate. *Nat Rev Mol Cell Biol* **21**, 607–632.

4 Scott TD, Sweeney K & McClean MN (2019) Biological signal generators: integrating synthetic biology tools and in silico control. *Curr Opin Syst Biol* **14**, 58–65.

5 Maeda T, Wurgler-Murphy SM & Saito H (1994) A two-component system that regulates an osmosensing MAP kinase cascade in yeast. *Nature* **369**, 242–245.

6 Maeda T, Takekawa M & Saito H (1995) Activation of yeast PBS2 MAPKK by MAPKKKs or by binding of an SH3-containing osmosensor. *Science* **269**, 554–558.

7 Posas F & Saito H (1997) Osmotic activation of the HOG MAPK pathway via Ste11p MAPKKK: Scaffold role of Pbs2p MAPKK. *SCIENCE* **276**, 1702–1708.

8 Brewster JL, Valoir T de, Dwyer ND, Winter E & Gustin MC (1993) An osmosensing signal transduction pathway in yeast. *Science* **259**, 1760–1763.

9 Posas F, Chambers JR, Heyman JA, Hoeffler JP, Nadal E de & Ariño J (2000) The Transcriptional Response of Yeast to Saline Stress. *J Biol Chem* **275**, 17249–17255.

10 Rep M, Krantz M, Thevelein JM & Hohmann S (2000) The Transcriptional Response of Saccharomyces cerevisiae to Osmotic Shock. *J Biol Chem* **275**, 8290–8300.

11 Roberts RL & Fink GR (1994) Elements of a single map kinase cascade in Saccharomyces cerevisiae mediate two developmental programs in the same cell type: Mating and invasive growth. *GENES DEV* **8**, 2974–2985.

12 Simon M-N, Virgilio CD, Souza B, Pringle JR, Abo A & Reed SI (1995) Role for the Rho-family GTPase Cdc42 in yeast mating-pheromone signal pathway. *Nature* **376**, 702–705.

13 Moskow JJ, Gladfelter AS, Lamson RE, Pryciak PM & Lew DJ (2000) Role of Cdc42p in Pheromone-Stimulated Signal Transduction in Saccharomyces cerevisiae. *Molecular and Cellular Biology* **20**, 7559–7571.

14 Van Drogen F, O'Rourke SM, Stucke VM, Jaquenoud M, Neiman AM & Peter M (2000) Phosphorylation of the MEKK Ste11p by the PAK-like kinase Ste20p is required for MAP kinase signaling in vivo. *Curr Biol* **10**, 630–639.

15 Leberer E, Wu C, Leeuw T, Fourest-Lieuvin A, Segall JE & Thomas DY (1997) Functional characterization of the Cdc42p binding domain of yeast Ste20p protein kinase. *EMBO J* **16**, 83–97.

16 Peter M, Neiman AM, Park HO, van Lohuizen M & Herskowitz I (1996) Functional analysis of the interaction between the small GTP binding protein Cdc42 and the Ste20 protein kinase in yeast. *EMBO J* **15**, 7046–7059.

17 Neiman AM & Herskowitz I (1994) Reconstitution of a yeast protein kinase cascade in vitro: Activation of the yeast MEK homologue STE7 by STE11. *PROC NATL ACAD SCI U S A* **91**, 3398–3402.

18 Zheng C-F & Guan K-L (1994) Activation of MEK family kinases requires phosphorylation of two conserved Ser/Thr residues. *EMBO Journal* **13**, 1123–1131.

19 Errede B, Gartner A, Zhou Z, Nasmyth K & Ammerer G (1993) MAP kinase-related FUS3 from S. cerevisiae is activated by STE7 in vitro. *Nature* **362**, 261–264.

20 Gartner A, Nasmyth K & Ammerer G (1992) Signal transduction in Saccharomyces cerevisiae requires tyrosine and threonine phosphorylation of FUS3 and KSS1. *Genes and Development* **6**, 1280–1292.

21 Ma D, Cook JG & Thorner J (1995) Phosphorylation and localization of Kss1, a MAP kinase of the Saccharomyces cerevisiae pheromone response pathway. *MOL BIOL CELL* **6**, 889–909.

22 Bardwell L, Cook JG, Chang EC, Cairns BR & Thorner J (1996) Signaling in the yeast pheromone response pathway: specific and high-affinity interaction of the mitogen-activated protein (MAP) kinases Kss1 and Fus3 with the upstream MAP kinase kinase Ste7. *Molecular and Cellular Biology* **16**, 3637–3650.

23 Elion EA, Brill JA & Fink GR (1991) Functional Redundancy in the Yeast Cell Cycle: FUS3 and KSS1 Have Both Overlapping and Unique Functions. *Cold Spring Harbor Symposia on Quantitative Biology* **56**, 41–49.

24 Breitkreutz A, Boucher L & Tyers M (2001) MAPK specificity in the yeast pheromone response independent of transcriptional activation. *Current Biology* **11**, 1266–1271.

25 Schwartz MA & Madhani HD (2006) Control of MAPK signaling specificity by a conserved residue in the MEK-binding domain of the yeast scaffold protein Ste5. *Curr Genet* **49**, 351–363.

26 Winters MJ & Pryciak PM (2018) Analysis of the thresholds for transcriptional activation by the yeast MAP kinases Fus3 and Kss1. *Molecular Biology of the Cell* **29**, 669–682.

27 Sabbagh W, Flatauer LJ, Bardwell AJ & Bardwell L (2001) Specificity of MAP kinase signaling in yeast differentiation involves transient versus sustained MAPK activation. *Mol Cell* **8**, 683–691.

28 Bardwell L, Cook JG, Zhu-Shimoni JX, Voora D & Thorner J (1998) Differential regulation of transcription: Repression by unactivated mitogen-activated protein kinase Kss1 requires the Dig1 and Dig2 proteins. *Proceedings of the National Academy of Sciences* **95**, 15400–15405.

29 O'Rourke SM & Herskowitz I (1998) The Hog1 MAPK prevents cross talk between the HOG and pheromone response MAPK pathways in Saccharomyces cerevisiae. *Genes Dev* **12**, 2874–2886.

30 Harris K, Lamson RE, Nelson B, Hughes TR, Marton MJ, Roberts CJ, Boone C & Pryciak PM (2001) Role of scaffolds in MAP kinase pathway specificity revealed by custom design of pathway-dedicated signaling proteins. *Curr Biol* **11**, 1815–1824.

31 McClean MN, Mody A, Broach JR & Ramanathan S (2007) Cross-talk and decision making in MAP kinase pathways. *Nat Genet* **39**, 409–414.

32 Westfall PJ & Thorner J (2006) Analysis of Mitogen-Activated Protein Kinase Signaling Specificity in Response to Hyperosmotic Stress: Use of an Analog-Sensitive HOG1 Allele. *Eukaryotic Cell* **5**, 1215–1228.

33 Westfall PJ, Patterson JC, Chen RE & Thorner J (2008) Stress resistance and signal fidelity independent of nuclear MAPK function. *Proceedings of the National Academy of Sciences* **105**, 12212–12217.

34 Reményi A, Good MC, Bhattacharyya RP & Lim WA (2005) The role of docking interactions in mediating signaling input, output, and discrimination in the yeast MAPK network. *Molecular Cell* **20**, 951–962.

35 Sikorski RS & Hieter P (1989) A system of shuttle vectors and yeast host strains designed for efficient manipulation of DNA in Saccharomyces cerevisiae. *Genetics* **122**, 19–27.

36 Patterson JC, Klimenko ES & Thorner J (2010) Single-Cell Analysis Reveals That Insulation Maintains Signaling Specificity Between Two Yeast MAPK Pathways with Common Components. *Sci Signal* **3**, ra75–ra75.

37 Madhani HD & Fink GR (1997) Combinatorial control required for the specificity of yeast MAPK signaling. *Science* **275**, 1314–1317.

38 Gimeno CJ, Ljungdahl PO, Styles CA & Fink GR (1992) Unipolar cell divisions in the yeast S. cerevisiae lead to filamentous growth: Regulation by starvation and RAS. *Cell* **68**, 1077–1090.

39 Dowell RD, Ryan O, Jansen A, Cheung D, Agarwala S, Danford T, Bernstein DA, Rolfe PA, Heisler LE, Chin B, Nislow C, Giaever G, Phillips PC, Fink GR, Gifford DK & Boone C (2010) Genotype to Phenotype: A Complex Problem. *Science* **328**, 469–469.

40 Chin BL, Ryan O, Lewitter F, Boone C & Fink GR (2012) Genetic Variation in Saccharomyces cerevisiae: Circuit Diversification in a Signal Transduction Network. *Genetics* **192**, 1523–1532.
41 Song G, Dickins BJA, Demeter J, Engel S, Dunn B & Cherry JM (2015) AGAPE (Automated Genome Analysis PipelinE) for Pan-Genome Analysis of Saccharomyces cerevisiae. *PLOS ONE* **10**, e0120671.
42 Nagiec MJ & Dohlman HG (2012) Checkpoints in a Yeast Differentiation Pathway Coordinate Signaling during Hyperosmotic Stress. *PLOS Genetics* **8**, e1002437.
43 Hao N, Behar M, Parnell SC, Torres MP, Borchers CH, Elston TimothyC & Dohlman HG (2007) A Systems-Biology Analysis of Feedback Inhibition in the Sho1 Osmotic-Stress-Response Pathway. *Curr Biol* **17**, 659–667.
44 Hersen P, McClean MN, Mahadevan L & Ramanathan S (2008) Signal processing by the HOG MAP kinase pathway. *Proceedings of the National Academy of Sciences* **105**, 7165–7170.
45 Macia J, Regot S, Peeters T, Conde N, Solé R & Posas F (2009) Dynamic Signaling in the Hog1 MAPK Pathway Relies on High Basal Signal Transduction. *Sci Signal* **2**, ra13–ra13.
46 Granados AA, Crane MM, Montano-Gutierrez LF, Tanaka RJ, Voliotis M & Swain PS (2017) Distributing tasks via multiple input pathways increases cellular survival in stress. *eLife Sciences* **6**, e21415.
47 Bonhivers M, Carbrey JM, Gould SJ & Agre P (1998) Aquaporins in Saccharomyces: GENETIC AND FUNCTIONAL DISTINCTIONS BETWEEN LABORATORY AND WILD-TYPE STRAINS*. *Journal of Biological Chemistry* **273**, 27565–27572.
48 Carbrey JM, Bonhivers M, Boeke JD & Agre P (2001) Aquaporins in Saccharomyces: Characterization of a second functional water channel protein. *Proceedings of the National Academy of Sciences* **98**, 1000–1005.
49 Laizé V, Gobin R, Rousselet G, Badier C, Hohmann S, Ripoche P & Tacnet F (1999) Molecular and Functional Study ofAQY1fromSaccharomyces cerevisiae:Role of the C-Terminal Domain. *Biochemical and Biophysical Research Communications* **257**, 139–144.
50 Miermont A, Waharte F, Hu S, McClean MN, Bottani S, Léon S & Hersen P (2013) Severe osmotic compression triggers a slowdown of intracellular signaling, which can be explained by molecular crowding. *PNAS* **110**, 5725–5730.
51 Chan RK & Otte CA (1982) Physiological characterization of Saccharomyces cerevisiae mutants supersensitive to G1 arrest by a factor and alpha factor pheromones. *Molecular and Cellular Biology* **2**, 21–29.
52 Ballensiefen W & Schmitt HD (1997) Periplasmic Barl Protease of Saccharomyces Cerevisiae is Active Before Reaching its Extracellular Destination. *European Journal of Biochemistry* **247**, 142–147.
53 Manney TR (1983) Expression of the BAR1 gene in Saccharomyces cerevisiae: induction by the alpha mating pheromone of an activity associated with a secreted protein. *Journal of Bacteriology* **155**, 291–301.
54 Hagen DC, McCaffrey G & Sprague GF (1991) Pheromone response elements are necessary and sufficient for basal and pheromone-induced transcription of the FUS1 gene of Saccharomyces cerevisiae. *Molecular and Cellular Biology* **11**, 2952–2961.
55 Remize F, Cambon B, Barnavon L & Dequin S (2003) Glycerol formation during wine fermentation is mainly linked to Gpd1p and is only partially controlled by the HOG pathway. *Yeast* **20**, 1243–1253.
56 Mitchell A, Wei P & Lim WA (2015) Oscillatory stress stimulation uncovers an Achilles' heel of the yeast MAPK signaling network. *Science* **350**, 1379–1383.
57 BIONDI RM & NEBREDA AR (2003) Signalling specificity of Ser/Thr protein kinases through docking-site-mediated interactions. *Biochemical Journal* **372**, 1–13.
58 Holland PM & Cooper JA (1999) Protein modification: Docking sites for kinases. *Current Biology* **9**, R329–R331.

59 Pryciak PM & Huntress FA (1998) Membrane recruitment of the kinase cascade scaffold protein Ste5 by the Gβγ complex underlies activation of the yeast pheromone response pathway. *Genes and Development* **12**, 2684–2697.

60 Zarrinpar A, Bhattacharyya RP, Nittler MP & Lim WA (2004) Sho1 and Pbs2 act as coscaffolds linking components in the yeast high osmolarity MAP kinase pathway. *Mol Cell* **14**, 825–832.

61 Flatauer LJ, Zadeh SF & Bardwell L (2005) Mitogen-activated protein kinases with distinct requirements for Ste5 scaffolding influence signaling specificity in Saccharomyces cerevisiae. *Mol Cell Biol* **25**, 1793–1803.

62 Gasch AP, Payseur BA & Pool JE (2016) The Power of Natural Variation for Model Organism Biology. *Trends in Genetics* **32**, 147–154.

63 Amberg DC, Burke DJ & Strathern JN (2005) *Methods in yeast genetics: a cold spring habor laboratory course manual* Cold Spring Harbor Laboratory Press, New York.

64 Gietz RD & Schiestl RH (2007) High-efficiency yeast transformation using the LiAc/SS carrier DNA/PEG method. *Nature Protocols* **2**, 31–34.

65 Kuang MC, Kominek J, Alexander WG, Cheng J-F, Wrobel RL & Hittinger CT (2018) Repeated Cis-Regulatory Tuning of a Metabolic Bottleneck Gene during Evolution. *Mol Biol Evol* **35**, 1968–1981.

66 Quan J & Tian J (2009) Circular Polymerase Extension Cloning of Complex Gene Libraries and Pathways. *PLOS ONE* **4**, e6441.

67 Quan J & Tian J (2011) Circular polymerase extension cloning for high-throughput cloning of complex and combinatorial DNA libraries. *Nat Protoc* **6**, 242–251.

68 Yvert G, Brem RB, Whittle J, Akey JM, Foss E, Smith EN, Mackelprang R & Kruglyak L (2003) Trans-acting regulatory variation in Saccharomyces cerevisiae and the role of transcription factors. *Nat Genet* **35**, 57–64.

69 Fang O, Hu X, Wang L, Jiang N, Yang J, Li B & Luo Z (2018) Amn1 governs post-mitotic cell separation in Saccharomyces cerevisiae. *PLOS Genetics* **14**, e1007691.

70 Kuzdzal-Fick JJ, Chen L & Balázsi G (2019) Disadvantages and benefits of evolved unicellularity versus multicellularity in budding yeast. *Ecology and Evolution* **9**, 8509–8523.

71 McIsaac RS, Silverman SJ, Parsons L, Xu P, Briehof R, McClean MN & Botstein D (2013) Visualization and Analysis of mRNA Molecules Using Fluorescence In Situ Hybridization in Saccharomyces cerevisiae. *JoVE (Journal of Visualized Experiments)*, e50382.

72 Raj A, van den Bogaard P, Rifkin SA, van Oudenaarden A & Tyagi S (2008) Imaging individual mRNA molecules using multiple singly labeled probes. *Nat Methods* **5**, 877–879.

73 History of Sigma - SGD-Wiki *https://wiki.yeastgenome.org/index.php/History_of_Sigma*.

74 Goldstein AL & McCusker JH (1999) Three new dominant drug resistance cassettes for gene disruption in Saccharomyces cerevisiae. *Yeast* **15**, 1541–1553.

75 Gietz RD & Akio S (1988) New yeast-Escherichia coli shuttle vectors constructed with in vitro mutagenized yeast genes lacking six-base pair restriction sites. *Gene* **74**, 527–534.

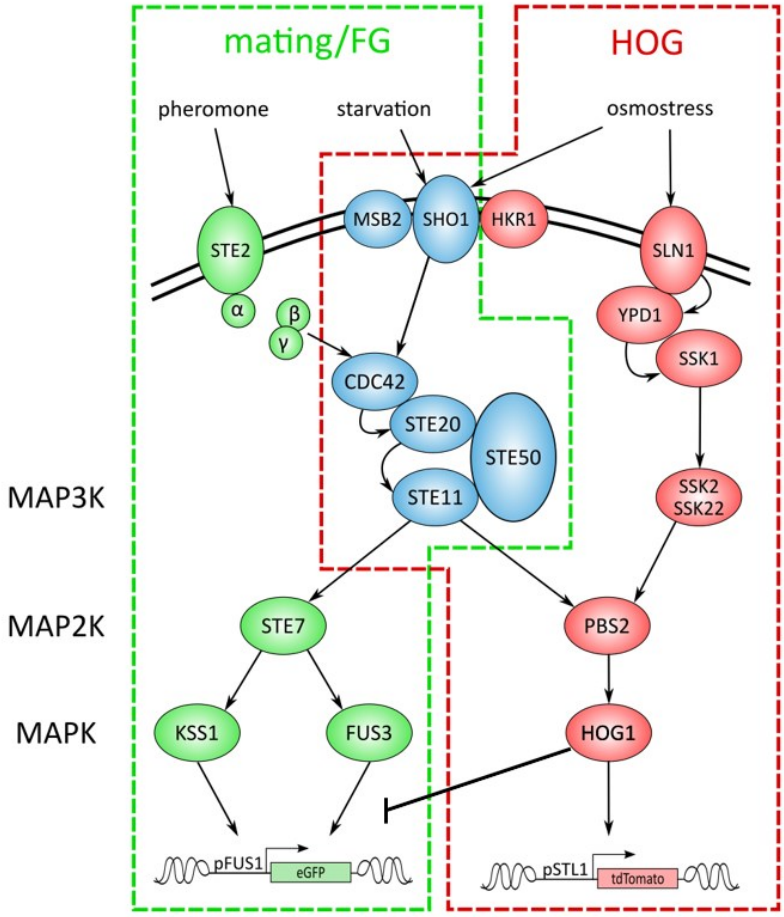

Figure 2.1: Yeast MAPK pathways

In yeast, the responses to pheromone, nutrient starvation, and hyperosmotic stress are controlled by mitogen-activated protein kinase (MAPK) networks termed the mating pathway, filamentous growth (FG) pathway, and the high osmolarity glycerol (HOG) pathway respectively. The HOG pathway is outlined in red, and the mating/FG pathways are outlined in green. Components belonging to the mating pathway only are shown in green; components belonging to the HOG pathway only are shown in red; blue components belong to more than one of the three pathways. In our experiments, activation of the HOG pathway results in expression of pSTL1-tdTomato and mating/FG pathway activity results in expression of pFUS1-eGFP.

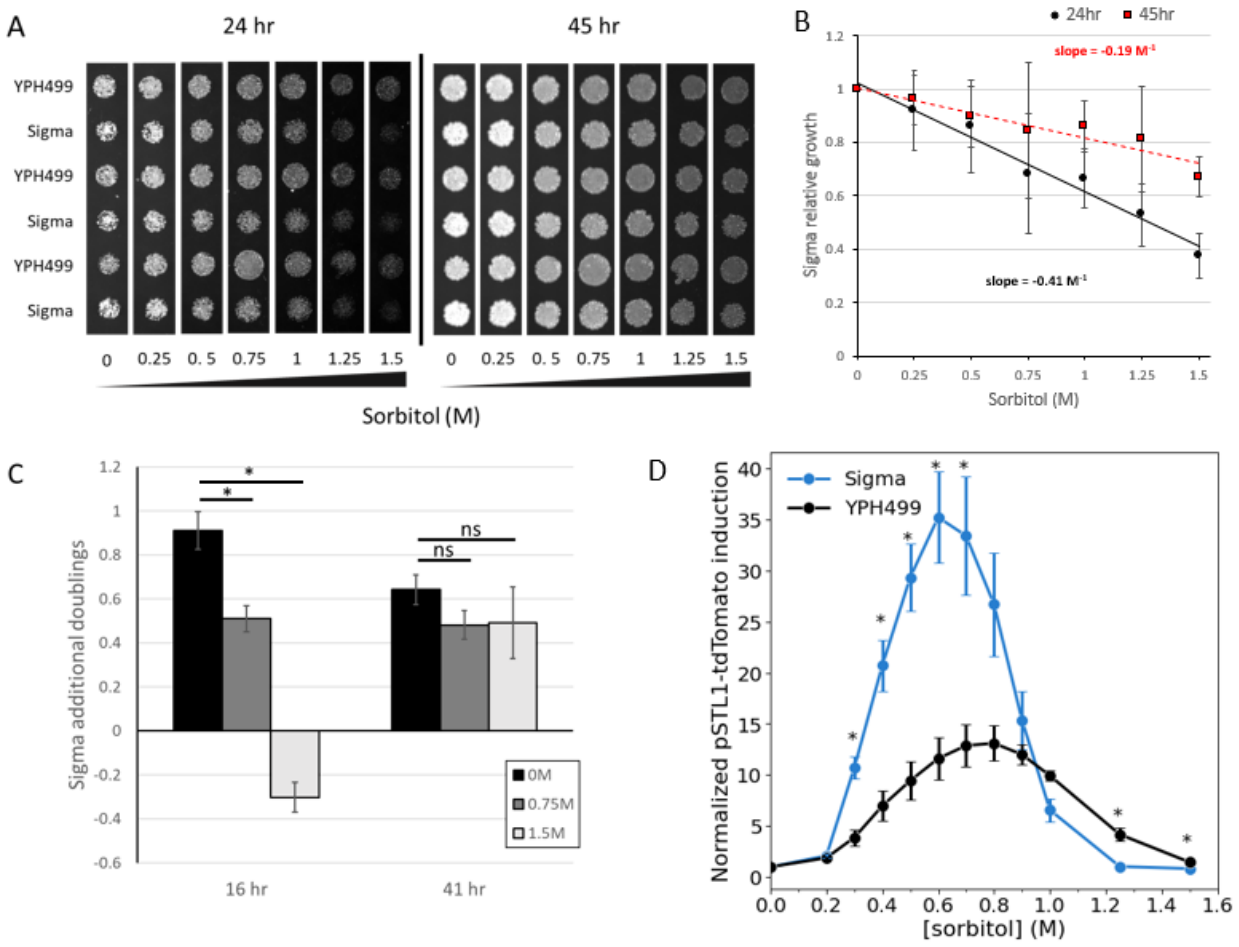

Figure 2.2: Sigma is more osmosensitive than YPH499

A: Spot tests of YPH499 and Sigma on varying concentrations of sorbitol after 24 hr (left) and 45 hr (right) at 30°C.

B: Quantification of the growth defect in Sigma relative to YPH499 as a function of sorbitol concentration. The quantification was done at 24 hr (black circles) and at 45 hr (red squares). The slope of the line represents the relative growth defect in Sigma per molar sorbitol. Plotted are mean ± standard error of the mean (s.e.m.) of 3 biological replicates.

C: Growth of YPH499 and Sigma in liquid YPD with or without sorbitol. OD600 measurements were used to calculate the number of doublings at 16 hr and 45 hr of 3 cultures each of Sigma and YPH499 in YPD with the indicated dose of sorbitol. Bars represent the mean ± s.e.m. of the difference between the Sigma

doublings and the YPH499 doublings. p-values calculated using two-sided student's t-test with equal variance. *p<0.05. n.s., not significant.

D: Induction of pSTL1-tdTomato in YPH499 (gray) and Sigma (blue) after 45 minutes in various doses of sorbitol. Plotted are mean ± s.e.m. of 3 biological replicates.

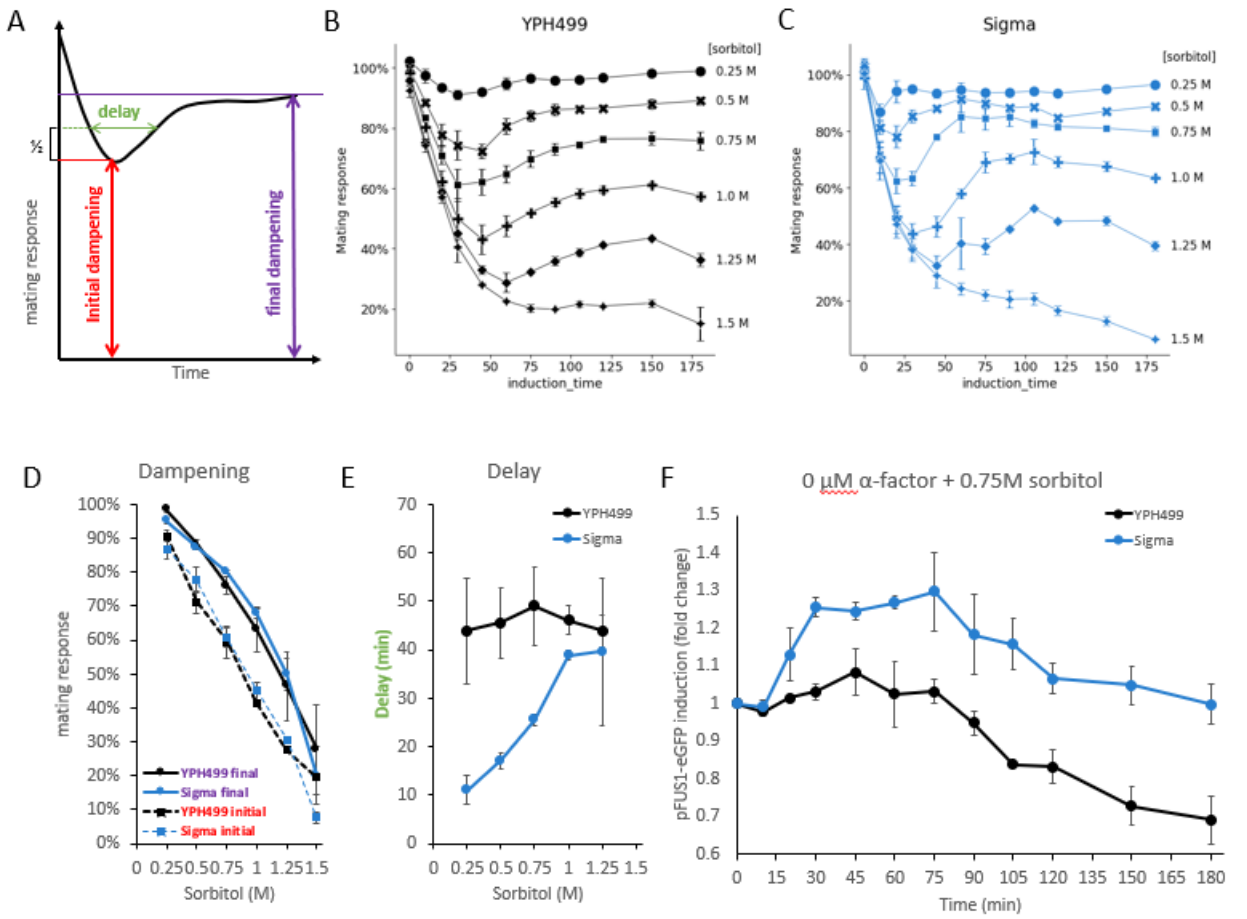

Figure 2.3: Effect of osmostress on mating pathway activation

A: Sorbitol disruption of the mating pathway consists of a strong initial dampening followed by recovery to a final dampening level. Initial dampening – minimum value of curve; final dampening – average of 150 min. and 180 min. time points. Delay is calculated as the full-width half minimum.

B: Effect of various concentrations of sorbitol on mating pathway induction in YPH499 at 10 µM α-factor. Points and error bars are mean ± standard error of the mean (s.e.m.) of 3 biological replicates (0.25M – 0.75M) or 2 biological replicates (1M – 1.5M).

C: Effect of various concentrations of sorbitol on mating pathway induction in Sigma at 10 µM α-factor. Points and error bars are mean ± s.e.m. of 3 biological replicates (0.25M – 0.75M) or 2 biological replicates (1M – 1.5M).

D: Initial and final dampening due to osmostress are identical in YPH499 and Sigma. Points and error bars are mean ± s.e.m. of 3 biological replicates (0.25M – 0.75M) or 2 biological replicates (1M – 1.5M).

E: Delay as a function of sorbitol in Sigma and YPH499. Sigma has a smaller delay at low-to-moderate concentrations of sorbitol. Points and error bars are mean ± s.e.m. of 3 biological replicates (0.25M – 0.75M) or 2 biological replicates (1M – 1.5M).

F: Induction of pFUS1-eGFP in Sigma in response to sorbitol alone. Points and error bars are mean ± s.e.m. of 2 biological replicates.

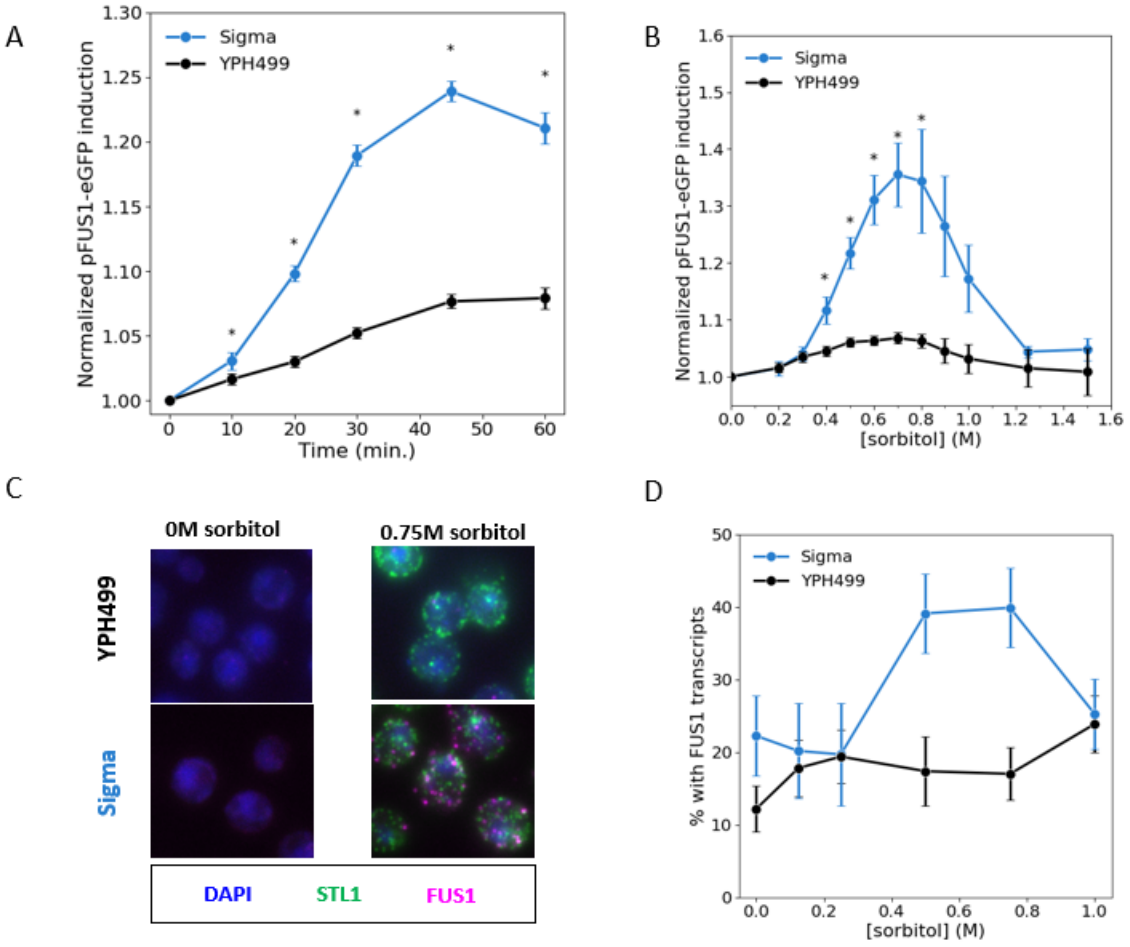

Figure 2.4: Sigma induces the mating pathway at certain levels of osmostress

A: Flow cytometry time course of sorbitol-induced pFUS1-eGFP induction in YPH499 and Sigma. Data for each strain is normalized to the t = 0 time point. (mean +/- s.e.m.; N = 19 biological replicates; Sigma t=60 is 17 biological replicates). * $p<0.05$, two-sided student's t-test with equal variance.

B: pFUS1-eGFP induction at 45 min. in the indicated concentration of sorbitol. Data for each strain is normalized to the [sorbitol] = 0 point. (mean +/- s.d.; n = 3 biological replicates). * $p<0.05$, two-sided student's t-test with equal variance.

C: Representative images of cells after a 10 minute induction with 0M sorbitol (left) or 0.75M sorbitol (right). Single mRNA transcripts appear as green (STL1) or magenta (FUS1) dots. Cells were additionally stained with DAPI (blue).

D: Proportion of cells with at least 1 FUS1 transcripts after 10 min induction with varying doses of sorbitol. Error bars represent at 95% confidence interval for the proportion of cells with FUS1 transcripts. Average N = 313 cells in each FISH experiment.

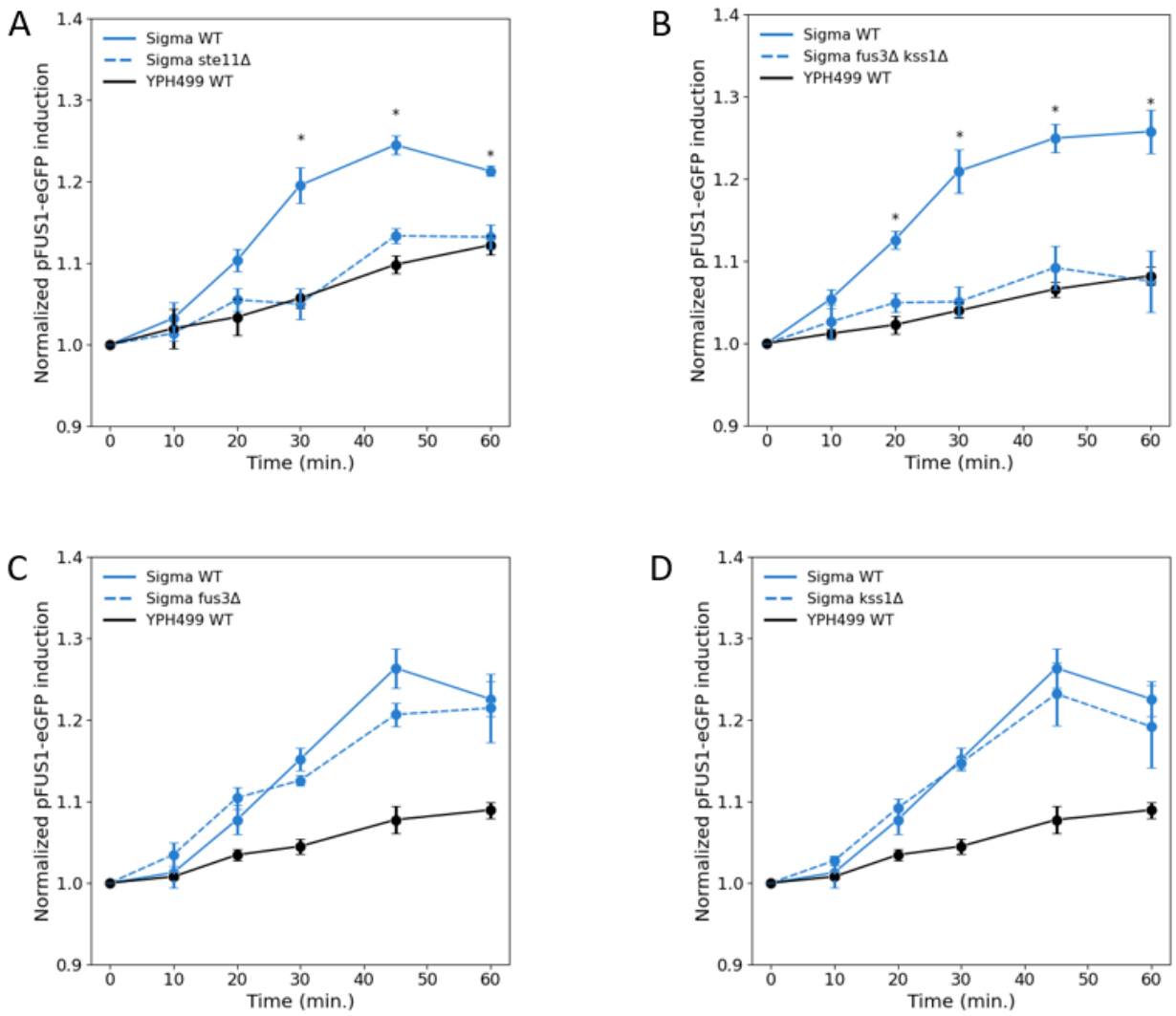

Figure 2.5: Crosstalk in Sigma is dependent on mating pathway components

Flow cytometry measurements of crosstalk in mating/FG pathway deletions. Each panel shows a Sigma background deletion (**A**: fus3Δ; **B**: kss1Δ; **C**: ste11Δ; **D**: fus3Δ kss1Δ) along with Sigma-background and YPH499-background wild-type controls. Measurements are normalized to the t = 0 timepoint. Plotted are mean +/- s.e.m.; n = 3 (panels A, C, D) or 4 (panel B) biological replicates. The wild-type controls were performed concurrently with the deletion in each panel. The fus3Δ and kss1Δ deletions (panels C and D) were measured simultaneously and the wild-type control lines are the same in both panels. *p<0.05, student's t-test with equal variance.

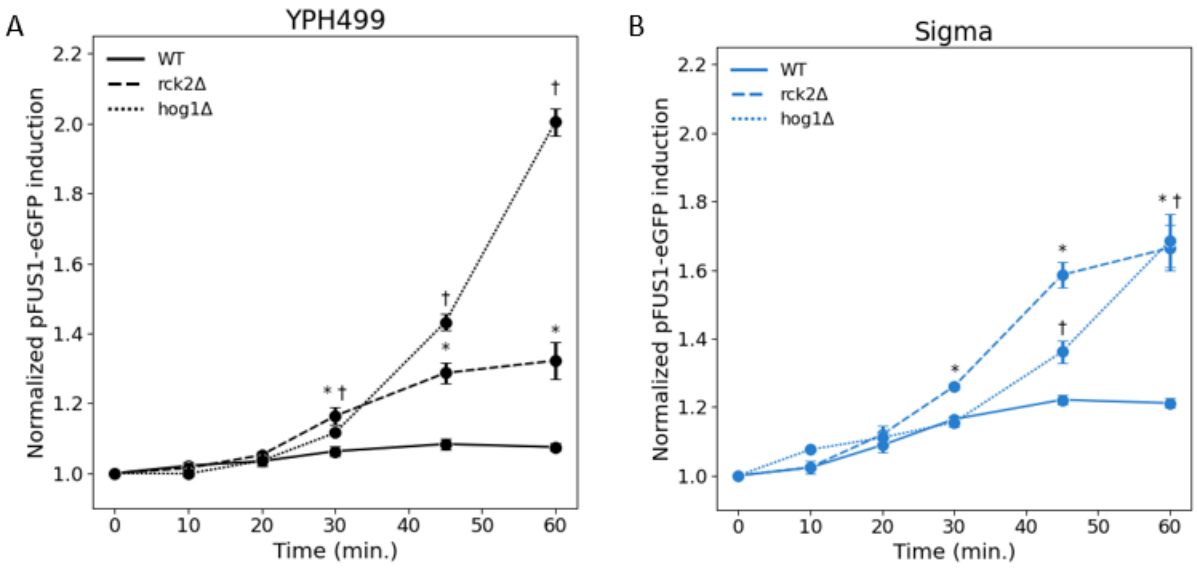

Figure 2.6: HOG-dependent suppression of crosstalk occurs late in a time course

Flow cytometry measurements of crosstalk in WT (–), *hog1Δ* (…), or *rck2Δ* (--) cells in the (A) YPH499 or (B) Sigma backgrounds. Measurements are normalized to the t = 0 time point. Mean ± s.e.m.; n = 3 biological replicates. A student's t-test with equal variance was performed between WT and *rck2Δ* (*) and between WT and *hog1Δ* (†). Markers represent points at which $p<0.05$.

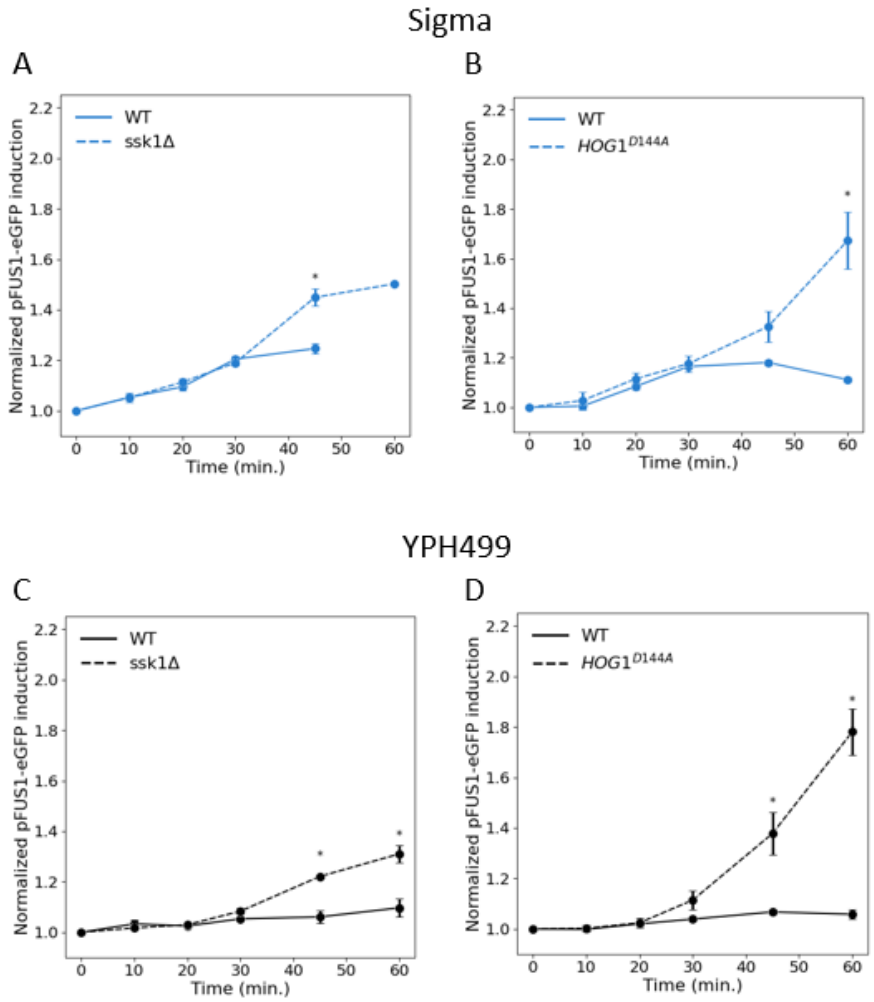

Figure 2.7: HOG pathway disruptions affect late crosstalk but not early crosstalk

Flow cytometry measurements of crosstalk in mutants which disrupt HOG pathway activity. Each panel shows a Sigma background or YPH499 background deletion of *SSK1* (panels **A, C**) and a kinase-dead *HOG1*^{D144A} mutant (panels **B, D**) along with a wild-type control. Measurements are normalized to the t = 0 time point. The wild-type controls were performed concurrently with the deletion in each panel. Mean +/- s.e.m.; N = 3 biological replicates. *p<0.05, student's t-test with equal variance.

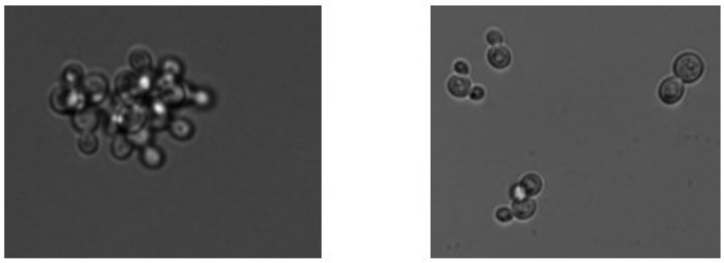

Figure 2.8: AMN1 affects clumpiness in Sigma

Introducing the *AMN1*^{D368V} allele significantly reduces clumpiness in the Sigma background.

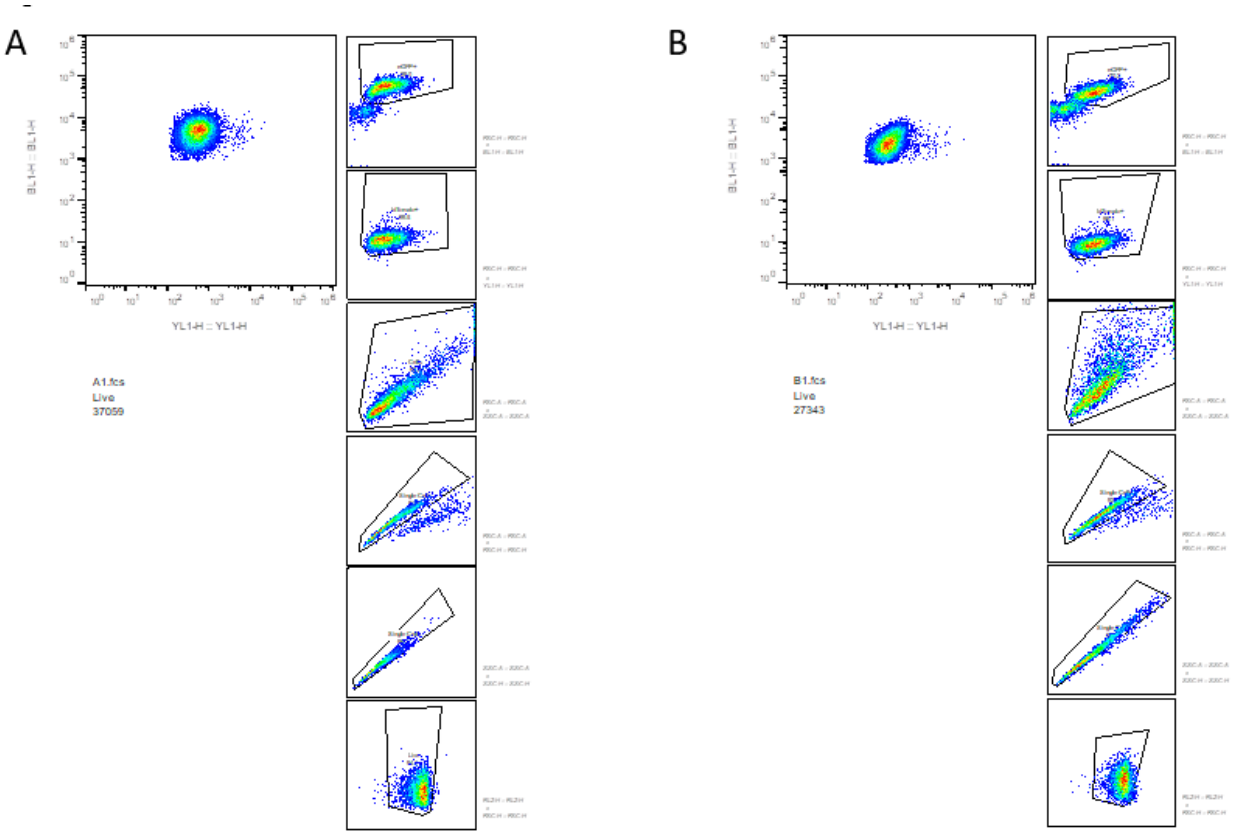

Figure 2.9: Flow cytometry gating

Representative examples of flow cytometry gating in the (**A**) YPH499 and (**B**) Sigma backgrounds.

SUPPORTING INFORMATION

Supplementary Table 2.1 List of yeast strains

Strain	Background	Genotype	Source
yMM0736 (YJP212)	YPH499[1]	MATa pSTL1::HA-tdTomato::ADE2 pFUS1::HA-eGFP::ADE1 bar1Δ::KanMX	[4]
yMM1052 (YJP406)	YPH499	yMM0736 ssk1Δ::TRP1	[4]
yMM1053 (YJP407)	YPH499	yMM0736 sho1Δ::HygMX	[4]
yMM1062	YPH499	yMM0736 fus3Δ::HygMX	This study
yMM1109	YPH499	yMM0736 ste11Δ::HygMX	This study
yMM1159	YPH499	yMM0736 kss1Δ::HygMX	This study
yMM1160	YPH499	yMM0736 fus3Δ::HygMX kss1Δ::NatMX	This study
yMM1722	YPH499	yMM0736 hog1Δ::HygMX	This study
yMM1723	YPH499	yMM0736 HOG1(D144A)	This study
yMM1724	YPH499	yMM0736 rck2Δ::HygMX	This study
yMM0964	Sigma[2]	MATa	David Botstein
yMM0985	Sigma	MATa bar1Δ::NatMX	This study
yMM1124	Sigma	MATa leu2Δ0 ura3Δ0	David Botstein
yMM1127	Sigma	MATa leu2Δ0 ura3Δ0 pSTL1::HA-tdTomato::LEU2	This study
yMM1128	Sigma	MATa leu2Δ0 ura3Δ0 pSTL1::HA-tdTomato::LEU2 bar1Δ::NatMX	This study

[1] YPH499 genotype: MATa ura3-52 lys2-801_amber ade2-101_ochre trp1-Δ63 his3-Δ200 leu2-Δ1 [1]
[2] Sigma2000, MATa prototroph derived from Σ1278b [2]

yMM1174	Sigma	MATa pSTL1::HA-tdtomato::LEU2 pFUS1::HA-eGFP::URA3 bar1Δ::NatMX	This study
yMM1179	Sigma	yMM1174 sho1Δ::HygMX	This study
yMM1180	Sigma	yMM1174 ste11Δ::HygMX	This study
yMM1181	Sigma	yMM1174 ssk1Δ::HygMX	This study
yMM1182	Sigma	yMM1174 kss1Δ::HygMX	This study
yMM1183	Sigma	yMM1174 fus3Δ::HygMX	This study
yMM1185	Sigma	yMM1174 fus3Δ::HygMX kss1Δ::KanMX	This study
yMM1583	Sigma	yMM1174 amn1Δ::KanMX	This study
yMM1584	Sigma	yMM1174 AMN1(D368V)	This study
yMM1725	Sigma	yMM1174 hog1Δ::HygMX	This study
yMM1726	Sigma	yMM1174 HOG1(D144A)	This study
yMM1727	Sigma	yMM1174 rck2Δ::HygMX	This study

Supplementary Table 2.2 List of plasmids

Plasmid	Description	Source
pMM0004	pRS406	[1]
pMM0025	pRS316 HOG1	Sharad Ramanathan
pMM0129	pFA6 NatMX	[3]
pMM0130	pFA6 HygMX	[3]
pMM0131	pFA6 KanMX	[3]
pMM0154	YIPlac128 pFUS1-HA-eGFP	[4]
pMM0155	YIPlac128 pSTL1-HA-tdtomato	[4]
pMM0292	YIPlac211	[5]
pMM0300	pYIPlac211 pFUS1-HA-eGFP	This study
pMM0887	pXIPHOS-NatMX pSNR52-KanMX sgRNA-tSNR52	Audrey Gasch
pMM0888	pXIPHOS-NatMX pSNR52-HygMX sgRNA-tSNR53	Audrey Gasch
pMM0889	pXIPHOS-NatMX pSNR52-tSNR54	Audrey Gasch
pMM0890	pXIPHOS-HygMX pSNR52-KanMX sgRNA-tSNR55	This study
pMM0891	pXIPHOS-HygMX pSNR52-tSNR56	This study
pMM0904	pHS2-KanMX	This study
pMM1232	pXIPHOS-KanMX pSNR52-HygMX sgRNA-tSNR53	This study
pMM1233	pXIPHOS-KanMX pSNR52-tSNR54	This study
pMM1234	pRS316 HOG1^{D144A}	This study

Supplementary Table 2.3 *STL1* FISH probe sequences

Sequence	Name
cagtgactggttctgcttat	STL1_1
caacttcttacccgtaagtc	STL1_2
cgtcatagatgcgatagtga	STL1_3
tcgtatccaaacagggagaa	STL1_4
tagacttgccatcaaccctt	STL1_5
ccattttctttggttgctgg	STL1_6
agttgcgtgtctgtcatgat	STL1_7
tcataacaggaggttgtagc	STL1_8
agaacctgcgaaacaaccta	STL1_9
caccgcagaacataacgaat	STL1_10
gaacccatcaggattaatgg	STL1_11
cggcaccaatgatggttatt	STL1_12
cacgaaatgcgcatgtagaa	STL1_13
ataaactggcctaatgccca	STL1_14
attcaaccctgttccaacac	STL1_15
gccaaacgggaatagtagat	STL1_16
gcaaccctctattttcagct	STL1_17
ccaaaagcaattgtggaacc	STL1_18
ctgttggtataagacaaccc	STL1_19
tttgcattgacacggggaat	STL1_20
agcaggaagagagcaaaaac	STL1_21
gtggcgattcaggtagttta	STL1_22
cgactttgagaaatcagcca	STL1_23
taccaagtagcgagcttctt	STL1_24
ttcctcatcatttggatccg	STL1_25

gtgaagcatagcaacttctg	STL1_26
gtttggtcctgttaacagca	STL1_27
ggagaacaaacttgacagtg	STL1_28
tctgaagattttgggacctg	STL1_29
gttgaagctgcaatcaaagc	STL1_30
gcagcgttacaaccagtaaa	STL1_31
ccccacctatgatcattgat	STL1_32
aaggcgtagattgttgcgaa	STL1_33
gcttacgtctacctagcttt	STL1_34
gacctgtggcacctaataaa	STL1_35
gcacctcttgcgttttcttt	STL1_36
gaacaaaaataagccgacgg	STL1_37
ggtgggtatatccatggtaa	STL1_38
gcacgaactttcattgatgc	STL1_39
tgtggagaaagcgtttgttg	STL1_40
ccgcaaagttacacaaccaa	STL1_41
caaccggactgtccaataaa	STL1_42
cggtttcagggtagaaaaag	STL1_43
gtcgatttcctccaaacttc	STL1_44
cctcgtatgctttagcaaag	STL1_45
tagcaactctccatggttga	STL1_46
agggataacttgggcaaatg	STL1_47
ggcatgatcttcgacttctt	STL1_48

Supplementary Table 2.4 *FUS1* FISH probe sequences

Sequence	Name
gtcgtctgcattattgttgc	FUS1_1
taaggtagtagacattgcgg	FUS1_2
ggaactagcttgcgaagata	FUS1_3
cgttactgttgttacactcg	FUS1_4
gagcgtattgatgtcgctat	FUS1_5
ccgccacattagaaaagagt	FUS1_6
gctgaagatgattttggctg	FUS1_7
gattgaaagcccaattgtgc	FUS1_8
cagaatattccgatgggaag	FUS1_9
gaaatggacaccgaattcct	FUS1_10
ttggaatcgtagctgacatg	FUS1_11
ttagtgcggcgacaatattc	FUS1_12
ccaaaataaccgtgagaacc	FUS1_13
tctgatcctcacacttactc	FUS1_14
gggtgtcgttatacttctca	FUS1_15
aagacatgttatcacccgag	FUS1_16
gcggtattatgggtttggaa	FUS1_17
ccgttttcttaggtgtcagt	FUS1_18
gaccaagcatatgggttctt	FUS1_19
ctttggggtctaacgaaatg	FUS1_20
ctttctcttcctccatttcg	FUS1_21
gtatacaggaatgcatccac	FUS1_22
gcatgctggattcaatatgg	FUS1_23
gacaccgtttttgagaagg	FUS1_24
ctcactcgtttttaacgcag	FUS1_25

gtggagattcgtaactccat	FUS1_26
tagaacccctcaagaaccat	FUS1_27
ggggtctttaaagaggtctt	FUS1_28
atttgcttcagttgtggagc	FUS1_29
acttatccgggagagcattt	FUS1_30
ctgactcattgaagtaaccc	FUS1_31
gatcgttcgtcaggcattat	FUS1_32
gaggcgtgttattatactcc	FUS1_33
cccaagttattcacactgtc	FUS1_34
ttgtgaatctggcgtggtat	FUS1_35
gccgtgattagatcgatgtt	FUS1_36
gtatatcactgaatggggtc	FUS1_37
ctcgtgtttctcagtgcttt	FUS1_38
ttgatggggtgggtattatc	FUS1_39
gcaatggtttagaacgtgac	FUS1_40
cctccccattatatttggag	FUS1_41
atgtcttccctaattggacg	FUS1_42
ggctcgtaatcctgaataac	FUS1_43
ccagcgagattcttatttcg	FUS1_44
ggtatgagtggccagaattt	FUS1_45
tttctaccagacaccatcca	FUS1_46
ctgacgtgaatagaaccctt	FUS1_47
gcctctatcttcattgaggt	FUS1_48

References

1 Sikorski RS & Hieter P (1989) A system of shuttle vectors and yeast host strains designed for efficient manipulation of DNA in Saccharomyces cerevisiae. *Genetics* **122**, 19–27.

2 History of Sigma - SGD-Wiki *https://wiki.yeastgenome.org/index.php/History_of_Sigma*.

3 Goldstein AL & McCusker JH (1999) Three new dominant drug resistance cassettes for gene disruption in Saccharomyces cerevisiae. *Yeast* **15**, 1541–1553.

4 Patterson JC, Klimenko ES & Thorner J (2010) Single-Cell Analysis Reveals That Insulation Maintains Signaling Specificity Between Two Yeast MAPK Pathways with Common Components. *Sci Signal* **3**, ra75–ra75.

5 Gietz RD & Akio S (1988) New yeast-Escherichia coli shuttle vectors constructed with in vitro mutagenized yeast genes lacking six-base pair restriction sites. *Gene* **74**, 527–534.

Chapter 3: Identification of genetic loci associated with differences in signaling in closely related strains of yeast

This chapter is in preparation for submission.

Taylor Scott constructed strains and plasmids, performed experiments, and analyzed the data. Althys Cao assisted in strain construction and performed experiments. Morgan Lekschas assisted in strain construction and performed experiments. Taylor Scott and Megan McClean wrote the paper.

ABSTRACT

Mitogen-activated protein kinase networks are a fundamental archetype of signaling present in all eukaryotes. In the budding yeast *Saccharomyces cerevisiae,* the response to pheromone is governed by one such network, known as the mating pathway. The precise signaling response to pheromone is tuned differently in different laboratory strains, despite the pathway existing in a functioning form in these strains. For example, in the strain Σ1278b, signal leaks from the osmotic stress response pathway into the mating pathway, a process known as crosstalk, while no such leakage occurs in the YPH499 strain background. Separately, basal expression of a mating pathway reporter, pFUS1-eGFP, is significantly higher in the YPH499 background than in the Σ1278b background. Here we identify genetic loci associated with these signaling phenotypes through a bulk segregant approach. Specifically, we show that the left arm of chromosome III may regulate basal expression of the mating pathway reporter and identify *STE50* and *FYV5* as genes which have a significant, strain dependent effect on reporter expression. We also show that a locus on chromosome XV is associated with crosstalk in the Σ1278b background, although we were unable to identify a specific gene causing this phenotype. Our results demonstrate that differences among closely related laboratory strains are an important tool for studying how small changes alter signaling despite the overall network remaining intact.

INTRODUCTION

Cells exist in a dynamic environment and must coordinate the response to distinct stimuli. The response to a specific stimulus is accomplished via a series of tightly regulated molecular reactions which collectively form a signaling network. Mitogen-activated protein kinase (MAPK) networks are found in every eukaryote and are among the best studied signaling network archetypes, consisting of a characteristic three step kinase cascade: the MAP kinase kinase kinase (MAP3K) phosphorylates and activates the MAP kinase kinase (MAP2K), which phosphorylates and activates the MAPK [1]. The upstream activation of the MAP3K and the downstream targets of the MAPK vary, and MAPK networks have been implicated in disease etiology, drug development [2], and *in silico* control of cellular systems [3].

Mating in yeast is controlled by a MAPK network. For simplicity, we will describe the system as it exists in MATa cells (Figure 3.1A); the same network structure exists in MATα cells, although some components are mating-type specific (e.g., MATa cells express an α-factor specific receptor, Ste2p [4], while MATα cells express an a-factor specific receptor, Ste3p [5]). Mating pathway signaling begins when the pheromone α-factor binds the G protein coupled receptor Ste2p [4]. Upon stimulation, release of the G protein βγ heterodimer [6–10] results in activation of Cdc42p through its activator Cdc24p[11] and subsequent activation of Ste20p [12]. Once activated, Ste20p initiates the 3 step MAPK cascade [13,14]: Ste11p (MAP3K) → Ste7p (MAP2K) → Fus3p and Kss1p (MAPK). Fus3p and Kss1p phosphorylate the transcription factor Ste12p, which regulates many genes important for mating and cell fusion [15,16]. Efficient signaling through the mating pathway requires both association of Ste11p with the adaptor protein Ste50p [17] and assembly of the cascade on the scaffold protein Ste5p [14].

The mating pathway is notable for its extensive regulation, both under pheromone stimulation and basally. Ste12p upregulates expression of mating MAPK components, including Ste2p Fus3p, and Ste12p itself[18–20], all of which are a form of positive feedback from the mating pathway onto itself. Contrastingly, active Fus3p directly inhibits the MAPK cascade by phosphorylating key components of the cascade [21–23], a form of negative autoregulation. Basal mating pathway activity is therefore a delicate balance between activation and inhibition. A slight increase in activity of any kinase could conceivably be amplified into a large change in transcriptional activation, or it could lead to no change due to the increased negative feedback. The mating pathway's interruption of the cell cycle implies a benefit towards downregulation of the pathway when pheromone is absent, and an increase in basal mating pathway activity has been linked to a growth defect under unstimulated conditions [24].

The yeast MAPK networks are also a model system for studying how signaling networks remain insulated despite sharing components (Figure 3.1B). The filamentous growth (FG) pathway is activated under starvation, and while it has an upstream activation mechanism distinct from mating pathway activation, the MAPK cascade is nearly identical to the mating MAPK cascade: Ste11p → Ste7p → Kss1p (but not Fus3p) [25,26]. The high osmolarity glycerol (HOG) pathway controls the response to osmotic stress and contains an upstream activation branch in which the Cdc42p-Ste20p complex phosphorylates and activates the MAP3K Ste11p. Ste11p then activates the MAP2K Pbs2p, which activates the MAPK Hog1p [27]. Despite the three pathways sharing the Cdc42p-Ste20p → Ste11p activation step, the pathways are insulated, and it has been shown that (in general) signal does not leak from the HOG pathway to the mating/FG pathways, a phenomenon commonly dubbed "crosstalk" [28]. The lack of crosstalk in wild type cells is well studied, and various approaches have been taken to identify the root cause of signaling insulation in the yeast MAPK networks, including deletion and mutation studies [28], experiments with inhibitable kinases [29,30], oscillatory stress [31], and experiments with kinase-substrate fusion constructs [32]. These approaches, while providing valuable information about the

network structure, produce gross network rearrangements and therefore do not address whether small modifications to the network, changes in expression or point mutations, can also produce crosstalk.

We have recently reported that crosstalk occurs at certain doses of osmostress in wild type cells of the Σ1278b background ("Sigma") [33]. Importantly, the overall network structure in the Sigma background is intact: the known signaling components are present with no obvious loss-of-function mutations. This suggests that the existing diversity of yeast laboratory strains provides a means by which to discover how small network perturbations affect signal flow (and crosstalk in particular) through MAPK networks. Here, we have crossed the Sigma background with the YPH499 background (congenic with S288C) to identify genetic loci associated with crosstalk and differences in basal expression of a mating pathway reporter. We used a bulk segregant analysis (Figure 3.2) to identify quantitative trait loci (QTL) associated with these phenotypes and we tested genes inside these QTL to determine whether they substantially affect signal flow through the mating/FG MAPK networks.

RESULTS

Crosstalk and basal mating pathway activity are heritable traits

We wished to understand the genetic basis of differences in mating signaling in the two parental strains, so we performed QTL mapping using a bulk segregant approach. The parental strains were crossed and the resulting diploid sporulated, yielding a collection of 744 segregant MATa haploids. We measured the phenotypes of these spores and 606 segregants yielded data of sufficient quality. For the crosstalk, the induction of the mating reporter in response to osmostress (Figure 3.3A), the distribution of spores was unimodal (mean 1.16) and closer to the YPH499 parent controls (mean 1.11) than the Sigma parent controls (mean 1.41). Nonetheless, the spores were generally distributed between the two parents, and a significant number of spores (29%) showed crosstalk more than two standard deviations from the

YPH499 parent mean. The calculated broad-sense heritability $H^2 = 0.61$ indicated that approximately 60% of the variation among the spores was due to genetic factors.

The distribution of basal mating pathway activity among the spores (Figure 3.3B) was bimodal. In general, the segregants were biased toward higher basal pFUS1-eGFP expression. For example, 24% of segregants showed basal pFUS1-eGFP more than two standard deviations higher than the YPH499 (high parent) mean, while only 8% of segregants showed basal pFUS1-eGFP more than two standard deviations lower than the Sigma (low parent) mean. We calculated the broad-sense heritability $H^2 = 0.98$, indicating that nearly all of variation among the segregants was due to genetic factors.

Several genetic loci are linked to crosstalk and basal pFUS1-eGFP expression

After sequencing pools of the highest and lowest phenotyped spores for each of our traits, we used MULTIPOOL[34] to calculate LOD scores across the genome for the above crosstalk trait and for basal pFUS1-eGFP expression. For crosstalk (Figure 3.4A), we found significant peaks on chromosomes II, VIII, XII, and XV. The most significant peak, found on chromosome XV, had a maximum LOD score of 7.9 and the MULTIPOOL output showed that up to 90% of reads in the low bulk matched the YPH499 parent (Figure 3.4B). We found 2-LOD support intervals around our significant peaks and used these boundaries to define our QTL. Full details of the QTL, including a list of the genes with non-silent mutations found in the QTL, can be found in Table 3.1. For simplicity, we included only mutations in open reading frames and did not include additional potential regulatory mutations.

For basal pFUS1-eGFP expression, we found significant peaks on chromosomes III, IV, VIII, XIII, and two peaks on chromosome XV. The most significant peak was found on chromosome III (LOD score = 24) and examination of the MULTIPOOL output for chromosome III (Figure 3.5) revealed that a substantial portion of the left arm of chromosome III (positions 11,000 – 70,000) showed significant segregation among the two bulks (estimated alle frequency of the high parent in the high bulk > 75%). As with

crosstalk, we defined our QTL using a 2-LOD support interval around each peak. A summary of the QTL and genes with non-silent mutations can be found in Table 3.2. Again, potential regulatory mutations were not included.

STE50 and *FYV5* affect basal pFUS1-eGFP expression in a strain dependent manner

We manually examined the list of genes with non-silent mutations on chromosome III and identified *STE50* and *FYV5* as potential regulators of basal pFUS1-eGFP expression. Ste50p is an adaptor protein which binds Ste11p during mating pathway activation [17], and mutations in *STE50* have been identified which alter mating pathway activity in response to pheromone [35]. Fyv5p has been shown to repress haploid specific genes (including *FUS1*) in MATα cells by heterodimerizing with Matalpha2p [36]. We used a CRISPR-based strategy to introduce the YPH499 alleles of *STE50* (Figure 3.6A) and *FYV5* (Figure 3.6B) into the Sigma background, and vice versa. The *STE50* allele in the Sigma background significantly increased basal pFUS1-eGFP expression: $STE50^{Sigma}$ = 3,227 ± 98 compared to $STE50^{YPH499}$ = 4,069 ± 102 (mean ± s.e.m). Interestingly, introducing the Sigma allele in the YPH499 background produced no significant change in basal pFUS1-eGFP expression: $STE50^{Sigma}$ = 9,076 ± 237 compared to $STE50^{YPH499}$ = 9,831 ± 749 (mean ± s.e.m).

Swapping the *FYV5* alleles produced unexpected results. In the Sigma background, the YPH499 allele did not significantly alter basal pFUS1-eGFP expression: $FYV5^{Sigma}$ = 3,227 ± 227 compared to $FYV5^{YPH499}$ = 3,334 ± 158 (mean ± s.e.m.). In the YPH499 background, however, the Sigma allele *increased* basal pFUF1-eGFP expression: $FYV5^{Sigma}$ = 25,463 ± 1,245 compared to $FYV5^{YPH499}$ = 12,164 ± 508 (mean ± s.e.m.). This is the opposite of what we anticipated – the Sigma parent had lower basal pFUS1-eGFP expression, so we expected that introducing Sigma alleles into the YPH499 background should lower pFUS1-eGFP expression.

Allele swaps did not identify a causal gene for crosstalk

We manually screened the genes appearing in the crosstalk QTL for genes which had previously been implicated in either HOG pathway or mating pathway signaling. We introduced the YPH499 allele into the Sigma background (and vice versa) and measured crosstalk in the original strains, deletion strains, and the strains containing the alternate alleles (Table 3.3). Some genes affected crosstalk only in the deletion strains; for example, crosstalk was significantly reduced in the Sigma-background *ldb19Δ* strain but was unaffected in YPH499-background *ldb19Δ* strain. Crosstalk was not meaningfully different in the *LDB19* alternate allele strains. Crosstalk was significantly increased in both strain backgrounds in the *rck2Δ* strains. In the YPH499 background, the Sigma *RCK2* allele slightly (but significantly) increased crosstalk, while the YPH499 allele did not affect crosstalk in the Sigma background. Crosstalk was unaffected by the *STE20* allele swaps in both strain backgrounds.

DISCUSSION

We showed that two closely related laboratory strains, YPH499 and Σ1278b, have heritable differences in both basal mating pathway induction and crosstalk from the HOG pathway into other MAPK pathways. While we have, for simplicity, referred to crosstalk as occurring between the HOG and mating pathway, an important piece of context is that the mating MAPK pathway is nearly identical to the filamentous growth (FG) pathway [26,37]. Therefore, our pFUS1-eGFP reporter is perhaps better described as a mating/FG pathway reporter, and crosstalk could be described as signal leaking from the HOG pathway into the FG pathway. We therefore might expect to see some differences because the YPH499 background, like the S288C background, is filamentation deficient due to truncation of the transcription factor *FLO8* [38,39], which is activated by the cyclic AMP (but not the MAPK) portion of the filamentous growth pathway [40]. Sigma, on the other hand, has a functional copy of *FLO8* and is therefore filamentation-competent [38]. An intriguing hypothesis is that the mating/FG pathways are differentially regulated because the YPH499 background has lost selective pressure to maintain the FG pathway,

particularly under stress conditions. The filamentous growth pathway and the HOG pathway are tightly linked, and two membrane-bound activators of the HOG pathway, Sho1p [41,42] and Msb2p [43], have also been implicated in activation of the FG MAPK pathway [44]. Although crosstalk is commonly understood in the context of the shared Ste20p→Ste11p activation step, it is possible that the critical connection between the yeast MAPK pathways is the upstream activation of Sho1p and Msb2p. Future studies of other yeast strains, particularly laboratory and wild strains which maintain the FG pathway, will provide insight into how common crosstalk from the HOG into the mating/FG pathways is, and whether this trait is linked to the ability to activate the FG pathway.

Our screen for QTL associated with high basal expression of pFUS1-eGFP revealed that the trait was associated with the left arm of chromosome III. Several important genes associated with mating are found on chromosome III, including *STE50*, *FYV5*, *FUS1* itself, the *MAT* locus, and the silent mating loci HML and HMR. Of these, only *STE50* and *FYV5* were present in our QTL. We showed that *STE50* and *FYV5* both regulate basal expression of the mating pathway reporter, although in a strain dependent fashion. It is interesting to note that only *STE50* is directly part of the mating pathway, serving as an adaptor protein between the Cdc42p-Ste20p complex and the MAP3K Ste11p. *FYV5*, in contrast, has been shown to repress the haploid specific genes (and *FUS1* specifically) by heterodimerizing with MATalpha2. Given the complex autoregulation of the mating MAPK pathway as well as the additional layer of regulation occurring due to the genes in the MAT locus, it is unsurprising that basal expression of mating reporters is epistatic. While the process of mating is, overall, beneficial for yeast, activation of the mating MAPK pathway may be deleterious for an individual cell if no mating partner is present. The mating pathway interferes with the cell cycle [45], and it has been shown that increased expression of a *FUS1* reporter is associated with a growth defect in S288C cells [24]. Future studies should explore the distinction between mating MAPK activity and regulation by the MAT locus, perhaps by using different reporters subject to alternate forms of regulation. For example, interesting insight may be obtained by comparing a *FAR1*

reporter, which is directly repressed by the a1-α2 complex [46], and a *FUS1* reporter, which, although it is haploid specific [47], is not thought to be regulated by the a1-α2 complex [46]. Additionally, a survey of other laboratory and wild strains, particularly those with a well-documented history, may provide insight into how regulation of the mating pathway is evolutionarily conserved.

As we have demonstrated, regulation of the yeast MAPK pathways is complex, both basally and under stimulation. Our results suggest that more sensitive genetic techniques are necessary to fully understand how different strains achieve the necessary balance between activation of the mating pathway in the presence of pheromone and no activation in the absence of pheromone or in the presence of other stimuli. A previous genetic study of MAPK signaling in twelve strains revealed subtle interactions between the HOG pathway and the general stress machinery [48]. A similar approach focused on crosstalk and basal mating activity could be used to identify important genes for regulating these phenotypes. Nonetheless, our finding that crosstalk and basal mating pathway activity are both heritable traits with unknown genetic regulators demonstrates that the existing diversity of yeast strains can yield valuable insights, even in a well-characterized model system.

MATERIALS AND METHODS

Yeast strains and methods

Yeast culture and growth were performed using standard methods [49] and transformations were done using the standard lithium acetate transformation protocol [50]. Allele swaps were performed using a CRISPR method as described previously [33]. A complete list of strains and plasmids can be found in Table 3.4 and Table 3.5. For flow cytometry experiments, cultures were grown in low fluorescence media (1.7 g/L Yeast Nitrogen Base without ammonium sulfate, without folic acid, without riboflavin [MP Biomedicals # 114030512]; 5 g/L ammonium sulfate; 20 g/L dextrose) supplemented with amino acids. Other experiments were performed in standard YPD media.

Cross preparation

The YPH499- and Sigma-background parental strains (yMM0736 and yMM1584 respectively) were engineered for mating as follows (Figure 3.7). A synthetic gene array mating type selection cassette [51] was amplified from a strain harboring this cassette (a gift from Audrey Gasch) and integrated into each strain at the *HO* locus. This cassette allows for selection of MATa cells using hygromycin (Figure 3.7A).

To generate isogenic MATα strains of each background (Figure 3.7B), the strains were then diploidized using pHS2 (Addgene plasmid # 81037; a gift from John McCusker), a replicative plasmid containing a functional *HO* gene. After transformation, colonies were passaged three times in non-selective YPD media to lose the plasmid and single colonies were tested for mating type using colony PCR [52]. Diploid colonies were sporulated in liquid media using a high-efficiency protocol for each strain background [53]. Briefly, YPH499-background strains were grown to mid-log in PSP2 media (0.1% yeast extract, 0.67% yeast nitrogen base without amino acids, 1% potassium acetate, 0.25X amino acid supplement)[53], washed 2X in 1% KOAc + 0.25X amino acid supplement, re-suspended in 1% KOAc + 0.25X amino acid supplement, and incubated shaking at 30°C for 3-4 days until tetrads formed. Sigma-background strains were grown to mid-log in YPD media, washed 2X in 1% KOAc, re-suspended in 1% KOAc, and incubated shaking at room temperature for 3-4 days until tetrads formed. Spores were harvested by first digesting the ascii with β-glucuronidase and vortexing the digested tetrads with acid-washed beads for 2 minutes. Spores were enriched by vortexing, allowing the hydrophobic spores to adhere to the wall of a microcentrifuge tube. After washing with sterile H_2O, spores were harvested in 0.01% IGEPAL CA-630 and plated on YPD Agar plates. Colonies were checked for mating type using colony PCR and MATα colonies were selected. The mating types of these colonies were confirmed by a test-cross with the original parental strain.

Sigma and YPH499 Cross and Sporulation

After generating isogenic MATa and MATα strains of both backgrounds, the two backgrounds were crossed by streaking onto YPD Agar plates and incubating at 30°C for 4 hours. The presence of zygotes was confirmed by microscopy, and the mating patch was re-streaked for single colonies. Diploid colonies were identified by colony PCR. The cross was performed in both directions (Sigma MATa x YPH499 MATα and Sigma MATα x YPH499 MATa) to avoid selecting one strain background's MAT locus. A diploid colony from each cross was sporulated following the Sigma sporulation protocol above. Spores were harvested and enriched as above and plated onto YPD+Hygromycin agar plates to select for MATa spores. After single colonies formed, 372 colonies from each cross were picked into YPD+Hygromycin media in a 384-deep well plate and stored in 15% glycerol at -80°C.

Phenotyping

The spores from the two crosses were phenotyped using a 96-well format flow cytometry protocol as described previously [33]. Each 96-well plate contained a YPH499 and Sigma parental strain as a control. Spores were induced with osmostress media (final concentration 0.75M sorbitol LFM) and non-osmostress media (0M sorbitol LFM) for 30 minutes. Crosstalk was calculated for each spore by taking the median eGFP in the osmostress sample divided by the median eGFP in the non-osmostress sample. Basal pFUS1-eGFP was found by taking the median eGFP in the non-osmostress sample. Upon examining the results, we found that the two crosses did not produce substantially different distributions of crosstalk or basal pFUS1-eGFP among the spores (Figure 3.8). We therefore considered the spores from both crosses together in our future analyses. Broad-sense heritability is defined as the variation among the segregants not attributable to environmental variance, $H^2 = \left(s_{seg}^2 - s_{env}^2\right)/s_{seg}^2$. We took the variance among our parent strain controls (Sigma, n = 6; YPH499, n = 7) as our environmental variance. The two strain backgrounds did not have significantly different variances (*F*-test, crosstalk p = 0.15, basal pFUS1-eGFP p

= 0.97) and we therefore used the pooled variance of the controls as our estimate for environmental variance: $s_{env}^2 = (n_1 s_1^2 + n_2 s_2^2)/(n_1 + n_2)$.

Pooling and Sequencing

After phenotyping the spores, the 120 highest and lowest spores were picked to form the high bulk and the low bulk respectively. We formed these bulks for crosstalk and for basal pFUS1-eGFP. Spores picked for the bulks were phenotyped a second time to confirm that the spores in the high bulk significantly differed from the spores in the low bulk (Figure 3.9). The spores were grown up (separately) overnight in YPD media and an equal number of cells (approximately 150,000) from each spore were combined to form the high bulk and low bulk pools. Genomic DNA from the pools was extracted using the Qiagen DNEasy Blood and Tissue kit. Genomic DNA was also extracted from the parental strains (yMM1597 and yMM1598). Genomic DNA was sequenced on the NovaSeq 6000 (150bp paired end reads) at the UW-Madison Biotechnology Center DNA Sequencing Facility. Parental strains were sequenced to depth of approximately 20X and the pools were sequenced to a depth of approximately 360X. Reads were trimmed using TrimGalore [54,55] prior to analysis.

QTL analysis

Reads from the parental strains were aligned to the S288C reference genome vR64.2.1 using bwa-mem [56] (with the default parameters) and variants were called using GATK HaplotypeCaller (--ploidy 1) [57,58]. To avoid biasing the pool alignments, a variant reference genome was constructed using GATK FastaAlternateReferenceMaker. Sites at which both parents share a SNP were replaced by the common allele; sites at which only one parent had a SNP were replaced by an allele not found in either parent. Reads from the pools were aligned to this alternate reference and a pileup was created at the SNP sites in the parent strains. The number of reads belonging to each parent was calculated from the pileup and LOD scores at each site were calculated using MULTIPOOL (-N 120) [34]. We chose a LOD threshold of 3 for identifying QTL. A 2-LOD support interval was found for each peak above this threshold and variants

from the two parents inside these intervals were processed using the Ensembl Variant Effects Predictor web interface [59]. We judged that, for basal pFUS1-eGFP expression, two peaks on the left arm of chromosome III were present and we considered the peaks to be separate QTL. The Variant Effects Predictor tool identifies genes with mutations as well as the type of mutation (silent, missense, frameshift, etc.). Genes with non-silent mutations were found within each QTL. A complete list of genes is given in Table 3.1 (crosstalk) and Table 3.2 (basal pFUS1-eGFP). Manually examining the basal pFUS1-eGFP QTL on chromosome III, we observed that *STE50* partially overlapped the QTL, although the variants in this gene fall outside the 2-LOD interval. We performed in the allele swap because of Ste50p's important role in mating pathway signaling.

REFERENCES

1 Widmann C, Gibson S, Jarpe MB & Johnson GL (1999) Mitogen-Activated Protein Kinase: Conservation of a Three-Kinase Module From Yeast to Human. *Physiological Reviews* **79**, 143–180.

2 Braicu C, Buse M, Busuioc C, Drula R, Gulei D, Raduly L, Rusu A, Irimie A, Atanasov AG, Slaby O, Ionescu C & Berindan-Neagoe I (2019) A Comprehensive Review on MAPK: A Promising Therapeutic Target in Cancer. *Cancers (Basel)* **11**, 1618.

3 Scott TD, Sweeney K & McClean MN (2019) Biological signal generators: integrating synthetic biology tools and in silico control. *Curr Opin Syst Biol* **14**, 58–65.

4 Burkholder AC & Hartwell LH (1985) The yeast α-factor receptor: structural properties deduced from the sequence of the STE2 gene. *Nucleic Acids Research* **13**, 8463–8475.

5 Hagen DC, McCaffrey G & Sprague GF (1986) Evidence the yeast STE3 gene encodes a receptor for the peptide pheromone a factor: gene sequence and implications for the structure of the presumed receptor. *Proceedings of the National Academy of Sciences* **83**, 1418–1422.

6 Blumer KJ & Thorner J (1990) Beta and gamma subunits of a yeast guanine nucleotide-binding protein are not essential for membrane association of the alpha subunit but are required for receptor coupling. *Proceedings of the National Academy of Sciences* **87**, 4363–4367.

7 Blinder D, Bouvier S & Jenness DD (1989) Constitutive mutants in the yeast pheromone response: ordered function of the gene products. *Cell* **56**, 479–486.

8 Cole GM, Stone DE & Reed SI (1990) Stoichiometry of G protein subunits affects the Saccharomyces cerevisiae mating pheromone signal transduction pathway. *Mol Cell Biol* **10**, 510–517.

9 Nomoto S, Nakayama N, Arai K & Matsumoto K (1990) Regulation of the yeast pheromone response pathway by G protein subunits. *EMBO J* **9**, 691–696.

10 Whiteway M, Hougan L & Thomas DY (1990) Overexpression of the STE4 gene leads to mating response in haploid Saccharomyces cerevisiae. *Mol Cell Biol* **10**, 217–222.

11 Zhao ZS, Leung T, Manser E & Lim L (1995) Pheromone signalling in Saccharomyces cerevisiae requires the small GTP-binding protein Cdc42p and its activator CDC24. *Mol Cell Biol* **15**, 5246–5257.

12 Moskow JJ, Gladfelter AS, Lamson RE, Pryciak PM & Lew DJ (2000) Role of Cdc42p in Pheromone-Stimulated Signal Transduction in Saccharomyces cerevisiae. *Molecular and Cellular Biology* **20**, 7559–7571.

13 Wu C, Whiteway M, Thomas DY & Leberer E (1995) Molecular Characterization of Ste20p, a Potential Mitogen-activated Protein or Extracellular Signal-regulated Kinase Kinase (MEK) Kinase Kinase from Saccharomyces cerevisiae(∗). *Journal of Biological Chemistry* **270**, 15984–15992.

14 Chol K-Y, Satterberg B, Lyons DM & Elion EA (1994) Ste5 tethers multiple protein kinases in the MAP kinase cascade required for mating in S. cerevisiae. *Cell* **78**, 499–512.

15 Elion EA, Satterberg B & Kranz JE (1993) FUS3 phosphorylates multiple components of the mating signal transduction cascade: evidence for STE12 and FAR1. *MBoC* **4**, 495–510.

16 Hagen DC, McCaffrey G & Sprague GF (1991) Pheromone response elements are necessary and sufficient for basal and pheromone-induced transcription of the FUS1 gene of Saccharomyces cerevisiae. *Molecular and Cellular Biology* **11**, 2952–2961.

17 Xu G, Jansen G, Thomas DY, Hollenberg CP & Rad MR (1996) Ste50p sustains mating pheromone-induced signal transduction in the yeast Saccharomyces cerevisiae. *MOL MICROBIOL* **20**, 773–783.

18 Hartig A, Holly J, Saari G & MacKay VL (1986) Multiple regulation of STE2, a mating-type-specific gene of Saccharomyces cerevisiae. *Mol Cell Biol* **6**, 2106–2114.

19 Ren B, Robert F, Wyrick JJ, Aparicio O, Jennings EG, Simon I, Zeitlinger J, Schreiber J, Hannett N, Kanin E, Volkert TL, Wilson CJ, Bell SP & Young RA (2000) Genome-Wide Location and Function of DNA Binding Proteins. *Science* **290**, 2306–2309.

20 Roberts CJ, Nelson B, Marton MJ, Stoughton R, Meyer MR, Bennett HA, He YD, Dai H, Walker WL, Hughes TR, Tyers M, Boone C & Friend † Stephen H. (2000) Signaling and Circuitry of Multiple MAPK Pathways Revealed by a Matrix of Global Gene Expression Profiles. *Science* **287**, 873–880.
21 Yu RC, Pesce CG, Colman-Lerner A, Lok L, Pincus D, Serra E, Holl M, Benjamin K, Gordon A & Brent R (2008) Negative feedback that improves information transmission in yeast signalling. *Nature* **456**, 755–761.
22 Cole GM & Reed SI (1991) Pheromone-induced phosphorylation of a G protein β subunit in S. cerevisiae is associated with an adaptive response to mating pheromone. *Cell* **64**, 703–716.
23 Gartner A, Nasmyth K & Ammerer G (1992) Signal transduction in Saccharomyces cerevisiae requires tyrosine and threonine phosphorylation of FUS3 and KSS1. *Genes and Development* **6**, 1280–1292.
24 Lang GI, Murray AW & Botstein D (2009) The cost of gene expression underlies a fitness trade-off in yeast. *PNAS* **106**, 5755–5760.
25 Cullen PJ & Sprague Jr. GF (2012) The regulation of filamentous growth in yeast. *Genetics* **190**, 23–49.
26 Liu H, Styles CA & Fink GR (1993) Elements of the Yeast Pheromone Response Pathway Required for Filamentous Growth of Diploids. *Science* **262**, 1741–1744.
27 Hohmann S (2002) Osmotic Stress Signaling and Osmoadaptation in Yeasts. *Microbiol Mol Biol Rev* **66**, 300–372.
28 O'Rourke SM & Herskowitz I (1998) The Hog1 MAPK prevents cross talk between the HOG and pheromone response MAPK pathways in Saccharomyces cerevisiae. *Genes Dev* **12**, 2874–2886.
29 Westfall PJ & Thorner J (2006) Analysis of Mitogen-Activated Protein Kinase Signaling Specificity in Response to Hyperosmotic Stress: Use of an Analog-Sensitive HOG1 Allele. *Eukaryotic Cell* **5**, 1215–1228.
30 Patterson JC, Klimenko ES & Thorner J (2010) Single-cell analysis reveals that insulation maintains signaling specificity between two yeast MAPK pathways with common components. *Sci Signal* **3**.
31 Mitchell A, Wei P & Lim WA (2015) Oscillatory stress stimulation uncovers an Achilles' heel of the yeast MAPK signaling network. *Science* **350**, 1379–1383.
32 Harris K, Lamson RE, Nelson B, Hughes TR, Marton MJ, Roberts CJ, Boone C & Pryciak PM (2001) Role of scaffolds in MAP kinase pathway specificity revealed by custom design of pathway-dedicated signaling proteins. *Curr Biol* **11**, 1815–1824.
33 Scott TD, Xu P & McClean MN (2022) Strain dependent differences in coordination of yeast signaling networks. *bioRxiv*, 2022.06.09.495559.
34 Edwards MD & Gifford DK (2012) High-resolution genetic mapping with pooled sequencing. *BMC Bioinformatics* **13**, S8.
35 Sharmeen N, Sulea T, Whiteway M & Wu C (2019) The adaptor protein Ste50 directly modulates yeast MAPK signaling specificity through differential connections of its RA domain. *Mol Biol Cell* **30**, 794–807.
36 Li D, Dong Y, Jiang Y, Jiang H, Cai J & Wang W (2010) A de novo originated gene depresses budding yeast mating pathway and is repressed by the protein encoded by its antisense strand. *Cell Res* **20**, 408–420.
37 Roberts RL & Fink GR (1994) Elements of a single map kinase cascade in Saccharomyces cerevisiae mediate two developmental programs in the same cell type: Mating and invasive growth. *GENES DEV* **8**, 2974–2985.
38 Liu H, Styles CA & Fink GR (1996) Saccharomyces cerevisiae S288C Has a Mutation in FL08, a Gene Required for Filamentous Growth. *Genetics* **144**, 967–978.
39 Song G, Dickins BJA, Demeter J, Engel S, Dunn B & Cherry JM (2015) AGAPE (Automated Genome Analysis PipelinE) for Pan-Genome Analysis of Saccharomyces cerevisiae. *PLOS ONE* **10**, e0120671.

40 Rupp S, Summers E, Lo HJ, Madhani H & Fink G (1999) MAP kinase and cAMP filamentation signaling pathways converge on the unusually large promoter of the yeast FLO11 gene. *EMBO J* **18**, 1257–1269.

41 Maeda T, Takekawa M & Saito H (1995) Activation of yeast PBS2 MAPKK by MAPKKKs or by binding of an SH3-containing osmosensor. *Science* **269**, 554–558.

42 Posas F & Saito H (1997) Osmotic activation of the HOG MAPK pathway via Ste11p MAPKKK: Scaffold role of Pbs2p MAPKK. *SCIENCE* **276**, 1702–1708.

43 O'Rourke SM & Herskowitz I (2002) A third osmosensing branch in Saccharomyces cerevisiae requires the Msb2 protein and functions in parallel with the Sho1 branch. *Mol Cell Biol* **22**, 4739–4749.

44 Cullen PJ, Sabbagh W, Graham E, Irick MM, van Olden EK, Neal C, Delrow J, Bardwell L & Sprague GF (2004) A signaling mucin at the head of the Cdc42- and MAPK-dependent filamentous growth pathway in yeast. *Genes Dev* **18**, 1695–1708.

45 Chang F & Herskowitz I (1990) Identification of a gene necessary for cell cycle arrest by a negative growth factor of yeast: FAR1 is an inhibitor of a G1 cyclin, CLN2. *Cell* **63**, 999–1011.

46 Nagaraj VH, O'Flanagan RA, Bruning AR, Mathias JR, Vershon AK & Sengupta AM (2004) Combined analysis of expression data and transcription factor binding sites in the yeast genome. *BMC Genomics* **5**, 59.

47 McCaffrey G, Clay FJ, Kelsay K & Sprague GF (1987) Identification and regulation of a gene required for cell fusion during mating of the yeast Saccharomyces cerevisiae. *Mol Cell Biol* **7**, 2680–2690.

48 Treusch S, Albert FW, Bloom JS, Kotenko IE & Kruglyak L (2015) Genetic Mapping of MAPK-Mediated Complex Traits Across S. cerevisiae. *PLOS Genetics* **11**, e1004913.

49 Amberg DC, Burke DJ & Strathern JN (2005) *Methods in yeast genetics: a cold spring habor laboratory course manual* Cold Spring Harbor Laboratory Press, New York.

50 Gietz RD & Schiestl RH (2007) High-efficiency yeast transformation using the LiAc/SS carrier DNA/PEG method. *Nature Protocols* **2**, 31–34.

51 Tong AHY, Evangelista M, Parsons AB, Xu H, Bader GD, Pagé N, Robinson M, Raghibizadeh S, Hogue CWV, Bussey H, Andrews B, Tyers M & Boone C (2001) Systematic Genetic Analysis with Ordered Arrays of Yeast Deletion Mutants. *Science* **294**, 2364–2368.

52 Huxley C, Green ED & Dunbam I (1990) Rapid assessment of S. cerevisiae mating type by PCR. *Trends in Genetics* **6**, 236.

53 Elrod SL, Chen SM, Schwartz K & Shuster EO (2009) Optimizing Sporulation Conditions for Different Saccharomyces cerevisiae Strain Backgrounds. In *Meiosis: Volume 1, Molecular and Genetic Methods* (Keeney S, ed), pp. 21–26. Humana Press, Totowa, NJ.

54 Krueger F, James F, Ewels P, Afyounian E & Schuster-Boeckler B (2021) FelixKrueger/TrimGalore. .

55 Martin M (2011) Cutadapt removes adapter sequences from high-throughput sequencing reads. *EMBnet.journal* **17**, 10–12.

56 Li H (2013) Aligning sequence reads, clone sequences and assembly contigs with BWA-MEM. **arXiv**, 1303.3997.

57 Auwera GV der & O'Connor B (2020) *Genomics in the Cloud: Using Docker, GATK, and WDL in Terra*, 1st edition O'Reilly Media, Sebastopol, CA.

58 Poplin R, Ruano-Rubio V, DePristo MA, Fennell TJ, Carneiro MO, Auwera GAV der, Kling DE, Gauthier LD, Levy-Moonshine A, Roazen D, Shakir K, Thibault J, Chandran S, Whelan C, Lek M, Gabriel S, Daly MJ, Neale B, MacArthur DG & Banks E (2018) Scaling accurate genetic variant discovery to tens of thousands of samples. *bioRxiv*, 201178.

59 McLaren W, Pritchard B, Rios D, Chen Y, Flicek P & Cunningham F (2010) Deriving the consequences of genomic variants with the Ensembl API and SNP Effect Predictor. *Bioinformatics* **26**, 2069–2070.

60 Sikorski RS & Hieter P (1989) A system of shuttle vectors and yeast host strains designed for efficient manipulation of DNA in Saccharomyces cerevisiae. *Genetics* **122**, 19–27.

61 History of Sigma - SGD-Wiki *https://wiki.yeastgenome.org/index.php/History_of_Sigma*.

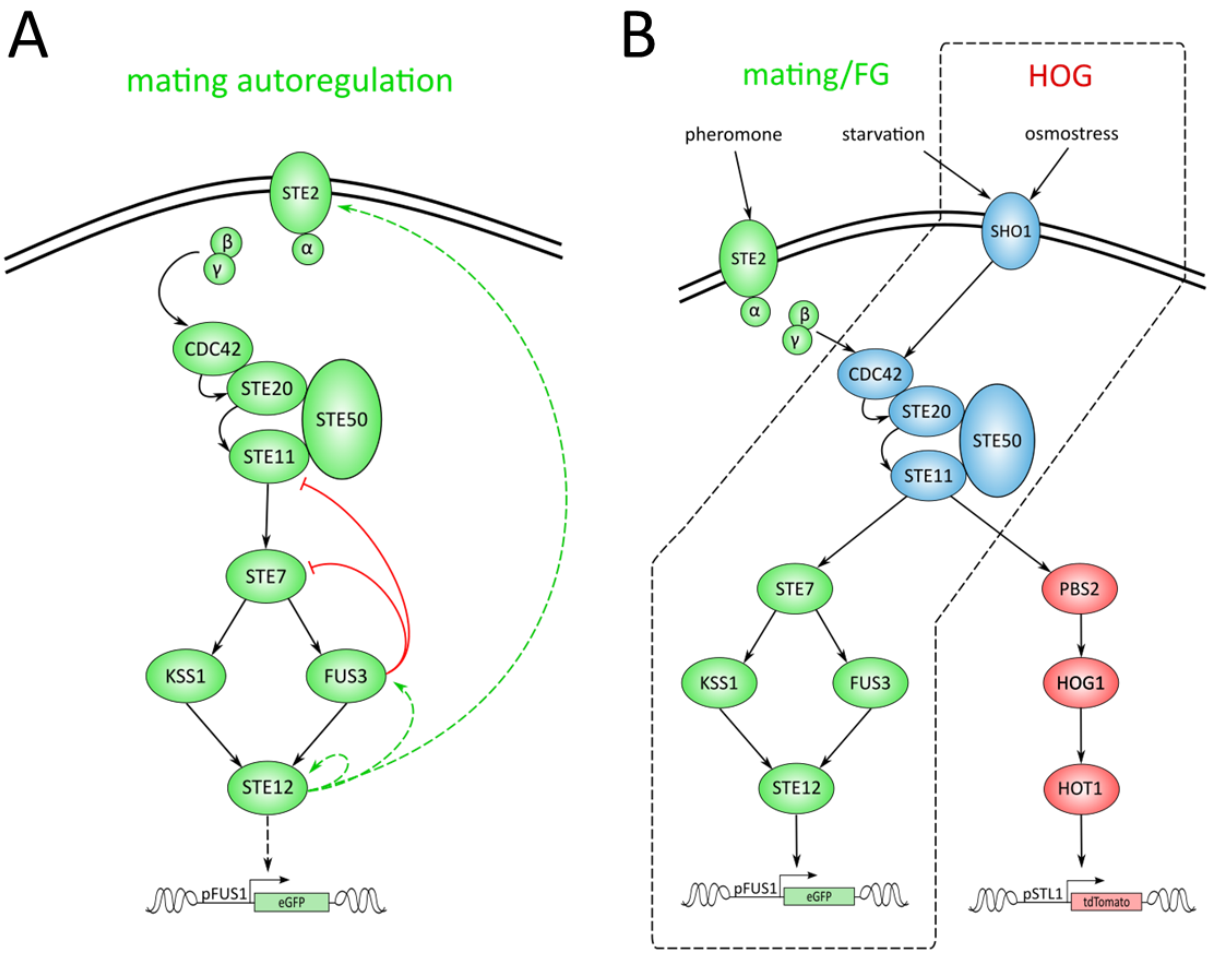

Figure 3.1 The mating pathway is subject to extensive autoregulation and is connected to other MAPK pathways.

A: Several feedback mechanisms allow for positive and negative autoregulation of the mating pathway. Active Fus3p inhibits Ste11p and Ste7p. Activation of the transcription factor Ste12p induces expression of Fus3p, Ste11p, and Ste2p. Solid lines indicate activation (arrows) or inhibition (bars). Dashed lines represent transcriptional activation. Green lines indicate positive feedback mechanisms. Red lines represent negative feedback mechanisms.

B: The mating pathway shares many activation components with the filamentous growth (FG) pathway which is activated by nutrient starvation. Additionally, the high osmolarity glycerol (HOG) pathway shares an upstream activation mechanism with the mating/FG pathways, specifically activation of Ste11p by Ste20p. Crosstalk occurs when signal from an osmotic shock (ordinarily activating the HOG pathway) also activates transcription of mating pathway genes (dashed outline). Mating components are depicted in green. HOG components are depicted in red. Components shared by more than one pathway are depicted in blue.

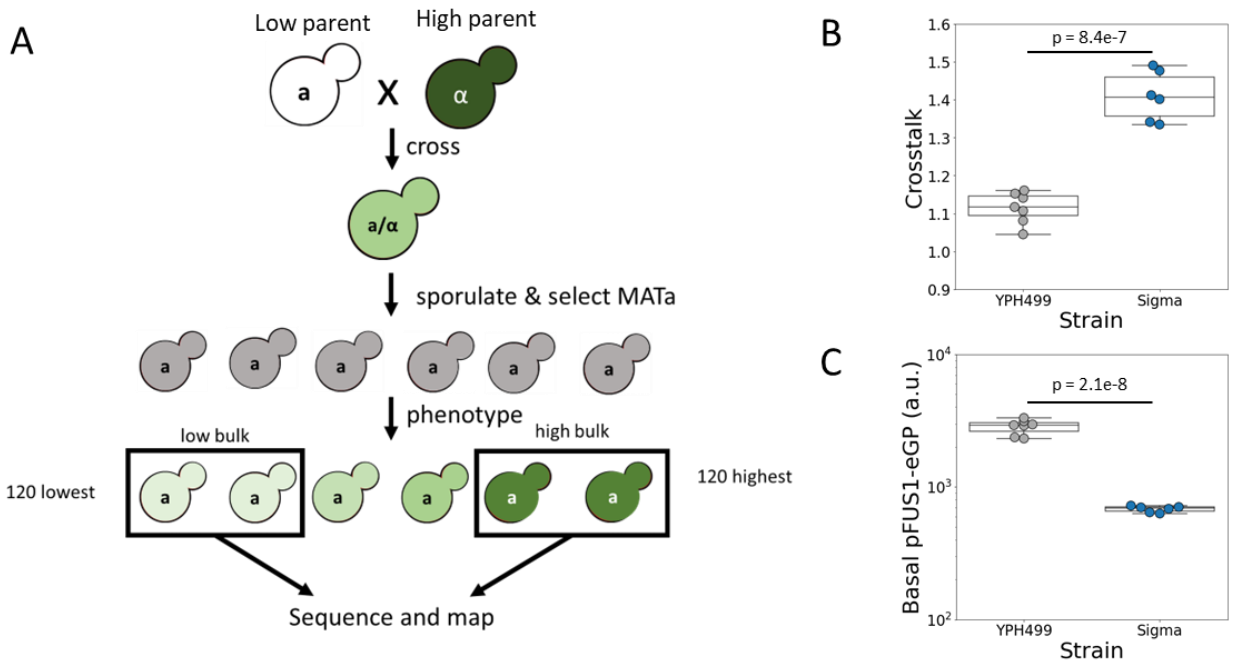

Figure 3.2 Strategy to identify QTL associated with crosstalk and basal pFUS1-eGFP.

A: Bulk segregant approach to identifying QTL in yeast. The two parent strains (with differing phenotypes, here denoted high and low) are crossed to form a diploid. The diploid is sporulated and MATa colonies are selected for phenotyping. After phenotyping, the lowest phenotyped colonies and the highest phenotyped colonies are pooled into the low bulk and high bulk respectively for sequencing.

B: YPH499 (gray dots, left) and Sigma (blue dots, right) parent strains show differing levels of crosstalk. Parent strain measurements were collected as controls during phenotyping of the segregant colonies. The difference between the parent strains is statistically significant ($p = 8.4\times10^{-7}$, student's t-test with equal variance).

C: YPH499 (gray dots, left) and Sigma (blue dots, right) parent strains show differing levels of basal pFUS1-eGFP. Parent strain measurements were collected as controls during phenotyping of the segregant colonies. The difference between the parent strains is statistically significant ($p = 2.8\times10^{-8}$, student's t-test with equal variance).

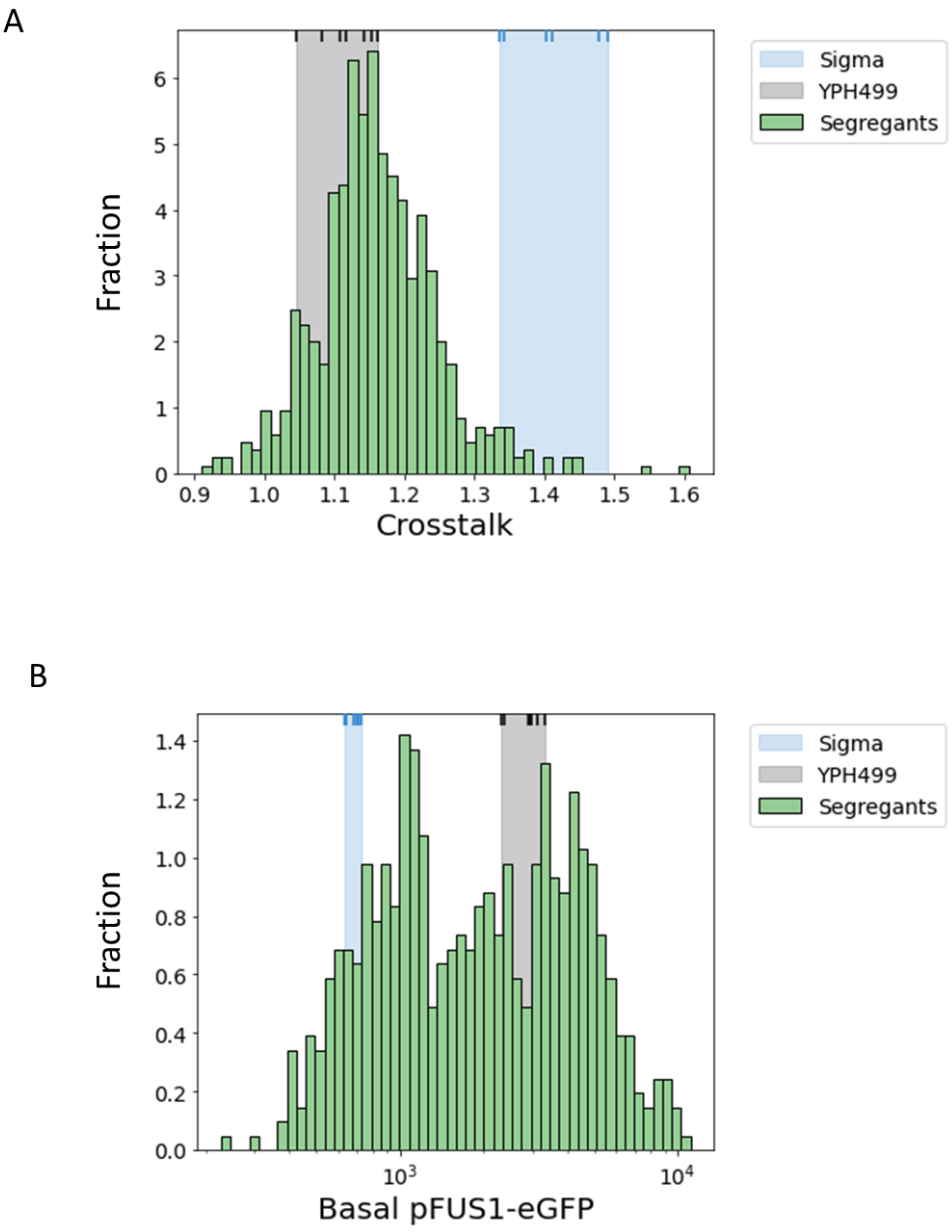

Figure 3.3 Distribution of segregant phenotypes.

Distribution of segregant phenotypes for (A) crosstalk and (B) basal pFUS1-eGFp expression. Green histograms are the phenotypes of the segregants. Blue shaded region is the observed range of the Sigma parent strain control, with blue tick marks at the observed phenotypic values. Gray shaded region is the observed range of the YPH499 parent strain control, with the black tick marks at the observed phenotypic values.

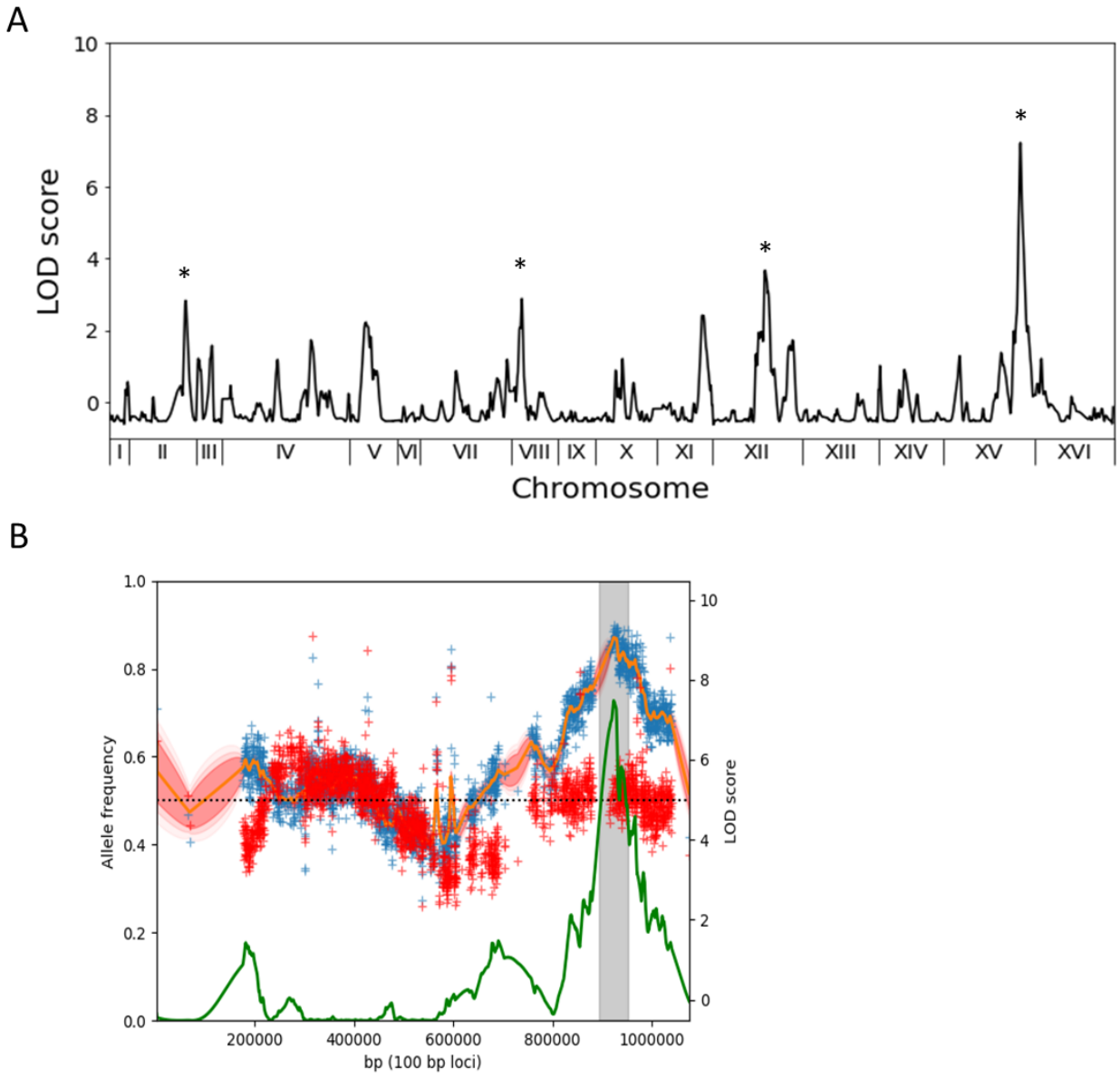

Figure 3.4 QTL associated with the crosstalk phenotype.

A: Profile of LOD scores across the genome for QTL associated with crosstalk. Stars indicate peaks above our significance threshold of 3.

B: MULTIPOOL output showing the prominent peak on chromosome XV. The green line is the LOD score at each locus on the chromosome. Blue crosses represent the fraction of YPH499 variants (low parent) in the low bulk. Red crosses represent the fraction of YPH499 variants in the high bulk. The gray shaded

region is a 1.5-LOD support interval automatically calculated by MULTIPOOL around the largest peak. We expanded this interval to a 2-LOD support interval when defining our QTL.

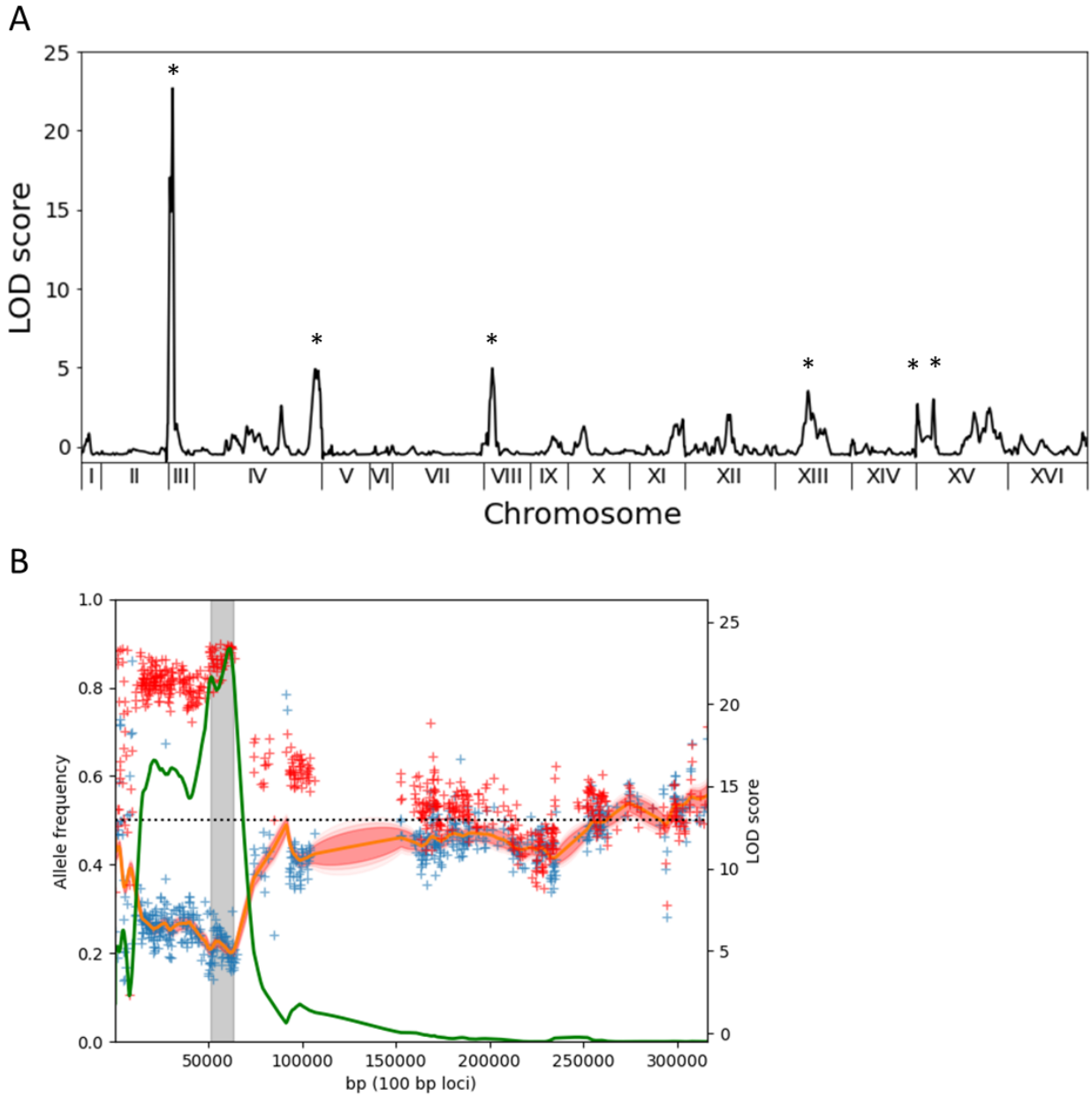

Figure 3.5 QTL associated with basal pFUS1-eGFP expression.

A: Profile of LOD scores across the genome for QTL associated with basal pFUS1-eGFP expression. Stars indicate peaks above our significance threshold of 3.

B: MULTIPOOL output showing the peaks on the left arm of chromosome III. The green line is the LOD score at each locus on the chromosome. Red crosses represent the fraction of YPH499 variants (high parent) in the high bulk. Blue crosses represent the fraction of YPH499 variants in the low bulk. The gray

shaded region is a 1.5-LOD support interval automatically calculated by MULTIPOOL around the largest peak. We expanded this interval to a 2-LOD support interval when defining our QTL.

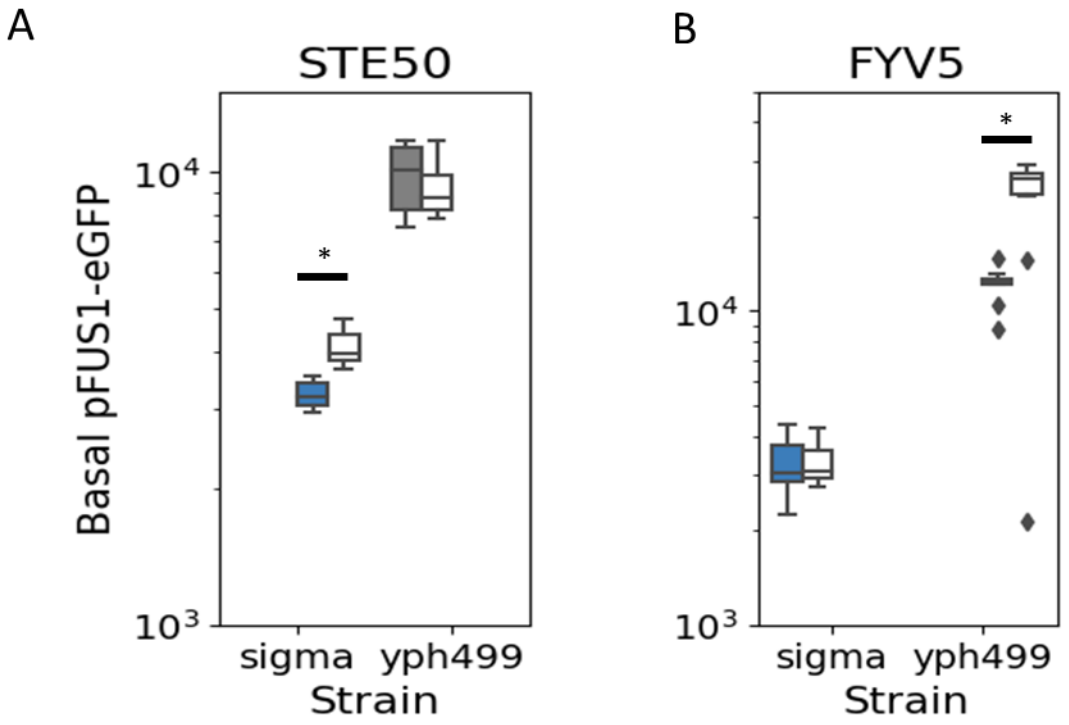

Figure 3.6 *STE50* and *FYV5* regulate basal pFUS1-eGFP expression in a strain dependent manner.

A: Basal pFUS1-eGFP expression measured in Sigma (left) and YPH499 (right) strain backgrounds with the native allele of *STE50* (blue and gray shaded boxes) or the *STE50* allele from the opposite strain background (white boxes). Basal pFUS1-eGFP expression is significantly higher in the Sigma background with the YPH499 allele of *STE50* (student's t-test with equal variance; $p = 8.2 \times 10^{-5}$; N = 6 (Sigma WT); N = 12 (allele swap)). Basal pFUS1-eGFP in the allele swap in the YPH499 background is not significant (student's t-test with equal variance; p = 0.23; N = 6 (Sigma WT); N = 24 (allele swap)).

B: Basal pFUS1-eGFP expression measured in Sigma (left) and YPH499 (right) strain backgrounds with the native allele of *FYV5* (blue and gray shaded boxes) or the *FYV5* allele from the opposite strain background (white boxes). Basal pFUS1-eGFP expression is significantly higher in the YPH499 background with the Sigma allele of *FYV5* (student's t-test with equal variance; $p = 2.2 \times 10^{-4}$; N = 10 (YPH499 WT); N = 12 (allele swap)). The swap in the Sigma background is not significantly different (p = 0.70; N = 10 (Sigma WT); N = 12 (allele swap)).

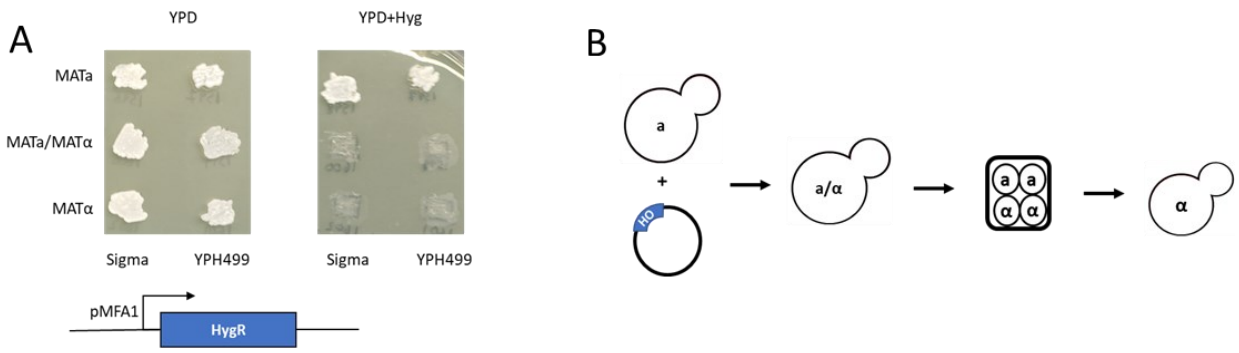

Figure 3.7 Preparation of Sigma and YPH499 background strains for the cross.

A: YPH499 and Sigma background strains were transformed with a pMFA1-HygR cassette, which allows for selection of MATa cells on YPD+Hygromycin agar plates.

B: The MATa YPH499 and Sigma strains were diploidized by transformation of a plasmid containing a functional HO gene. Diploid colonies were selected and sporulated, then spores were prepped and MATα colonies were identified by colony PCR.

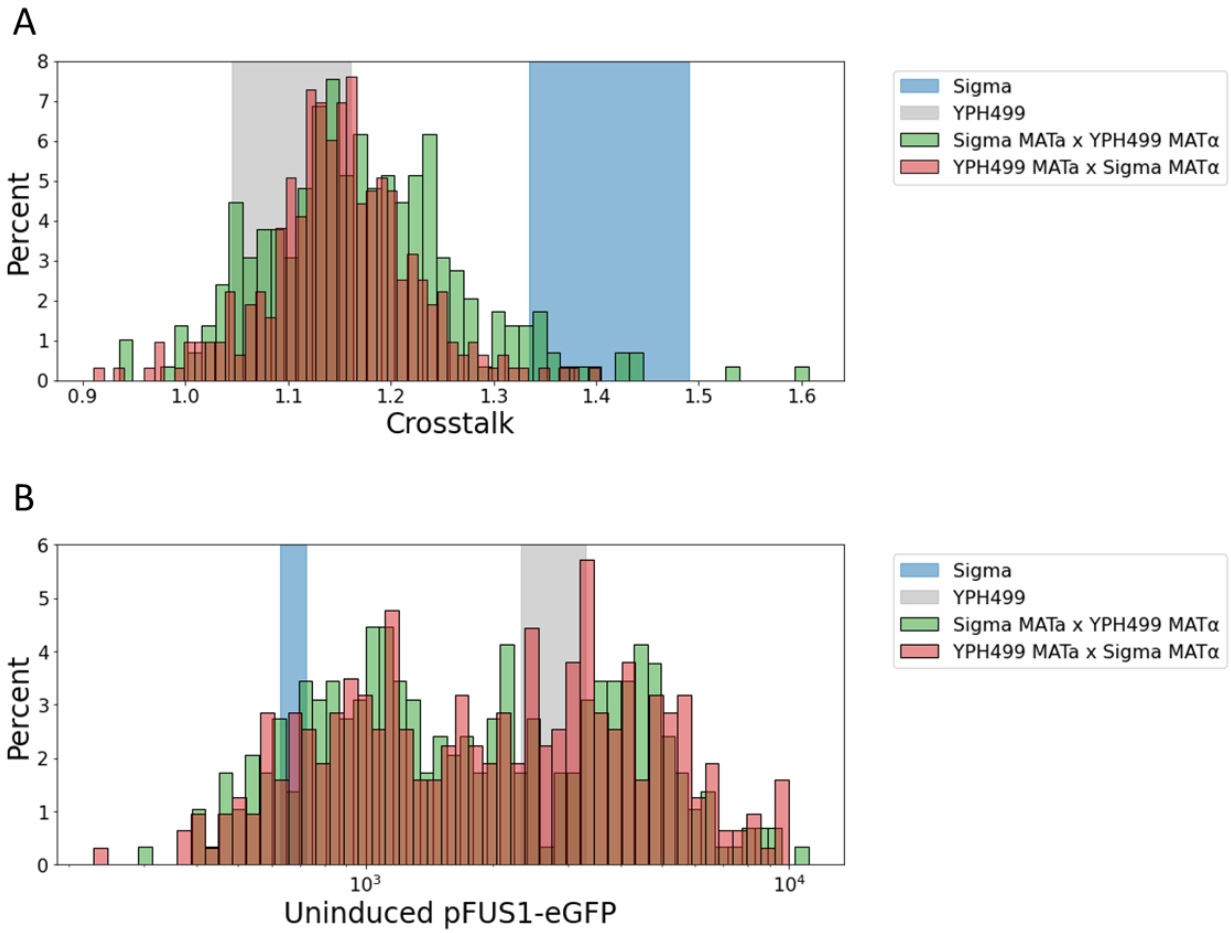

Figure 3.8 The strain background of the MATa parent does not affect the phenotypes of the segregants.

Phenotypic distribution of the segregants measured for (A) crosstalk or (B) basal pFUS1-eGFP expression. The segregants are grouped by the strain background of the MATa parent: Sigma (green) or YPH499 (red). Shaded regions represent the observed range of Sigma (blue) or YPH499 (gray) wild type controls run alongside the segregants.

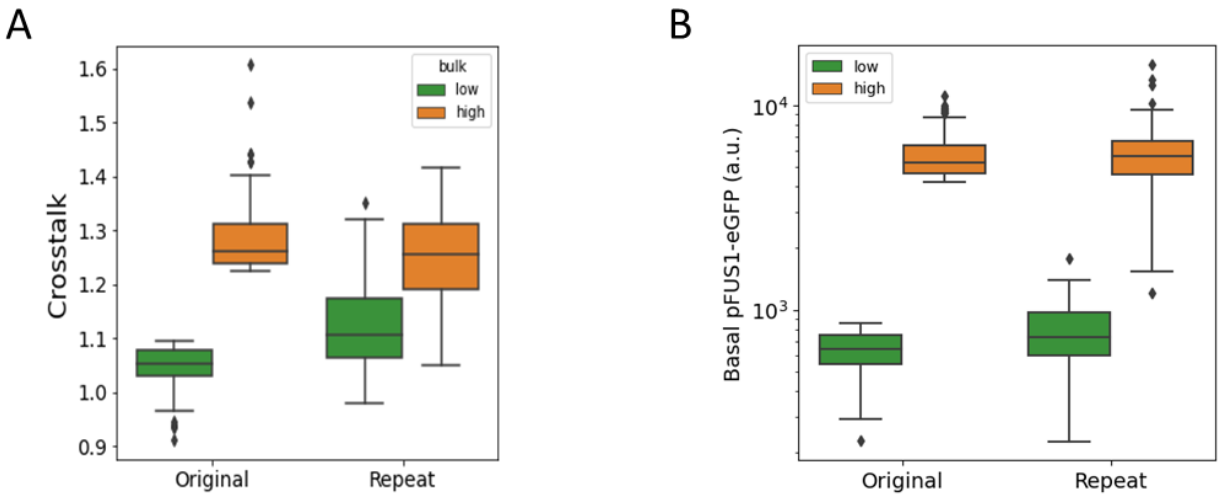

Figure 3.9 The separation of the high and low bulks is not due to technical variation.

After the original phenotyping experiments (left), the spores for the bulks were chosen and phenotyping was repeated for these spores (right). For both crosstalk (A) and basal pFUS1-eGFP (B), the spores in the low bulk (green) were on average lower than the spores in the high group (orange). The differences between the bulks for crosstalk ($p = 1.3 \times 10^{-25}$; N = 120, each bulk) and basalpFUS1-eGFP ($p = 1.7 \times 10^{-66}$; N = 120, each bulk) were statistically significant (student's t-test with equal variance).

Table 3.1 Genes appearing in crosstalk QTL.

Chromosome	Gene	Symbol	Num. variants*
chrII:664,700 – 725,100			
chrII	YBR223C	TDP1	5
chrII	YBR224W	-	4
chrII	YBR225W	-	3
chrII	YBR226C	-	3
chrII	YBR227C	MCX1	2
chrII	YBR228W	SLX1	4
chrII	YBR229C	ROT2	10
chrII	YBR230C	OM14	1
chrII	YBR230W-A	-	2
chrII	YBR231C	SWC5	3
chrII	YBR234C	ARC40	2
chrII	YBR235W	VHC1	1
chrII	YBR236C	ABD1	2
chrII	YBR237W	PRP5	15
chrII	YBR238C	-	1
chrII	YBR239C	ERT1	1
chrII	YBR240C	THI2	1
chrII	YBR241C	-	1
chrII	YBR253W	SRB6	2
chrII	YBR255W	MTC4	3
chrVII:89,400 – 147,900			
chrVIII	YHL002W	HSE1	1
chrVIII	YHL003C	LAG1	1
chrVIII	YHL004W	MRP4	1
chrVIII	YHL005C	-	1
chrVIII	YHL006C	SHU1	1
chrVIII	YHL007C	STE20	4
chrVIII	YHL008C	-	59
chrVIII	YHR001W	OSH7	2
chrVIII	YHR002W	LEU5	1
chrVIII	YHR003C	TCD1	2
chrVIII	YHR004C	NEM1	4
chrVIII	YHR005C	GPA1	4
chrVIII	YHR006W	STP2	4
chrVIII	YHR007C	ERG11	2
chrVIII	YHR007C-A	-	1
chrVIII	YHR009C	TDA3	3
chrVIII	YHR012W	VPS29	3
chrVIII	YHR013C	ARD1	1
chrVIII	YHR014W	SPO13	5

chrVIII	YHR015W	MIP6	4
chrVIII	YHR016C	YSC84	1
chrVIII	YHR017W	YSC83	1
chrVIII	YHR018C	ARG4	1
chrVIII	YHR020W	-	1
chrXII:619,600 – 693,500			
chrXII	YLR246W	ERF2	3
chrXII	YLR247C	IRC20	12
chrXII	YLR248W	RCK2	5
chrXII	YLR249W	YEF3	2
chrXII	YLR251W	SYM1	1
chrXII	YLR252W	-	2
chrXII	YLR253W	MCP2	1
chrXII	YLR255C	-	2
chrXII	YLR256W	HAP1	10
chrXII	YLR257W	-	1
chrXII	YLR258W	GSY2	1
chrXII	YLR260W	LCB5	2
chrXII	YLR261C	VPS63	3
chrXII	YLR262C	YPT6	1
chrXII	YLR263W	RED1	13
chrXII	YLR264C-A	-	1
chrXII	YLR264W	RPS28B	1
chrXII	YLR265C	NEJ1	9
chrXII	YLR266C	PDR8	8
chrXII	YLR267W	BOP2	5
chrXII	YLR269C	-	2
chrXII	YLR271W	CMG1	3
chrXII	YLR272C	YCS4	2
chrXII	YLR273C	PIG1	15
chrXV: 901,400 – 931,200			
chrXV	YOR321W	PMT3	1
chrXV	YOR322C	LDB19	1
chrXV	YOR323C	PRO2	1
chrXV	YOR324C	FRT1	1
chrXV	YOR326W	MYO2	6

* Number of variants which exist between the YPH499 and Sigma parent strains

Table 3.2 Genes appearing in basal pFUS1-eGFP QTL.

Chromosome	Gene	Symbol	Num. variants*
chrIII:56,700 – 63,700			
chrIII	YCL032C	STE50	1
chrIII	YCL033C	MXR2	1
chrIII	YCL034W	LSB5	2
chrIII	YCL036W	GFD2	5
chrIII	YCL037C	SRO9	1
chrIII:15,200 – 38,700			
chrIII	YCL050C	APA1	1
chrIII	YCL051W	LRE1	5
chrIII	YCL052C	PBN1	2
chrIII	YCL055W	KAR4	1
chrIII	YCL057W	PRD1	4
chrIII	YCL058C	FYV5	3
chrIII	YCL059C	KRR1	1
chrIII	YCL061C	MRC1	14
chrIII	YCL063W	VAC17	7
chrIII	YCL064C	CHA1	2
chrIV:1,418,000 – 1,514,100			
chrIV	YDR498C	SEC20	1
chrIV	YDR501W	PLM2	1
chrIV	YDR503C	LPP1	1
chrIV	YDR505C	PSP1	1
chrIV	YDR506C	GMC1	3
chrIV	YDR507C	GIN4	1
chrIV	YDR515W	SLF1	4
chrIV	YDR517W	GRH1	1
chrIV	YDR518W	EUG1	2
chrIV	YDR519W	FPR2	1
chrIV	YDR520C	URC2	3
chrIV	YDR521W	-	2
chrIV	YDR522C	SPS2	3
chrIV	YDR526C	-	1
chrIV	YDR527W	RBA50	2
chrIV	YDR528W	HLR1	1
chrIV	YDR530C	APA2	5
chrIV	YDR531W	CAB1	3
chrIV	YDR532C	KRE28	2
chrIV	YDR534C	FIT1	30
chrIV	YDR535C	-	1
chrIV	YDR537C	-	2
chrIV	YDR538W	PAD1	2

chrVIII:93,300 – 136,700			
chrVIII	YHL002W	HSE1	1
chrVIII	YHL003C	LAG1	1
chrVIII	YHL004W	MRP4	1
chrVIII	YHL005C	-	1
chrVIII	YHL006C	SHU1	1
chrVIII	YHL007C	STE20	4
chrVIII	YHL008C	-	44
chrVIII	YHR001W	OSH7	2
chrVIII	YHR002W	LEU5	1
chrVIII	YHR003C	TCD1	2
chrVIII	YHR004C	NEM1	4
chrVIII	YHR005C	GPA1	4
chrVIII	YHR006W	STP2	4
chrVIII	YHR007C	ERG11	2
chrVIII	YHR007C-A	-	1
chrVIII	YHR009C	TDA3	3
chrVIII	YHR012W	VPS29	3
chrVIII	YHR013C	ARD1	1
chrVIII	YHR014W	SPO13	5
chrVIII	YHR015W	MIP6	4
chrXIII:382,100 – 489,500			
chrXIII	YMR053C	STB2	3
chrXIII	YMR054W	STV1	1
chrXIII	YMR056C	AAC1	1
chrXIII	YMR057C	-	1
chrXIII	YMR058W	FET3	6
chrXIII	YMR060C	SAM37	1
chrXIII	YMR062C	ARG7	1
chrXIII	YMR063W	RIM9	1
chrXIII	YMR064W	AEP1	1
chrXIII	YMR065W	KAR5	2
chrXIII	YMR066W	SOV1	4
chrXIII	YMR067C	UBX4	3
chrXIII	YMR068W	AVO2	1
chrXIII	YMR070W	MOT3	6
chrXIII	YMR071C	TVP18	1
chrXIII	YMR075C-A	-	1
chrXIII	YMR075W	RCO1	1
chrXIII	YMR076C	PDS5	2
chrXIII	YMR078C	CTF18	2
chrXIII	YMR080C	NAM7	1
chrXIII	YMR081C	ISF1	5
chrXIII	YMR082C	-	3
chrXIII	YMR084W	-	3

chrXIII	YMR085W	-	2
chrXIII	YMR086C-A	-	1
chrXIII	YMR086W	SEG1	5
chrXIII	YMR087W	-	2
chrXIII	YMR088C	VBA1	1
chrXIII	YMR089C	YTA12	2
chrXIII	YMR090W	-	1
chrXIII	YMR092C	AIP1	2
chrXIII	YMR094W	CTF13	1
chrXIII	YMR097C	MTG1	1
chrXIII	YMR098C	ATP25	1
chrXV: 186,400 – 221,500			
chrXV	YOL058W	ARG1	2
chrXV	YOL059W	GPD2	1
chrXV	YOL060C	MAM3	3
chrXV	YOL062C	APM4	2
chrXV	YOL063C	CRT10	12
chrXV	YOL064C	MET22	2
chrXV	YOL065C	INP54	8
chrXV	YOL066C	RIB2	2
chrXV	YOL068C	HST1	1
chrXV	YOL069W	NUF2	2
chrXV	YOL070C	NBA1	1
chrXV	YOL072W	THP1	1
chrXV	YOL073C	DSC2	1
chrXV	YOL075C	-	4
chrXV	YOL076W	MDM20	8
chrXV	YOL155C	HPF1	9

* Number of variants which exist between the YPH499 and Sigma parent strains

Table 3.3 Effects of allele swaps on crosstalk.

	Strain	YPH499			Sigma		
	Genotype	WT	Δ	swap	WT	Δ	swap
Gene	STE20	1.12±0.02†	N.D.	1.12±0.01$^{n.s.}$	1.31±0.01	N.D.	1.32±0.01$^{n.s.}$
	RCK2	1.07±0.02	1.27±0.03***	-	1.23±0.03	1.67±0.04***	1.20±0.01$^{n.s.}$
		1.15±0.02	1.37±0.04***	1.19±0.01**	1.49±0.04	1.92±0.04***	-
	LDB19	1.23±0.02	1.25±0.02$^{n.s.}$	1.26±0.01$^{n.s.}$	1.47±0.01	1.18±0.02***	1.44±0.01**
	MYO2	1.09±0.004	N.D.	1.08±0.004$^{n.s}$	N.D.	N.D.	N.D.

†All values are mean ± s.e.m. crosstalk measurements of at least 6 biological replicates. Experiments in the same row were performed on the same day.
n.s., not significant
N.D., not done
*p<0.05
**p<0.01
***p<0.001
P-values compare the mutant to the WT of the same strain background with a one-sided student's t-test with equal variance.

Table 3.4 Yeast strain table.

Strain	Background	Genotype	Source
yMM0736 (YJP212)	YPH499[3]	MATa pSTL1::HA-tdTomato::ADE2 pFUS1::HA-eGFP::ADE1 bar1Δ::KanMX	[30]
yMM11584	Sigma[4]	MATa pSTL1::HA-tdtomato::LEU2 pFUS1::HA-eGFP::URA3 bar1Δ::NatMX AMN1(D68V)	[33]
yMM1597	YPH499	yMM0736 hoΔ::pMFA1::HygMX	This study
yMM1598	Sigma	yMM1584 hoΔ::pMFA1::HygMX	This study
yMM1599	YPH499	yMM1597 diploid	This study
yMM1600	Sigma	yMM1598 diploid	This study
yMM1601	YPH499	yMM1597 MATα	This study
yMM1602	Sigma	yMM1598 MATα	This study
yMM1609	YPH499/Sigma	yMM1598 x yMM1601	This study
yMM1610	YPH499/Sigma	yMM1597 x yMM1602	This study
yMM1653	YPH499	yMM0736 diploid	This study
yMM1655	YPH499	yMM1653 MYO2/myo2Δ::HygMX	This study
yTS0001	YPH499	yMM1653 MYO2/MYO2(Sigma)	This study
yTS0002	YPH499	yMM0736 MYO2(Sigma)	This study
yTS0003	YPH499	yMM0736 ste50Δ::HygMX	This study
yTS0004	YPH499	yMM0736 STE50(Sigma)	This study
yTS0005	YPH499	yMM0736 fyv5Δ::HygMX	This study
yTS0006	YPH499	yMM0736 FYV5(Sigma)	This study
yTS0007	YPH499	yMM0736 ste20Δ::HygMX	This study
yTS0008	YPH499	yMM0736 STE20(Sigma)	This study
yMM1724	YPH499	yMM0736 rck2Δ::HygMX	[33]
yTS0009	YPH499	yMM0736 RCK2(Sigma)	This study
yTS0010	YPH499	yMM0736 ldb19Δ::HygMX	This study
yTS0011	YPH499	yMM0736 LDB19(Sigma)	This study
yTS0012	YPH499	yMM0736 pmt3Δ::HygMX	This study
yTS0013	YPH499	yMM0736 PMT3(Sigma)	This study
yTS0014	Sigma	yMM1584 ste50Δ::HygMX	This study
yTS0015	Sigma	yMM1584 STE50(Sigma)	This study
yTS0016	Sigma	yMM1584 fyv5Δ::HygMX	This study
yTS0017	Sigma	yMM1584 FYV5(Sigma)	This study
yTS0018	Sigma	yMM1584 ste20Δ::KanMX	This study

[3] YPH499 genotype: MATa ura3-52 lys2-801_amber ade2-101_ochre trp1-Δ63 his3-Δ200 leu2-Δ1 [60]
[4] Sigma2000, MATa prototroph derived from Σ1278b [61]

yTS0019	Sigma	yMM1584 STE20(Sigma)	This study
yTS0020	Sigma	yMM1584 rck2Δ::HygMX	This study
yTS0021	Sigma	yMM1584 RCK2(Sigma)	This study
yTS0022	Sigma	yMM1584 ldb19Δ::HygMX	This study
yTS0023	Sigma	yMM1584 LDB19(Sigma)	This study
yTS0024	Sigma	yMM1584 pmt3Δ::HygMX	This study
yTS0025	Sigma	yMM1584 PMT3(Sigma)	This study

Table 3.5 Plasmid table.

Plasmid	Description	Source
pMM0815	pHS2	Addgene# 81037
pMM0887	pXIPHOS-NatMX pSNR52-KanMX sgRNA-tSNR52	Audrey Gasch
pMM0888	pXIPHOS-NatMX pSNR52-HygMX sgRNA-tSNR53	Audrey Gasch
pMM0889	pXIPHOS-NatMX pSNR52-tSNR54	Audrey Gasch
pMM0890	pXIPHOS-HygMX pSNR52-KanMX sgRNA-tSNR55	[33]
pMM0891	pXIPHOS-HygMX pSNR52-tSNR56	[33]
pMM0904	pHS2-KanMX	[33]
pMM1232	pXIPHOS-KanMX pSNR52-HygMX sgRNA-tSNR53	[33]
pMM1233	pXIPHOS-KanMX pSNR52-tSNR54	[33]

Chapter 4: Conclusions and Future Directions

Taylor Scott wrote the chapter.

CONCLUSIONS AND FUTURE DIRECTIONS

In this thesis, I demonstrated that many features of yeast mitogen activated protein kinase (MAPK) signaling are impacted by the strain background. Specifically, I showed that in the Sigma background crosstalk occurs between the HOG and the mating pathways in wild type cells under certain osmostress conditions, and that this crosstalk is not regulated by the well-known inhibition by Hog1p. I showed that this crosstalk and basal expression of pFUS1-eGFP (a reporter for mating pathway activity) are heritable traits, and I mapped these phenotypes to QTL. From this QTL analysis, I identified two genes, *STE50* and *FYV5*, which regulate basal mating pathway expression in a strain dependent manner. These results are important for understanding how signaling through a network can be altered despite apparently having the same components and reactions.

Distinct phases of crosstalk regulation

I identified crosstalk in the Sigma background, and by comparing crosstalk in wildtype cells to crosstalk in HOG pathway deletions, I discovered that there are distinct phases of crosstalk regulation during an osmotic shock. Early in a time course (roughly 20-30 minutes post-shock), crosstalk is permitted in the Sigma background but suppressed in the YPH499 background. Late in a time course, the HOG pathway actively inhibits crosstalk in both strain backgrounds. The key finding that supports this theory is that in the Sigma background, disrupting the HOG pathway by deleting *HOG1*, rendering Hog1p kinase dead, or delaying Hog1p activation results in increased crosstalk only at 45 minutes and 60 minutes post-induction. This is after crosstalk in the Sigma background is first apparent, which occurs by 20 minutes post-induction. Similar results were seen in the YPH499 background, although I did observe a slight (but statistically significant) increase in crosstalk in the HOG pathway disruptions at 30 minutes post-induction. Previous studies have shown that the timing of Hog1p activity is important for insulating the HOG and mating pathways [1,2].

These time points are not precisely resolved: the time course experiments I performed consisted of only 6 time points. Better resolution would be achieved by using live-cell microscopy. These experiments were previously not possible due to the clumpy nature of the Sigma background. However, as part of this work, I introduced the *AMN1*^{D368V} allele[3] into the Sigma background strain with HOG and mating reporters, facilitating both higher throughput flow cytometry experiments (as I used it) and wildtype cells and in HOG pathway disrupted cells in both the Sigma and YPH499 backgrounds in order to determine when the excess crosstalk associated with deficient HOG signaling occurs. This would also reveal whether the timing of Hog1p inhibition of crosstalk varies by strain background, and whether this timing is associated with any important events in HOG pathway signaling (e.g., maximal Hog1p localization[4], cell size recovery [5], or gene induction). Microscopy could also be used to study strain dependent differences in crosstalk under more complex stress patterns. It has previously been shown that crosstalk between MAPK pathways occurs under rapidly oscillating stress, and the authors suggest that this crosstalk is due to the hyperactivation of the SHO1 branch of the HOG pathway [6]. Microscopy in microfluidic devices would enable experiments to determine whether crosstalk in the Sigma background can be increased using similar oscillatory stress, and whether more complex stress profiles (e.g., randomly changing osmolarity) influence the amount of crosstalk in either strain background. Complex, random stress profiles have been associated with SHO1 signaling previously [7], therefore I expect that they also will result in increased crosstalk, because crosstalk occurs through the SHO1 branch.

Genetic factors affecting crosstalk

I did not identify a causal gene for crosstalk in the Sigma background, despite showing that crosstalk is heritable and showing that a QTL on chromosome XV is associated with low crosstalk in the YPH499 background. It is unlikely that crosstalk is caused by a single gene – signaling through MAPK networks is complex with many regulating factors outside of the MAPK network itself, such as the cell cycle [8–10], metabolic state [11,12], flux across the membrane [5], ploidy[13], and mating type[14]. One strategy to

identify factors affecting crosstalk is to screen the knockout collection for crosstalk. The S288C deletion collection has been widely used for high-throughput screens [15] and a deletion collection has also been created in the Sigma background [16]. A direct comparison of crosstalk in these collections would reveal genetic factors which promote or suppress crosstalk in a strain dependent manner. These collections consist of individual strains with most of the 6000+ yeast genes deleted, and manually screening all of these strains with flow cytometry would be expensive, time consuming, and difficult. One strategy is to use liquid handling robots to automate the growth and induction. This would be particularly effective if the protocol can be adapted for a plate reader instead of flow cytometry because a plate reader can give real-time output during the induction. In order to facilitate this, the pSTL1-tdTomato reporter should be replaced with a fast-folding red fluorescent protein and both reporters should be moved to a plasmid, which can be transformed into the deletion collections with much higher efficiency than a genomic integration. Although these (and other) technical obstacles exist, these experiments would be powerful and would greatly expand our knowledge of how signaling components regulate the interaction of signaling networks.

A different approach to identifying factors affecting signaling is to use diversity among many different strains of yeast. In this work I examined two strains, YPH499 and Sigma, but many strains exist with varying amounts of similarity to the reference strain S288C [17]. It is interesting to note that S288C is filamentation deficient due truncation of *FLO8*, a defect in cyclic AMP signaling [18], and therefore may have lost selective pressure to allow signaling through the filamentous growth MAPK pathway under stress. A study of many yeast strains, those with intact filamentation and without, could determine whether loss of filamentation is associated with a lack of crosstalk. Collections of wild and laboratory yeast strains and species have been used to study the diversity of phenotypes [19–22]. Screening these or other collections for crosstalk would reveal whether crosstalk is common outside of laboratory strains. Crosses between these strains can also be used to increase the power of genetic mapping, as has been done with

MAPK traits previously [23]. As with the high throughput screening experiments above, these experiments would be facilitated by moving the fluorescent reporters to plasmids to allow for more efficient transformation. High efficiency transformation methods have been developed which work across strains and species [24], and these methods may be necessary when working with strains less tractable than the typical laboratory strains.

Genetic factors affecting basal mating activity

I showed that between the YPH499 and Sigma backgrounds there is a heritable difference in basal expression of a mating pathway reporter. This difference is associated with (predominantly) the left arm of chromosome III, as well as several less significant QTL on other chromosomes. Regulation of the mating pathway is critically important for the cell because unregulated MAPK signaling is associated with a cell cycle arrest [25,26]. I did not explore the relationship between increased basal pFUS1-eGFP expression in the YPH499 background and fitness, but it is interesting to note that, in general, Sigma grows better than YPH499 in liquid culture. A previous study identified a direct link between mating pathway activity and fitness, specifically finding that mutations in *GPA1* which result in increased pFUS1-eGFP expression are associated with a growth defect [27]. A survey of other yeast strains to determine whether, in general, increased pFUS1-eGFP expression is associated with lowered fitness would strengthen this conclusion and provide additional insight into the evolutionary balance of fitness and mating.

I identified two genes, *STE50* and *FYV5*, which affected basal pFUS1-eGFP expression in the strain backgrounds. Interestingly, the results were strain dependent: the YPH499 allele of *STE50* increased expression in the Sigma background, while the Sigma allele did not alter expression in the YPH499 background. Similarly, the Sigma allele of *FYV5* increased expression in the YPH499 background, while the YPH499 allele did not alter expression in the Sigma background. This finding underscores that regulation of the mating pathway is complex and epistatic. A higher resolution genetic study is necessary to identify all of the genes regulating mating activity in these strains. Rather than individually phenotyping

segregants, a more powerful approach would be to use fluorescence-activated cell sorting (FACS) to collect, at minimum, thousands of segregants into each of the two bulks. A larger population of segregants in the pools would increase the total number of recombination events and therefore improve the resolution of the mapping. A potential problem with this method is that my data showed that most of the left arm of chromosome III was associated with pFUS1-eGFP expression, indicating that several causal genes may exist on this chromosome. To further improve the power of the mapping, the segregant pool could be generated after several rounds of backcrossing. My work used a single cross (F2) which limits the number of potential recombination events. Previous works have used multiple backcrosses to reduce the linkage between nearby loci [28]. These experiments would also improve efforts to identify genes associated with crosstalk. I chose to phenotype a limited number of segregants because the vastly different pFUS1-eGFP expression levels between the two strain backgrounds means that FACS is not a viable means to generate large pools of high crosstalk and low crosstalk bulks. If the pFUS1-eGFP expression levels between the two strains can be equalized, then FACS can be used to generate much larger pools of high crosstalk and low crosstalk segregants and higher resolution mapping.

Conclusions

Signaling through MAPK pathways is highly conserved among eukaryotes [29], with implications in important biological fields, such as cancer biology, developmental biology, and control of cellular systems [30–32]. I used the yeast MAPK networks a model system to explore how diversity can exist in signaling output, despite the same pathway components being present and no obvious defects in activation. I showed that important signaling properties differ between two strains of yeast, specifically crosstalk between the HOG and mating pathways, basal mating pathway activity, and coordination of the response to multiple stimuli. In this thesis I have demonstrated that the complexity of signaling networks leaves many intricacies to be discovered, even in well-studied model systems. It shows that existing yeast strains are a powerful tool for understanding the signaling properties of MAPK networks.

REFERENCES

1 Patterson JC, Klimenko ES & Thorner J (2010) Single-Cell Analysis Reveals That Insulation Maintains Signaling Specificity Between Two Yeast MAPK Pathways with Common Components. *Sci Signal* **3**, ra75–ra75.

2 Westfall PJ & Thorner J (2006) Analysis of Mitogen-Activated Protein Kinase Signaling Specificity in Response to Hyperosmotic Stress: Use of an Analog-Sensitive HOG1 Allele. *Eukaryotic Cell* **5**, 1215–1228.

3 Kuzdzal-Fick JJ, Chen L & Balázsi G (2019) Disadvantages and benefits of evolved unicellularity versus multicellularity in budding yeast. *Ecology and Evolution* **9**, 8509–8523.

4 Ferrigno P, Posas F, Koepp D, Saito H & Silver PA (1998) Regulated nucleo/cytoplasmic exchange of HOG1 MAPK requires the importin beta homologs NMD5 and XPO1. *EMBO J* **17**, 5606–5614.

5 Miermont A, Waharte F, Hu S, McClean MN, Bottani S, Léon S & Hersen P (2013) Severe osmotic compression triggers a slowdown of intracellular signaling, which can be explained by molecular crowding. *PNAS* **110**, 5725–5730.

6 Mitchell A, Wei P & Lim WA (2015) Oscillatory stress stimulation uncovers an Achilles' heel of the yeast MAPK signaling network. *Science* **350**, 1379–1383.

7 Granados AA, Crane MM, Montano-Gutierrez LF, Tanaka RJ, Voliotis M & Swain PS (2017) Distributing tasks via multiple input pathways increases cellular survival in stress. *eLife Sciences* **6**, e21415.

8 Oehlen LJ & Cross FR (1994) G1 cyclins CLN1 and CLN2 repress the mating factor response pathway at Start in the yeast cell cycle. *Genes Dev* **8**, 1058–1070.

9 Wassmann K & Ammerer G (1997) Overexpression of the G1-cyclin gene CLN2 represses the mating pathway in Saccharomyces cerevisiae at the level of the MEKK Ste11. *J Biol Chem* **272**, 13180–13188.

10 Strickfaden SC, Winters MJ, Ben-Ari G, Lamson RE, Tyers M & Pryciak PM (2007) A Mechanism for Cell Cycle Regulation of MAP Kinase Signaling in a Yeast Differentiation Pathway. *Cell* **128**, 519–531.

11 Zi Z, Liebermeister W & Klipp E (2010) A Quantitative Study of the Hog1 MAPK Response to Fluctuating Osmotic Stress in Saccharomyces cerevisiae. *PLoS ONE* **5**, e9522.

12 Klipp E, Nordlander B, Krüger R, Gennemark P & Hohmann S (2005) Integrative model of the response of yeast to osmotic shock. *Nat Biotechnol* **23**, 975–982.

13 Cullen PJ & Sprague Jr. GF (2012) The regulation of filamentous growth in yeast. *Genetics* **190**, 23–49.

14 Bardwell L (2005) A walk-through of the yeast mating pheromone response pathway. *Peptides* **26**, 339–350.

15 Giaever G & Nislow C (2014) The Yeast Deletion Collection: A Decade of Functional Genomics. *Genetics* **197**, 451–465.

16 Ryan O, Shapiro RS, Kurat CF, Mayhew D, Baryshnikova A, Chin B, Lin Z-Y, Cox MJ, Vizeacoumar F, Cheung D, Bahr S, Tsui K, Tebbji F, Sellam A, Istel F, Schwarzmüller T, Reynolds TB, Kuchler K, Gifford DK, Whiteway M, Giaever G, Nislow C, Costanzo M, Gingras A-C, Mitra RD, Andrews B, Fink GR, Cowen LE & Boone C (2012) Global gene deletion analysis exploring yeast filamentous growth. *Science* **337**, 1353–1356.

17 Song G, Dickins BJA, Demeter J, Engel S, Dunn B & Cherry JM (2015) AGAPE (Automated Genome Analysis PipelinE) for Pan-Genome Analysis of Saccharomyces cerevisiae. *PLOS ONE* **10**, e0120671.

18 Liu H, Styles CA & Fink GR (1996) Saccharomyces Cerevisiae S288c Has a Mutation in Flo8, a Gene Required for Filamentous Growth. *Genetics* **144**, 967–978.

19 Schacherer J, Shapiro JA, Ruderfer DM & Kruglyak L (2009) Comprehensive polymorphism survey elucidates population structure of Saccharomyces cerevisiae. *Nature* **458**, 342–345.

20 Sylvester K, Wang Q-M, James B, Mendez R, Hulfachor AB & Hittinger CT (2015) Temperature and host preferences drive the diversification of Saccharomyces and other yeasts: a survey and the discovery of eight new yeast species. *FEMS Yeast Research* **15**, fov002.

21 Molinet J & Cubillos FA (2020) Wild Yeast for the Future: Exploring the Use of Wild Strains for Wine and Beer Fermentation. *Frontiers in Genetics* **11**.

22 García-Béjar B, Arévalo-Villena M, Guisantes-Batan E, Rodríguez-Flores J & Briones A (2020) Study of the bioremediatory capacity of wild yeasts. *Sci Rep* **10**, 11265.

23 Treusch S, Albert FW, Bloom JS, Kotenko IE & Kruglyak L (2015) Genetic Mapping of MAPK-Mediated Complex Traits Across S. cerevisiae. *PLoS Genet* **11**.

24 Alexander WG, Doering DT & Hittinger CT (2014) High-Efficiency Genome Editing and Allele Replacement in Prototrophic and Wild Strains of Saccharomyces. *Genetics* **198**, 859–866.

25 Gartner A, Jovanović A, Jeoung DI, Bourlat S, Cross FR & Ammerer G (1998) Pheromone-dependent G1 cell cycle arrest requires Far1 phosphorylation, but may not involve inhibition of Cdc28-Cln2 kinase, in vivo. *Mol Cell Biol* **18**, 3681–3691.

26 Chang F & Herskowitz I (1990) Identification of a gene necessary for cell cycle arrest by a negative growth factor of yeast: FAR1 is an inhibitor of a G1 cyclin, CLN2. *Cell* **63**, 999–1011.

27 Lang GI, Murray AW & Botstein D (2009) The cost of gene expression underlies a fitness trade-off in yeast. *PNAS* **106**, 5755–5760.

28 Parts L, Cubillos FA, Warringer J, Jain K, Salinas F, Bumpstead SJ, Molin M, Zia A, Simpson JT, Quail MA, Moses A, Louis EJ, Durbin R & Liti G (2011) Revealing the genetic structure of a trait by sequencing a population under selection. *Genome Res* **21**, 1131–1138.

29 Widmann C, Gibson S, Jarpe MB & Johnson GL (1999) Mitogen-Activated Protein Kinase: Conservation of a Three-Kinase Module From Yeast to Human. *Physiological Reviews* **79**, 143–180.

30 Braicu C, Buse M, Busuioc C, Drula R, Gulei D, Raduly L, Rusu A, Irimie A, Atanasov AG, Slaby O, Ionescu C & Berindan-Neagoe I (2019) A Comprehensive Review on MAPK: A Promising Therapeutic Target in Cancer. *Cancers (Basel)* **11**, 1618.

31 Scott TD, Sweeney K & McClean MN (2019) Biological signal generators: integrating synthetic biology tools and in silico control. *Curr Opin Syst Biol* **14**, 58–65.

32 Lavoie H, Gagnon J & Therrien M (2020) ERK signalling: a master regulator of cell behaviour, life and fate. *Nat Rev Mol Cell Biol* **21**, 607–632.

Appendix A: Genetic basis of osmotolerance

Taylor Scott performed the experiments, analyzed the data, and wrote the appendix.

As I showed in Chapter 2, the YPH499 and Σ1278b ("Sigma") backgrounds are differently osmotolerant, with the YPH499 background showing better initial growth on YPD agar containing sorbitol (see Figure 2.2A, B). I attempted to map this phenotype to a genetic locus using a bulk segregant approach. Using the pool of segregants from YPH499 x Sigma crosses described in Chapter 3, I grew the segregants overnight in YPD and spotted onto YPD agar and YPD + 0.75M sorbitol agar. Spots were incubated at room temperature for 2 days before imaging on a ChemiDoc. Spot growth (intensity) was quantified using the Gel Analyzer tool in ImageJ [1] and grown on YPD+sorbitol was normalized to growth on YPD to obtain a value for osmotolerance for each segregant (Figure 1A).

As expected, the parent strain controls showed differing osmotolerance values, with the YPH499 background controls being more osmotolerant than the Sigma background controls (Figure 1A, $p = 1.3e-9$, student's t-test with equal variance, each strain $n = 8$). The osmotolerance of the segregants were distributed between the two parents (Figure 1C), and broad sense heritability was found to be 0.92, indicating that 92% of the variation among the segregants is due to genetic factors. The 120 most osmotolerant and 120 least osmotolerant segregants were pooled to form the high and low bulks and sequencing, mapping, and variant calling was performed as described in Chapter 3. LOD scores were calculated across the genome using MULTIPOOL (Figure 1D) [2]. I found a single peak on chromosome XV with a LOD score above the threshold of 3 (maximum LOD score = 35). Examining the MULTIPOOL output for chromosome XV (Figure 1E) shows that, at this peak, more than 90% of reads from the high bulk were from the YPH499 parent and fewer than 10% of reads in the low bulk were from the YPH499 parent. A 2-LOD support interval for this peak was found, and variants within this region were assessed for non-silent mutations in known genes using the web version of the Variant Effect Predictor tool [3]. Ten genes in this region have non-silent variations between YPH499 and Sigma. The list of genes can be found in Table 1. Due to time constrains, I did not perform allele swap of these genes to determine which, if any, causes

the difference in osmotolerance. None of the genes have previously been implicated in high osmolarity glycerol pathway signaling.

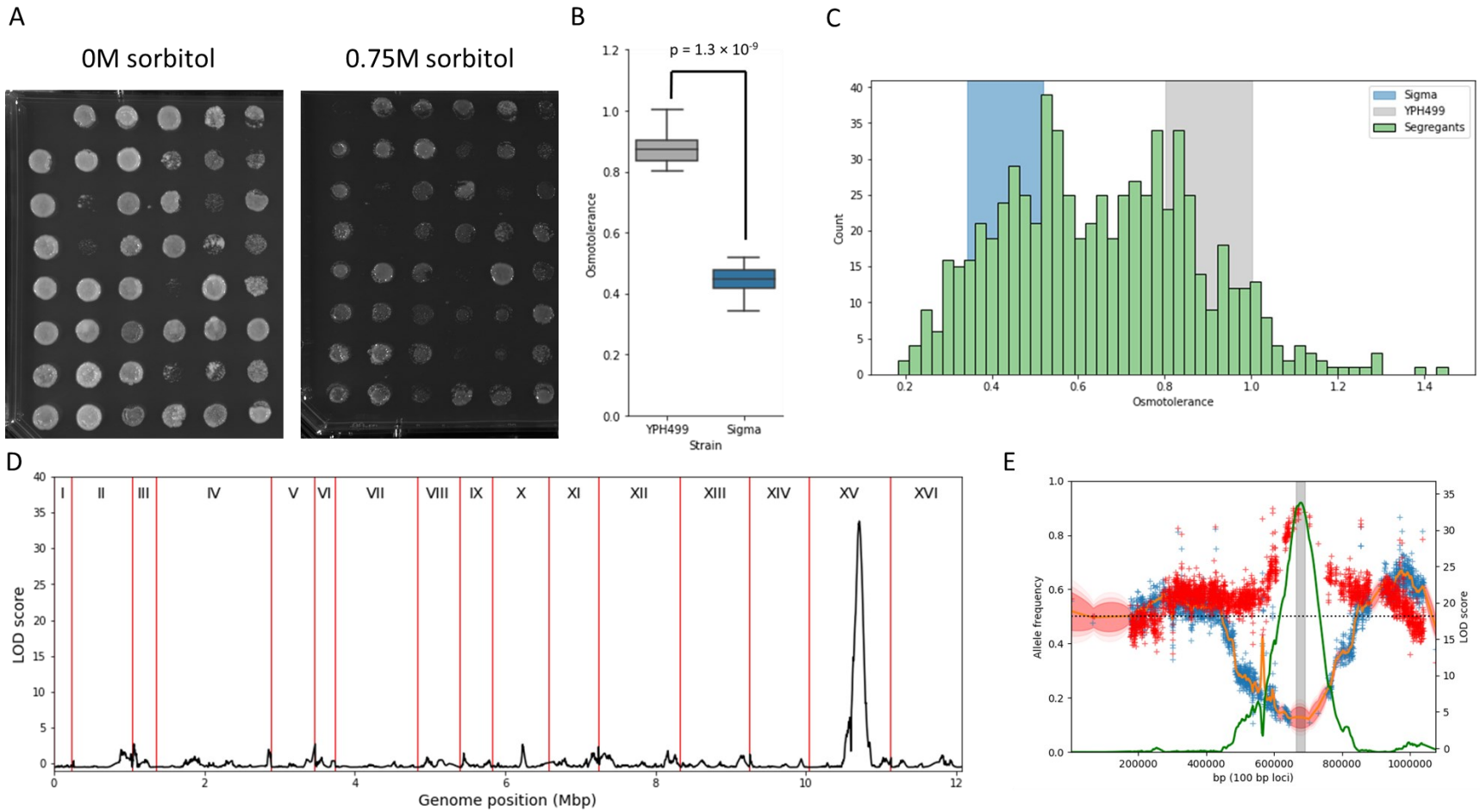

Figure 1 Mapping osmotolerance to a genomic locus.

(A) Representative images of spot growth images on YPD agar (left) and YPD agar + 0.75M sorbitol (right)

(B) The YPH499 parent controls (gray) are more osmotolerant than the Sigma parent controls (blue), p = 1.3e-9, student's t test with equal variance, n = 8 (each strain background).

(C) Osmotolerance of the segregants (green histogram) is distributed between the osmotolerance values of the parents strain controls.

(D) A single significant peak on chromosome XV (LOD = 34) was identified bulk segregant analysis.

(E) MULTIPOOL output of chromosome XV. Red, blue: percentage of reads in high, low bulk from YPH499 parent. Green, LOD score.

REFERENCES

1 Schneider CA, Rasband WS & Eliceiri KW (2012) NIH Image to ImageJ: 25 years of image analysis. *Nat Methods* **9**, 671–675.

2 Edwards MD & Gifford DK (2012) High-resolution genetic mapping with pooled sequencing. *BMC Bioinformatics* **13**, S8.

3 McLaren W, Pritchard B, Rios D, Chen Y, Flicek P & Cunningham F (2010) Deriving the consequences of genomic variants with the Ensembl API and SNP Effect Predictor. *Bioinformatics* **26**, 2069–2070.

Appendix B: Automated microcolony growth tracking in microfluidic devices

Taylor Scott wrote the software, performed the experiments, analyzed the data, and wrote the appendix.

Microfluidic devices allow for imaging single cells in dynamic environments. For example, it is possible to image yeast cells before and after a sorbitol osmoshock to observe how their growth, transcription, or physiology changes. The Cellasic Onix platform (EMD Millipore, Burlington, MA) traps cells between a glass slide and a PDMS ceiling in order to hold them in place over long (multi-day) experiments. Cells are seeded into the chamber at a low density (Figure 1A) and grow in distinct microcolonies over the course of the experiment (Figure 1B). I wrote Python software to process fluorescence microscopy images, automatically identify cells and microcolonies and calculate the growth rate of the each microcolony over the course of an experiment.

The cells I used had integrated *HTB2::mCherry* tags, labeling their nuclei and allowing for accurate cell identification via circle finding methods. I used the Laplacian of Gaussian (LoG) circle detector which is part of the scikit-image package [1]. LoG circle detection is a convolution-based method which detects circles of a fixed size. As with all convolution methods, the runtime is proportional to the size of the image scanned. However, the majority of the image is empty, particularly at the beginning of the experiment when the cells are seeded sparsely. To improve runtime, I do not detect circles in the entire image in every frame. Rather, I first define the boundaries of microcolonies by detecting circles in the last frame (when the colonies are at their largest). LoG detectors produce many false positives, so the detected spots are clustered by intensity in the original image and intensity in the LoG-transformed image using K-means clustering with two groups using scikit-learn [2]. True spots will be bright in both the original image (where they are fluorescent labeled nuclei) and in the LoG-transformed image (where they match the profile of a circle). In practice, there are many more false spots than true spots, so the smaller of the two clusters is taken to be the true spots. The true spots are expanded from the size of a nucleus to the size of a cell, and overlapping cells are grouped into a microcolony. The coordinates of each microcolony are then used to limit the search area for the LoG detector in the remaining frames (Figure 1). This greatly improves speed

and computational efficiency, because areas which are empty in the final frame are likely to be empty in the previous frames, and so they do not need to be searched for circles.

After the microcolonies are defined, the LoG detector identifies spots in each frame for each microcolony. As before, K-means clustering on the original intensity and the LoG-transformed intensity is used to identify true spots. The number of spots in each microcolony at each time point is recorded and used to track growth. Because each microcolony starts with a different number of cells, the final size of a colony is a misleading statistic for growth. A better approach is to calculate the number of doublings at each time point $D_t = \log\_2\,[N_t/N_0]$, where D_t is the number of doublings, N_t is the number of cells at time t, and N_0 is the number of cells at time 0. This metric, while noisy at the beginning of the experiment, provides a better view of colony growth relative to other colonies. In the example in Figure 2, two adjacent microcolonies (pink and green) are tracked over a 12-hour experiment. The pink colony begins with 3 cells and the green colony begins with 4 cells (Figure 2A). Considering the number of cells over time (Figure 2B), it seems as if the green colony is growing much faster than the pink colony. However, it clear from looking at the number of doublings that the two colonies are doubling at approximately the same rate, with each doubling approximately 4 times over the course of the experiment (Figure 2C). This is the expected behavior because the two colonies spatially close and subject to similar nutrient profiles.

This method can be used to detect the cell cycle interruption associated with an osmotic shock. Figure 3 shows the number of doublings over time for genetically identical cells grown in low fluorescence media for two hours before the media was switched to low fluorescence media without or with 1M sorbitol (Figures 3A and 3B respectively). The graph of doublings over time for cells subjected to 1M sorbitol plateaus for nearly 2 hours following the stress, demonstrating the high osmolarity glycerol (HOG) pathway's interruption of the cell cycle. A small plateau is seen in the cells not subjected to stress, likely a result of the media change, but the cells quickly recover and resume linear growth.

REFERENCES

1 Walt S van der, Schönberger JL, Nunez-Iglesias J, Boulogne F, Warner JD, Yager N, Gouillart E & Yu T (2014) scikit-image: image processing in Python. PeerJ 2, e453.

2 Pedregosa F, Varoquaux G, Gramfort A, Michel V, Thirion B, Grisel O, Blondel M, Prettenhofer P, Weiss R, Dubourg V, Vanderplas J, Passos A, Cournapeau D, Brucher M, Perrot M & Duchesnay É (2011) Scikit-learn: Machine Learning in Python. Journal of Machine Learning Research 12, 2825–2830.

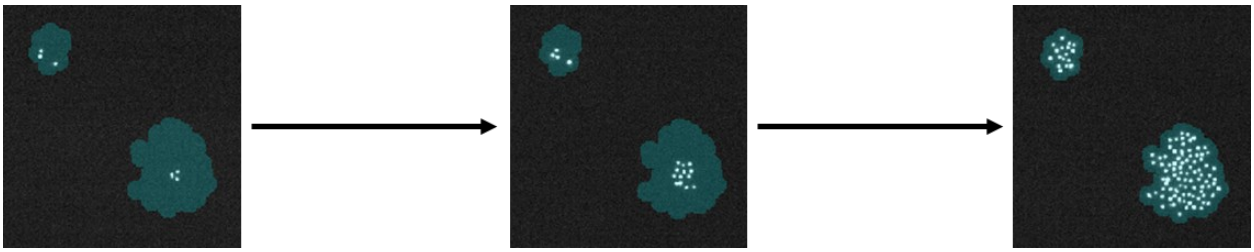

Figure 20 Colony growth is restricted to discrete areas

On the Cellasic platform, cells are held in place between the glass slide and a PDMS ceiling. Consequently, microcolonies grow within discrete areas of the frame. Depicted are two microcolonies growing over time. The growth is contained withing boundaries (blue) defined based on the last frame (rightmost image).

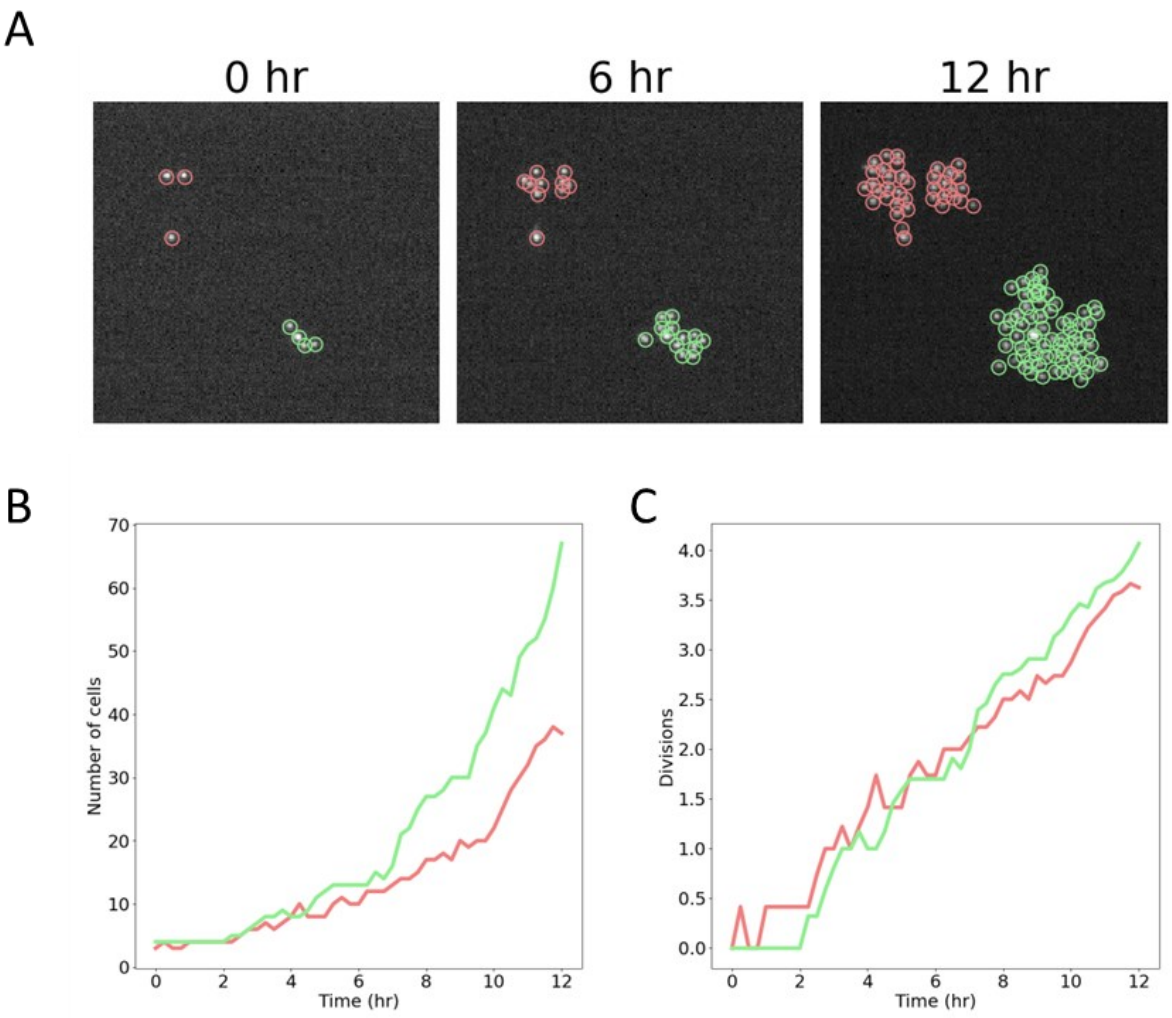

Figure 21 Doublings over time is an accurate way to quantify growth.

(A) Two colonies (pink and green) are spatially close to one another and start with different number of cells (pink, 3 cells; green, 4 cells). After 6 hours growth, the number of cells is similar in both colonies. After 12 hours growth, the green colony has many more cells than the pink colony.

(B) Tracking the number of cells over time, it appears the green colony is growing much faster than the pink colony.

(C) Tracking doublings over time, the two colonies have similar growth rates over the course of the experiment, both doubling approximately 4 times over the 12-hour time course.

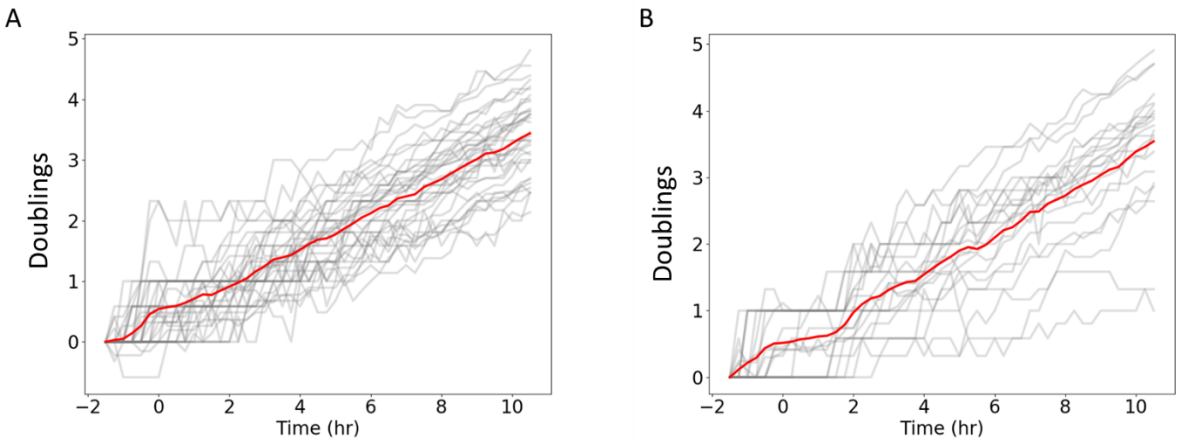

Figure 22 Growth defect due to osmostress can be identified using microcolony growth.

Yeast cells were grown for 2 hours without stimulus, then media was switched to media without osmostress (A) or with 1M sorbitol osmostress (right). Gray lines are the growth rates of individual microcolonies. Red lines are the mean growth rate for all microcolonies. The osmostress-induced interruption of the cell cycle is visible as a plateau in the mean number of doublings, which lasts for approximately two hours post-osmoshock.